Università degli Studi del Piemonte Orientale

"Amedeo Avogadro"

Dipartimento di Scienze Chimiche, Alimentari, Farmaceutiche e Farmacologiche

Dottorato di Ricerca in Biotecnologie Farmaceutiche ed Alimentari

XXVII ciclo a.a.2011-2014

DISSECTING CHANGES IN THE B CELL REPERTOIRE IN RESPONSE TO VACCINE ANTIGENS

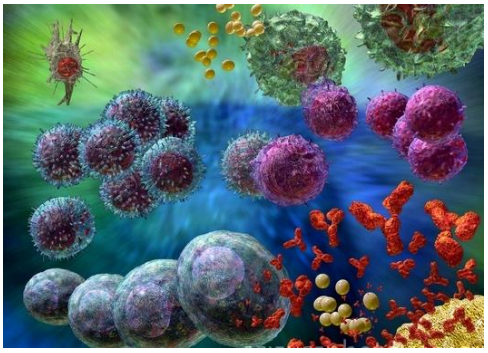

Liliana Alleri

Università degli Studi del Piemonte Orientale

"Amedeo Avogadro"

Dipartimento di Scienze Chimiche, Alimentari, Farmaceutiche e Farmacologiche

Dottorato di Ricerca in Biotecnologie Farmaceutiche ed Alimentari

XXVII ciclo a.a.2011-2014

DISSECTING CHANGES IN THE B CELL REPERTOIRE IN RESPONSE TO VACCINE ANTIGENS

Liliana Alleri

Supervised by Oretta Finco and Grazia Galli

PhD program co-ordinator Prof Menico Rizzi

Contents

1.1. Immunological memory is long-lived after infection or vaccination

The generation and the maintenance of a serological memory are fundamental for the immune system to remember the pathogens to which it was exposed. It has been so far demonstrated that a successful response remains in human sera for a lifetime after vaccination or infections (Amanna IJ1, 2006 Jun; Hammarlund E1, 2003 Sep). Different are the hypotheses suggested in the recent years to explain the mechanisms at the basis of such durable responses and it is noteworthy that all these hypotheses rely upon the establishment of a pool of Antigen-specific Plasmablasts (PBs) and Memory B cells (MBCs) (Mark K. Slifka, 1998; Traggiai E1, 2003 Jun 1) (Figure 1).

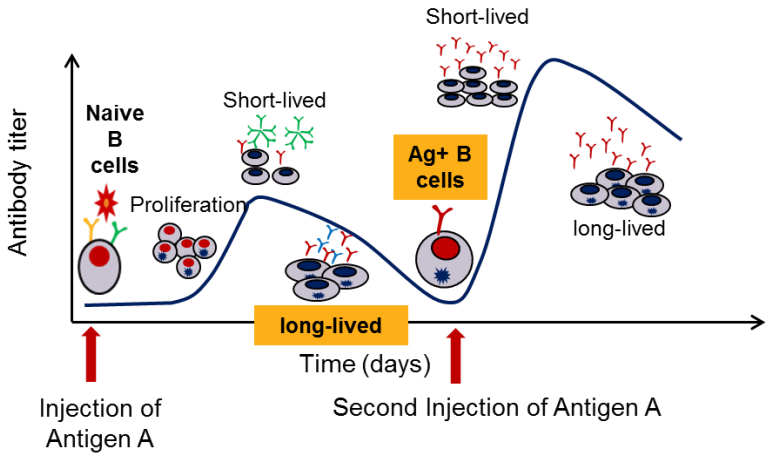

Figure 1_Mechanisms that establish and mantain serological memory

PBs are known to be the main source of antigen specific antibodies and these terminally differentiated B cells are able to maintain antibody level independently (Slifka MK1, 1998) or could require a refilling mediated by the continuous differentiation of MBCs into PBs (Amanna IJ1, 2006 Jun; Traggiai E1, 2003 Jun

1). Several are in fact the studies that supposed a requirement of MBCs for the antibody maintenance even if it seems that it is not likely to be a global mechanism for antibody maintenance (Ian J. Amanna, November 8, 2007).

Both PBs and MBCs are the result of adaptive immune responses. The adaptive capabilities of B cells strongly rely on two independent stages of development. The first one occurs in the bone marrow and is an antigen-independent process by which each B cells finally creates a unique receptor for recognition of pathogens. As a consequence, a large repertoire of antigen receptors is generated with the potential to specifically recognize many different pathogens. The naïve B cells generated in this way reach the secondary lymphoid organs where they eventually recognize eliciting agents. Following antigen recognition, the second stage of B cell development starts which is antigen-dependent and leads to the clonal expansion and receptor affinity maturation of the antigen-activated B cells. These latter events are the basis for generating effector cells that elicit strong response and long term memory in the form of MBCs and PBs (Figure 1).

1.2. Antigen-independent B cell differentiation in the bone marrow

In humans the development of B cells occurs in the bone marrow proceeding through different stages of maturation. It has been so far demonstrated that both the development and function of B cells critically depend on the B-cell antigen receptor (BCR) (Figure 2). In its simplest form, the BCR is a heterotetramer composed by two identical heavy chains (HCs) and two identical light chains (LCs). Each chain has a variable domain at its N-terminal end a constant region at its C-terminal end. The first step of BCR generation is the biosynthesis of the Variable domain and occurs in a pre-B cell state, when a random recombination between one Variable (V), Diversity (D, only for IGH) and Joining (J) genes takes

place at the DNA genomic level (Tonegawa, 1983). The rearranged VDJ genes, together with one Heavy Constant gene (for the heavy chain) or the rearranged VJ and Kappa or Lambda Constant genes (for the light chain) are transcribed as a pre-messenger RNA, then spliced and translated to obtain a heavy or a light chain, respectively. This step is followed by the combinatorial pairing of the heavy and light chains. All these steps are responsible for generating the broad diversity in the repertoire of the final BCR. The random process of genes recombination introduces or subtracts nucleotides at the joints between different gene segments, while at later stages the combinatorial pairing of the different possible combinations of heavy- and light-chain V regions forming the binding site of the immunoglobulin molecules increases further the repertoire's diversity. The variable antibody repertoire generated through these events is able to recognize both an enormous number of foreign antigens and the majority of the organism's self-tissues molecules.

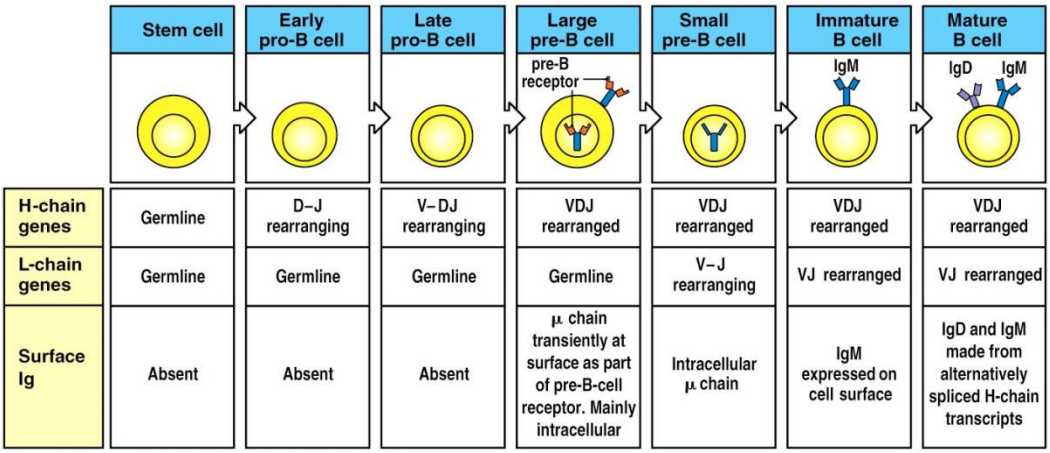

Figure 2_Maturation stages of B cell development in the bone marrow (From "The immune System" 3ed, Garland Science 2009).

1.3. Variations in the IG germline repertoire

Genes encoding for the Immunoglobulins (IG) are located at three primary loci in the human genome and specifically: IGH at 14q32.33, IGK at 2p11.2 and IGL 22q11.2 (Lefranc M-P, 2001). Each locus is composed by V, (D), J and C genes. The complete sequence of the human IGH locus has been reported for the first time by *Matsuda et al.* (Matsuda F, 1998) and comprised 44 functional/open reading frame (ORF) V genes, 85 pseudogenes, 27 D genes (whose 23 were functional) and 9 J genes (6 of which were functional). This full sequence was used by the international ImMunoGeneTics information system (IMGT) to determine the first official nomenclature of the IGH genes approved by the HUGO Nomenclature Committee (HGNC) in 1999. After this milestone and following sequencing of specific germline IGHV, IGHD and IGHJ genes and expressed IGHV gene repertoire, a comprehensive database of sequence variants has been created (IMGT).

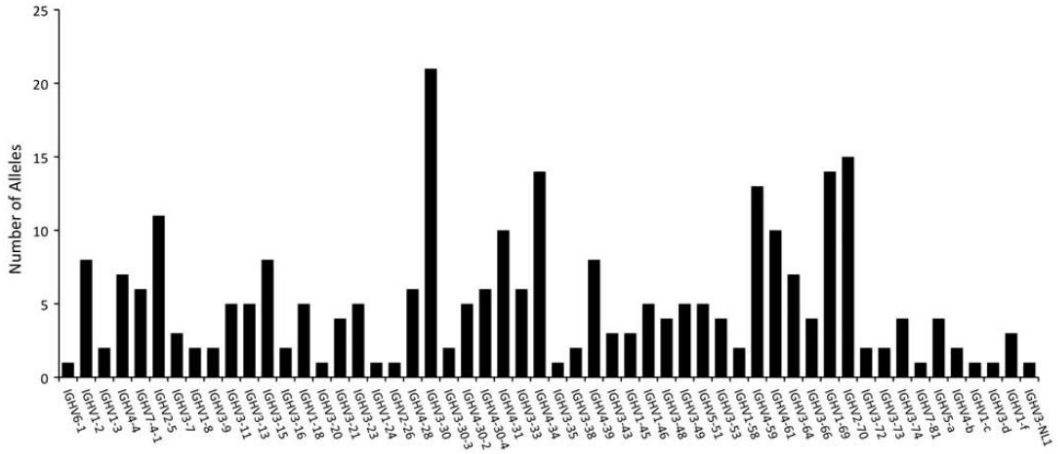

Figure 3_The number of known alleles for each of the mapped and unmapped IGHV genes (functional/ORF) (From Genes and Immunity 2012)

At least 55 functional/ORF IGHV genes are known and they are grouped in seven phylogenetically related subgroups (IGHV1 to IGHV7). The repertoire size of each of the seven subgroups is variable and ranges from 1 functional gene in subgroup IGHV6 to 24 genes in subgroup IGHV3. In this context further variability is generated by the difference observed in gene allelic richness among genes, even if knowledge about inter-allelic variations is still incomplete due to the paucity of studies investigating this aspect (Figure 3). Another aspect to take into account is the segmental duplication in the IGH locus, i.e. the presence of repetitive IGHV gene-containing segments occurring multiple times across the locus, which is thought to be responsible of the occurrence of large insertion/deletion variants in the region and of the Copy Number Variation (CNV) polymorphism in the IGH locus (Matsuda F, 1998).

1.4. Central and Pheripheral human B cell development

Ig can be produced as membrane bound receptors (i.e. the BCR), or secreted as antibodies during a humoral response. The N-terminal of each heavy and light chain is involved in antigen binding and the C-terminal determines the class of antibody and mediates effector functions (Kracker, 2004) (Figure 4). The two different C-terminal domains of the transmembrane and secreted forms of IgHC are encoded by separate exons of the heavy-chain constant regions (CH) gene: the membrane-coding (MC) sequence that encodes the transmembrane region and its cytoplasmic tail, and a secretion-coding (SC) sequence that encodes the carboxy terminus of the secreted form. The production of the two forms is the result of an alternative RNA processing of the initial transcript. Different CHs, which determine the class or isotype of the antibody and thus its effector functions, are encoded by separated genes at the HC locus. The five main isotypes of immunoglobulin are IgM, IgD, IgG, IgE, and IgA. In humans, IgG antibodies can be further subdivided into four subclasses (IgG1, IgG2, IgG3, and IgG4 according

to their abundance in serum), whereas IgA antibodies are found as two subclasses (IgA1 and IgA2). IgM forms pentamers in serum, which accounts for its high molecular weight. Secreted IgA can occur as either a monomer or as dimers.

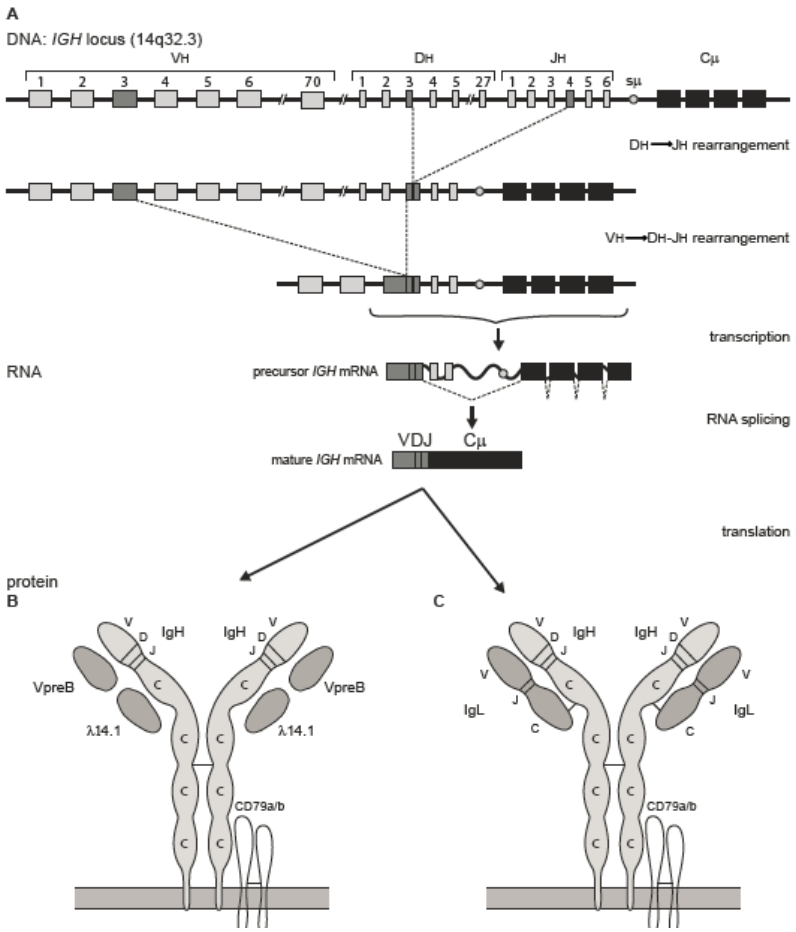

Figure 4_Schematic representation of IGH gene rearrangements

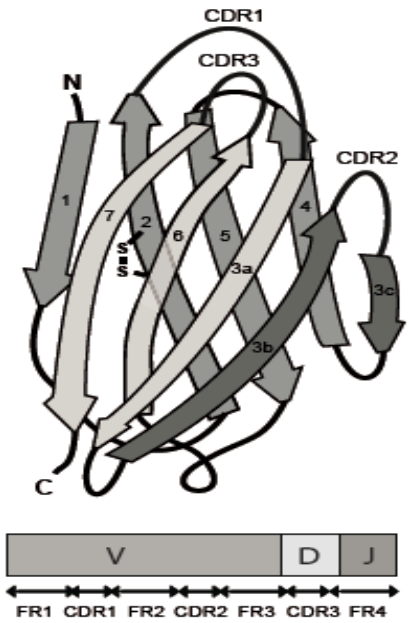

Figure 5_IgH variable domain structure.

Within the variable part of both heavy and light chains, three regions are key for antigen recognition. These are termed complementarity-determining region (CDR) 1, 2 and 3. The nucleotide sequence encoding the CDRs is particularly variable compared to the surrounding sequences which are termed framework regions. CDR1 and 2 are encoded within the V_H-gene segment. CDR3 comprises the entire joint region spanning from the conserved cysteine in the 3'-end of the V_H-gene to the conserved tryptophan in 5'-end of the J_H-gene. Framework residues, that represent about 85% of the V region, define the positioning of the CDRs so that the CDRs form three loops exposed on the surface of the chain and create a dock for antigen binding (Figure 5). The rearrangements of V(D)J gene segments take place at the late pro-B cell stage. They are rearranged together by the RAG1 and RAG2 enzymes, which recognize, bind and cleave specific recombination signalling sequences (RSS) flanking each V_H-, D- and J_H-gene segment (Max, 1979; Oettinger, 1990). The RSS is composed of a relatively conserved heptamer (5'-CACAGTG-3') separated from a conserved nonamer (5'-ACAAAAACC-3') by a non-conserved spacer region of either 12 or 23 nucleotides (Ramsden, 1994). Generally, a gene segment flanked by a 23-spacer RSS only joins with a gene segment flanked by a 12-spacer RSS. This is known as the 12/23 rule. On the IgH locus V_H- and J_H gene segments are flanked by 23-spacer RSS, while D-gene segments are flanked by 12- spacer RSS. This arrangement ensures that the gene segments are associated in the correct VHDJH configuration (Early, 1980). The first rearrangement occurs between a D- and a JH-gene segment, then a

VH gene segment rearranges to the DJH rearrangement. If the initial VHDJH-rearrangement is functional, further rearrangements on the other chromosome are inhibited. This mechanism, known as allelic exclusion, prevents each single B cell from expressing more than one type of BCR (Alt, 1984). When a VHDJH-rearrangement is transcribed it will pair with a surrogate light chain (SL), leading to the assembly of a pre-BCR that will be transported to the surface membrane of large pre-B cells (Min Zhang, 2004). Pre-BCR expression is the first vital checkpoint in B cell development and marks the transition from pro- to pre-B cell. Shortly after pre-BCRs have been exposed on the cell surface, several signalling cascades (Syk- and Akt-dependent) are activated modulating the expression of rag genes (U. Grawunder, 1995) and inhibiting further RAG-mediated rearrangement in the IgH gene locus. Signalling through the pre-BCR also stimulates cell proliferation, and differentiation to small post-mitotic pre-B cells that start rearranging the IgL chain genes. The variable part of the light chain is composed of a VL- and JL-gene segment. The VL-gene segments are flanked by 23-spacer RSSs and JL-gene segment by 12- spacer RSSs. If the VLJL-rearrangement is translatable, it will replace the surrogate IgL chain in the pre-PCR. This step constitutes the second checkpoint in early B cell development and marks the transition from pre-B cell to immature B cell.

Before leaving the bone marrow, immature B cells are also tested for self-tolerance: immature B cells whose BCRs bind with high affinity to the 'housekeeping' molecules expressed in the bone marrow cells (and thus are potentially autoreactive) receive an intracellular signal to halt their development; those B cells that do not recognize such molecules leave the bone marrow as naïve B cells reaching the peripheral blood and secondary lymphoid tissues. Naïve B cells recirculating in the blood and co-expressing surface bound Immunoglobulin M (IgM) and D (IgD) BCRs are susceptible to face different fates based on the nature of the antigen they encounter. In fact, the exposure to eliciting agents

typically results in an immune response that kills, clears, or neutralizes the invader. The ability of the immune system to respond more rapidly and effectively to antigens encountered previously, also referred as immunological memory, reflects the presence of clonally expanded populations of antigen-specific B and T lymphocytes. Memory immune responses are generally different from primary responses in terms of quality and kinetics. In fact, in secondary immune responses antibodies are produced faster and have a higher affinity for the antigen in respect to previous response. Thus immune memory resides both in the antibody that continues to be made and in the B cells and T cells that can rapidly interact to reproduce successful responses.

It is well established that the affinity maturation of the antibody repertoire and the isotype switch is associated with T cell-dependent antibody responses (TD), which strongly rely on the cognate guidance of T follicular helper cells (T_{FH} cells) and other accessory cells following initial priming and secondary challenge with antigen. During TD responses B cell differentiation occurs through two different pathways. The initial priming of naive B cells and subsequent cognate contact with T_{FH} cells initiates immunoglobulin class switching that results in the rapid differentiation of some B cells into Antibody Secreting Cells, also called short-lived Plasma cells, outside the B cell follicles of the secondary lymphoid organs. The initial B cell–T cell contact is also required to induce the formation of specialized areas of the secondary lymphoid organs, called Germinal Centers (GCs) (IC., 1994). GCs are the unique documented sites for coupling the diversification of BCR V gene sequences, with the selective expansion of those variants with improved binding affinity for antigen. In GCs, B cells activated by antigen-recognition start to proliferate rapidly and switch on a tightly regulated nuclear machinery leading to the generation of a multitude of clones carrying modified immunoglobulin BCRs (Figure 6). In this context the Activation-induced cytidine deaminase (AID) enzyme plays a central role (Muramatsu M, 2000) (Storb U,

2002); by deaminating deoxycytidine residues on DNA, AID paves the way to the introduction of point mutations, deletions and duplications in the germ-line sequence of the V,D,J gene segments encoding for the variable region of Immunoglobulins (IgV). Since Immunoglobulins bind to antigens through their IgV domains, this process, named Somatic HyperMutation (SHM), modulate, and might eventually re-shape, the specificity and overall binding affinity of the individuals' repertoire of B cells and secreted antibodies. In addition, AID activity is also involved in the initiation of the gene-re-arrangements required to switch the immunoglobulin constant region to a different class (IgG, IgA or IgE) best mediating specific immune responses (e.g. complement activation, opsonophacytosis, etc.).

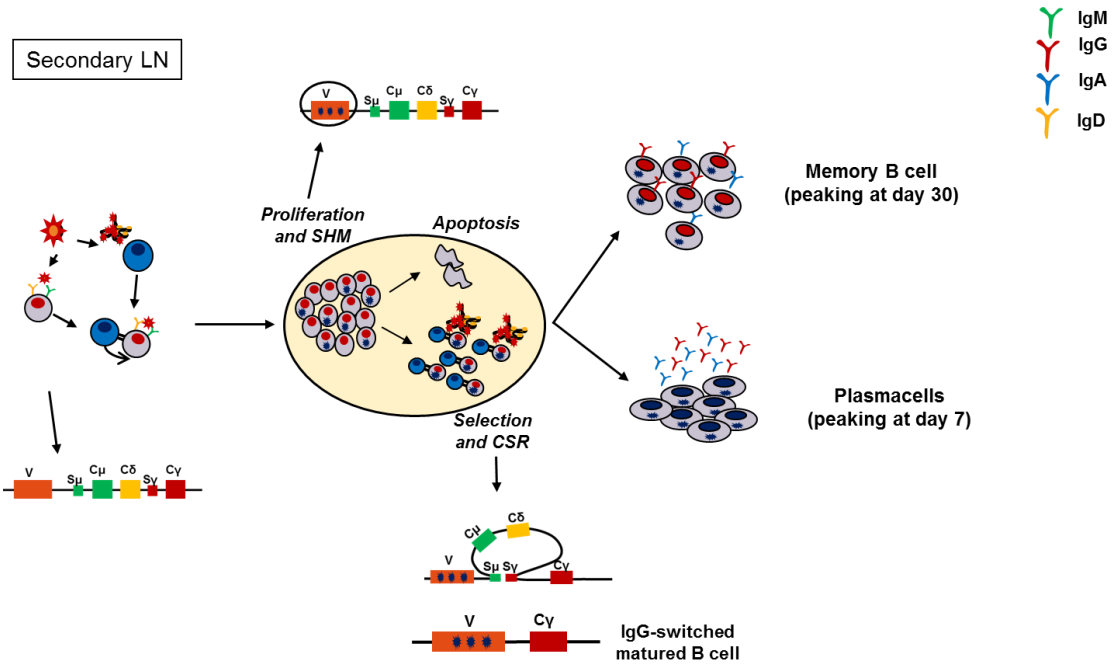

Figure 6_ T cell-dependent activation of B cells leads to the formation of GC in secondary lymphoid organs. Inside the GC, BCR is modified by Somatic HyperMutation and Class Switching. Both these events drive the differentiation of activated B cells into plasma cells or memory B cells in humans

Inside the GC proliferating B cells compete for antigen binding and access to survival signals delivered by T cells. Ultimately, this race ends with the survival of the clones that having acquired improved antigen-binding capacity will out-compete the others, which instead will die by neglect. While clonally expanded B cells are generated and selected, some of them differentiate into plasma cells that secrete antibodies whilst others will rest and become memory B cells that recirculate in the blood and will rapidly respond to subsequent antigenic re-stimulation. Ag-specific PBs and MBCs start to populate the human blood after infection or vaccination in different timeslots and with different kinetics. PBs, representing the early component of host defence, peak in the blood around day 8 after vaccination and return quickly to undetectable levels thereafter. Otherwise, Ag-specific MBCs circulate at enriched frequency in the blood peaking at 1 month after vaccination, and contracting slightly above or equal to baseline thereafter. Even if it is still controversial, there are several emerging evidences that Ag-specific PBs and MBCs undergo affinity maturation also without GC formation in extra-follicular pathways. It seems that of the B cells remaining in the outer follicle in the early stages of the B cell response, some migrate out and establish the foci of short lived Plasma cells, whereas others may be the B cells that are the origin of GC-independent memory (Tarlinton, 2012; David Tarlinton, 2013).

1.5. Diversity of B-cell memory

A substantial fraction of B cells in humans has encountered antigen and shows hallmarks of B-cell memory. One of these memory B cell hallmark is considered the expression of CD27 (Agematsu K, 1997), but recent studies have demonstrated that also CD27- cells can present with an activated phenotype and molecular signs of antigen experience (Fecteau JF, 2006; Cagigi A, 2009), suggesting that they could be memory cells. The majority of circulating memory B cells in healthy

adults is derived from GC dependent reactions. The earliest GC responses generate IgM+ cells. It has been demonstrated that these cells can undergo subsequent class switching, mostly to IgG, and clonally related IgM+ and IgG+ cells can be found in human GCs and blood (Seifert M, 2009). IgA+ and IgG+ GC-derived memory B cells occur later in the course of an immune response and carry high loads of SHM.

Terminal differentiation and survival of plasma cells

Plasma cells are derived from activated B cells through a different transcriptional program than memory B cells. Since plasma cells progressively loose membrane BCR expression while maturing, they depend on other mechanisms for survival. While most plasma cells are generated in lymphoid organs and long-lived plasma cells reside in bone marrow (Rozanski CH, 2011), small numbers can be found circulating in blood of healthy adults and the latter ones have high CD38, CD27 expression levels. Despite their low numbers in blood (1-5 cells/μl), plasma cells display large phenotypic heterogeneity. Interestingly, circulating IgA+ plasma cells are more frequent than IgM+ or IgG+. These IgA+ plasma cells display characteristics suggestive of a mucosal origin.

1.6. Tools to dissect the human BCR repertoire

Since the acquired immunity generates highly specific and long-lived antibody response, there is a growing interest in set up methodologies that can dissect this aspect of immune memory. It is clear that the specificity of the antibody responses for particular pathogens is achieved by the development of a vast diverse repertoire resulted by the recombination of the V-genes that finally enable antibodies recognizing an enormous numbers of potential epitopes.

To summarize, after this brief excursus on the B cell development, five are the principal mechanisms that mediate the diversity in the antigen combining site of the BCR repertoire; the first three mechanisms acting at immature B cell level whereas the last two after B cell activation:

1. Combinatorial diversity generated by V(D)J recombination,
2. Junctional diversity at the recombination sites of the V(D)J genes,
3. Random pairing of heavy and light chains to form the antigen binding site (Figure 7A);
4. Somatic hypermutation that introduces point mutation into the variable domain,
5. Class switch recombination that enables to change the isotypes and thus to determine a different effector function (Figure 7B).

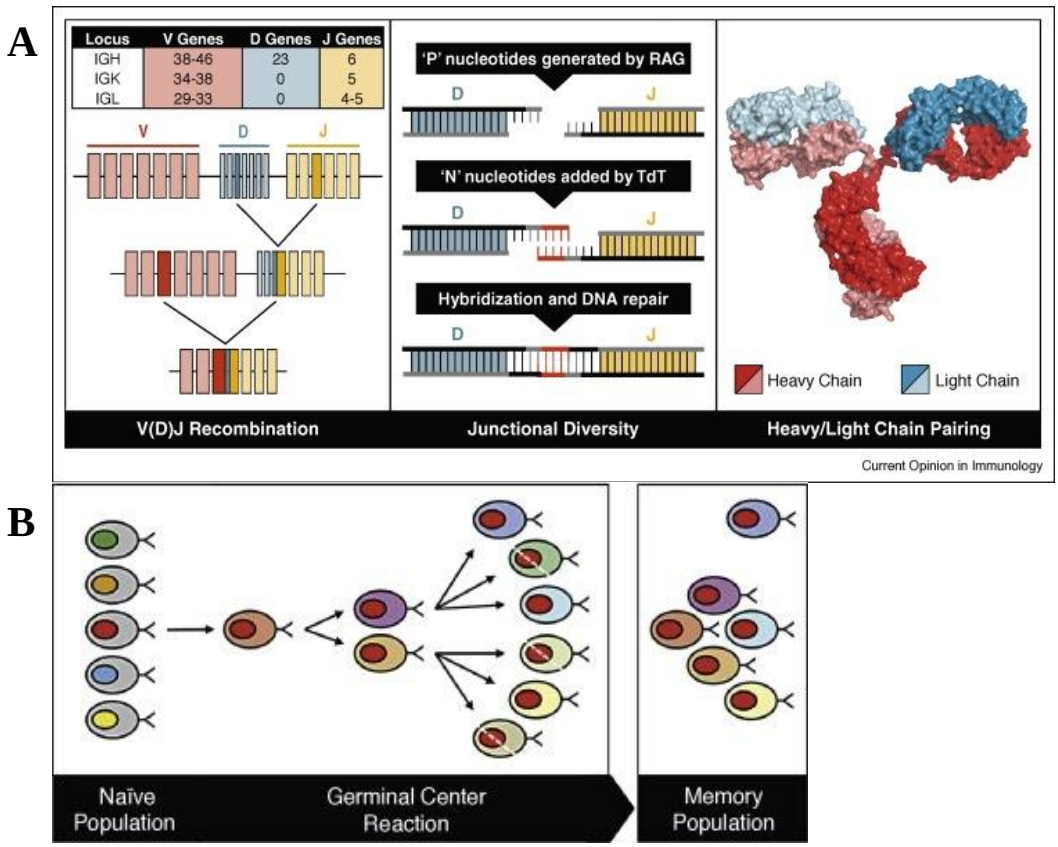

Figure 7_Mechanisms that mediate the diversity in the antigen combining site of the BCR repertoire. **A)** V(D)J recombination, Juntional diversity and VH/VL pairing; **B)** Generation of different variants by SHM and CSR after GC reaction (from Current opinion in Immunology, 2013)

Due to the importance of gaining insights on the BCR nature, different progresses have been done to dissect the Ab repertoire. The earliest studies were performed by using isoelectric focusing of Antibodies on polyacrylamide gel resolving the Abs into pattern of bands based on their isoelectric pH values (al, 1968). From this study, different steps forward have been done especially with the use of PCR, electrophoresis and sequencing methods for determining the exact nucleotide sequences that encode for specific antibodies (al, 1978). These studies paved the way to a huge number of studies addressing the study of the repertoire and making use of this information to produce human monoclonal antibodies with a defined specificity. Three are the main strategies used to dissect the repertoire that have also been used to produce human monoclonal antibodies:

1. Phage display technologies_ Phage display libraries have been constructed from IgV of vaccinated or infected subjects by sorting memory B cells and total peripheral blood mononuclear cell (PBMCs) populations containing all B cell subsets. Once B cells are isolated a random RT-PCR of VH and VL follows creating a combinatorial library of random VH and VL that can be expressed as single-chain variable antibody fragments (scFvs) on phage or antigen-binding fragments (Fabs) on yeast or mammalian cells (Figure 8). In this way a multitude of monoclonal antibodies with different specificities can be obtained and in fact this strategy has been used to isolate neutralizing antibodies specific for different numbers of pathogens such as West Nile virus, rabies virus, severe acute respiratory syndrome (SARS) virus, hepatitis A virus, HIV, hantavirus, Ebola virus, yellow fever virus, hepatitis C virus, measles virus and human and avian influenza virus strains, and so on. Even if this methodology has been an high-throughput way to produce antibodies, this is not the best way to obtain information about faithful representation of the physiological antibody gene pairs due to

the random pairing of immunoglobulin heavy and light chain variable regions that are cloned separately. Even if this random pairing enables to create a greater diversity of antibodies and it is a helpful strategy to generate higher affinity antibodies, it is not possible to obtain information about the process of affinity maturation that a given heavy and light chain pair went through.

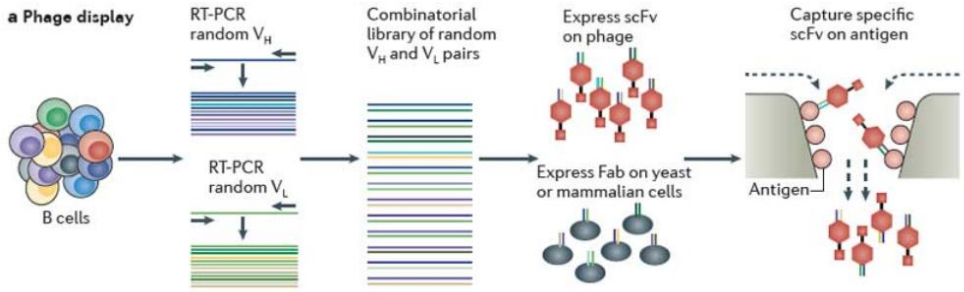

Figure 8_Scheme of the different steps to generate phage display libraries (from Nature Reviews Immunology, 2012)

2. B cell immortalization_ this methodology generally involves culturing total PBMCs or sorted IgG+ memory B cells from fresh or frozen samples in the presence of the Epstain Barr Virus (EBV), that can transform all pheripheral resting B cells subsets, together with Toll Like Receptor 9 (TLR9) and/or allogeneic irradiated mononuclear cells to provide co-stimulatory signals. Under these conditions, B cells are induced to proliferate and to secrete antibodies. After several days, supernatants from cultured cells are tested for antigen binding and/or functional activity. The B cells producing the antibodies of interest are cloned by limiting dilution and further screened for the desired reactivity at the single-cell level before individual VH and VL are cloned and sequenced (Traggiai, 2012) (Figure 9). By applying this

strategy the EBV-transformed B cell clones obtained can also be fused with myeloma cells to generate hybridomas, which facilitate the stable production of high levels of antibodies. This approach offers the opportunity to immortalize and obtain information about the antibodies produced from the pool of the antigen specific memory B cells.

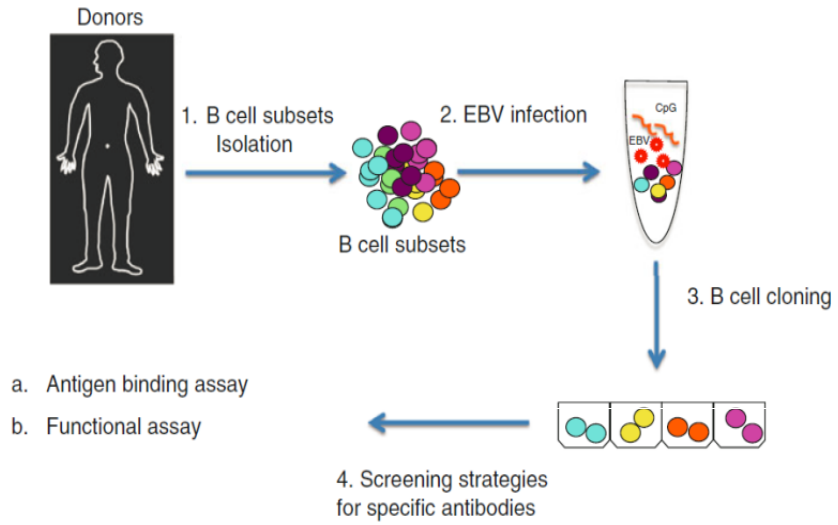

Figure 9_Scheme of the different steps required for human B cell immortalization (form Methods in Molecular Biology, 2012)

3. Single cell analysis of BCR repertoire_ An important advance in the study of the human BCR repertoire is represented by the single-cell reverse transcription PCR (RT-PCR) to isolate and amplify the cognate VH and VL genes from single B cells sorted by FACS (Thomas Tiller, 2008; Hua-Xin Liao, 2009) (Figure 10). This kind of approach enables to take a snapshot of the exact repertoire of the BCR expressed on the surface of particular B cells in a defined time slot. By using this approach information can be obtained also from rare, highly discrete B

cell subpopulations, such as MBCs, if those cells can be identified by FACS. This approach was firstly applied by Wardemann et al. to understand the tolerogenic selection of developing human B cell subpopulations. Thereafter, this strategy has been applied to investigate the different type and class of B cells in healthy, or immunocompromised individuals, or to study the repertoire of PBs and MBCs elicited by vaccination. There are a lot of studies focused on the repertoire of PBs isolated 7 days after vaccination because they are the first and robust source of antigen specific B cells and also because their identification by FACS basically relies upon the expression of Cluster of Differentiation (CD) surface markers. Moreover, since the time of antigen exposure is well defined, their dissection is particularly useful for examining the ongoing immune response to vaccines. For example, this method has been successful for analyzing the immune response to influenza, tetanus and anthrax vaccination. To a lesser extent also the repertoire of antigen-specific MBCs has been dissected. However the paucity of studies on this direction is ascribed to the lack of suitable tools for the identification of antigen specific Memory B cells, which circulate at very low frequencies in the blood as well as to the low efficiency in the recovery of VH and VL genes after RT-PCR. The identification of Ag-specific B cells has been so far challenging but several efforts have been done to solve this issue and one solution came from our laboratory (Bardelli M, 2013). All these studies basically rely on the use of fluorescent antigen baits or antigen tetramers to identify memory B cells engaged into BCR-specific interactions. Brightly labelled memory B cells are identified and isolated as single cells on a 96-well plate containing a lysis buffer that preserve mRNA. Thereafter, IgVH and VL genes are retro-transcribed and amplified by nested PCR .

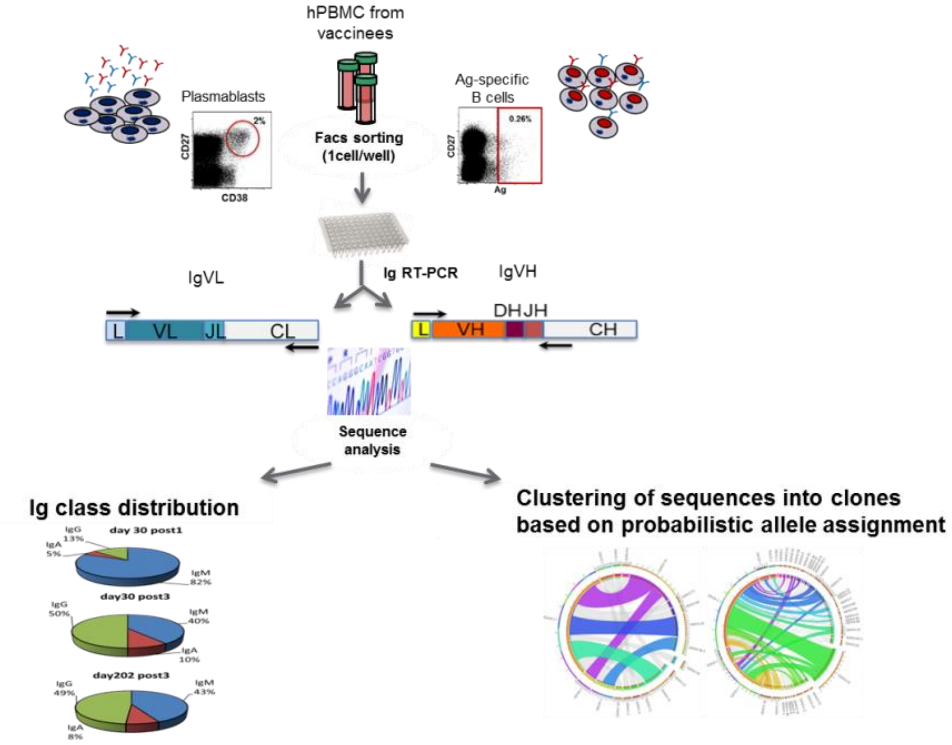

Figure 10_Schematic representation of scPCR approach to dissect changes in the repertoire of PBs and Ag-specific MBCs

Finally, various high-throughput technologies are emerging to generate a more comprehensive picture of the human B cell response. One promising approach is the use of next-generation sequencing to exhaustively sequence the entire B cell repertoire. The application of high throughput sequencing of paired VH and VL sequences to different B cell subsets isolated overtime following vaccination could be key to understand the specificity, the frequency and also the class of memory cells required to mediate protection, as well as the individual variability in the breadth of the response. Moreover, this analysis could be helpful in discriminating useless versus harming responses and thus to design better vaccine antigens able to stimulate and guide successful immune memory responses.

2.1. Classification of influenza viruses

Influenza viruses are members of the Orthomyxoviridae family (R.A. Lamb, 2001) and are basically classified into three subtypes: A, B and C. The principal differences between the three subgroups are based on the number of the segments present in the genome and thus on the antigenic features of their internal proteins, nucleoprotein and matrix. Influenza A and C viruses infect multiple species, while influenza B almost exclusively infects humans. Influenza A and B viruses are responsible of most of the cases of human disease and cause annual epidemics. They are antigenically distinct and do not exhibit cross-immunity or gene recombination. Influenza A viruses are essentially avian viruses that occasionally infect other species including humans. Avian infection is usually asymptomatic, and viruses replicate in the intestine of aquatic birds, creating that constitute a large reservoir of potential pandemic viruses.

The eight, negative-sense, RNA segments of the influenza virus genome encode 11 different proteins, of which 8 are packaged into the infectious, enveloped, virion. On the viral surface are the two main antigenic determinants of the virus, the spike glycoproteins: hemagglutinin (HA) and neuraminidase (NA). HA mediates viral entry into cells and has receptor binding and membrane fusion activity. NA mediates enzymatic cleavage of the viral receptor at late stages of infection, allowing for the release of progeny virions (A., 1957). A third integral membrane protein, M2, is a multi-functional, proton-selective, ion channel which has roles both in virus entry as well as in assembly and budding. Inside the viral envelope, the matrix protein (M1) provides structure to the virion and bridges interactions between the viral lipid membrane and the ribonucleoprotein (RNP) core. The RNP core is composed by the RNA polymerase complex proteins, PB1, PB2 and PA, and the nucleocapsid protein (NP) which mediates binding and packaging of the viral genome. During virus replication three other proteins are expressed that are not incorporated into the mature virion. Non-structural protein 1 (NS1) is a multi-

functional protein with a major role in evasion of the host immune system. NS2 (NEP) plays a crucial role in mediating the export of viral RNPs from the cell nucleus during replication (García-Sastre, 2011) (Figure 11).

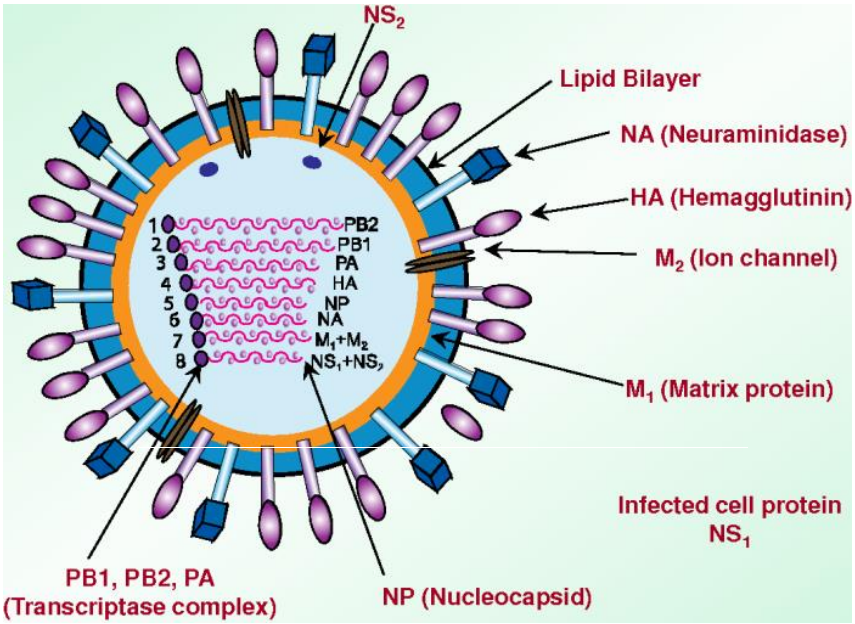

Figure 11_Schematic structure of the Influenza A virus and genomic organization

Influenza A viruses are grouped in subtyped based on sequence and antigenic of HA and NA. Up to now, 16 different HA and 9 NA have been described, most of which circulating in the avian reservoir. So far, cases of human infection resulting in annual epidemics have been attributed only to viruses carrying H1, H2,H3 and N1 or N2. When a virus strain with a new HA or NA subtype appears in the human population by genetic reassortment, it usually causes a pandemic because there is no preexisting immunity against the new virus. This was the case for example of the three pandemics that occurred during the last century (1918, 1957, and 1968) and also for the first pandemic of the 21st century, caused by the currently

circulating A (H1N1) 2009 virus, which was generated by gene reassortment between a virus present in pigs of North America and a virus that circulates in the swine population of Euroasia.

2.2. Virus replication cycle

The exact mechanism for fusion of virus and cell is well established and a strong contribution to this type of knowledge has been given by crystallographic analysis.
During the first steps of infection both HA and NA have crucial roles in mediating binding of the virus to the cell surface and release of the newly-formed viral particles, respectively.
HA owns its name to its capacity of causing agglutination of red blood cells *in vitro* and this peculiar characteristic is conferred by the capability of the glycoprotein to bind sialic acid residues exposed on cell surface. In most viral strains it is present as native un-cleaved form, also called HA0 monomer. Each HA monomer presents a host receptor binding site that allows the virus to recognize terminal sialic acid moieties on glycolipids and glycoproteins on the surface of host cells. Since there are many copies of HA on each influenza virus particle, the attachment of influenza virus on the host cell surface is multivalent and has high avidity despite low affinity. The specificity and the affinity of the viral HA for its receptor is a crucial characteristic of host transmission. Cleavage of the HA0 protein is mediated by host-produced trypsin-like proteases and produces two subunits: HA1 and HA2. The mature form of HA on infective viral particles is a homotrimeric structure where each HA molecule consists of a globular 'head' domain, made up exclusively by HA1, and a fibrous stem composed by the entire HA2 and part of HA1 that is inserted into the viral membrane. The HA C-terminal cytoplasmic tail interacts directly with the matrix protein layer immediately underneath the membrane envelope.

It is through the binding of HA to sialic acid residues that viral and host membranes fuse and thus the infective process starts by internalization of the virion inside the host cell through classical receptor mediated endocytosis in clathrin-coated vesicles. During the endocytosis process, the M2 protein allows for the influx of protons leading to an acidic environment (Matlin KS, 1981). The acidification of endosomes is critical for the next step of the replication cycle of the virus for two reasons:

6. It provokes a conformational change in the HA favoring the fusion of the viral and cellular membranes and this allows the virus to enter the cell cytoplasm
7. It promotes the uncoating of the virus and allows the RNPs to dissociate from the viral particle, such that they are released into the cytoplasm and transported to the cell nucleus.

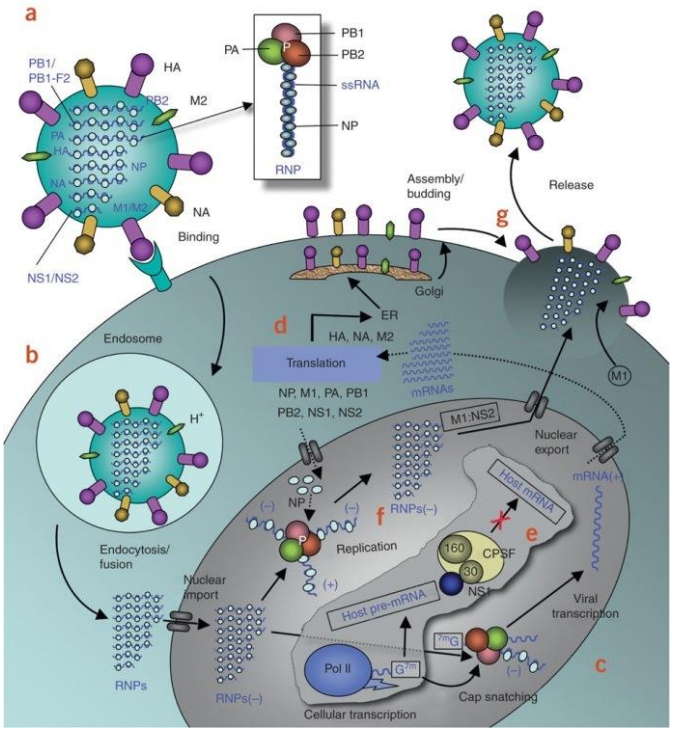

Figure 12_Entry and replication pathway of influenza virus (from Nature Structural & Molecular Biology,2010)

Once in the nucleus of infected cells, the viralRNA-dependent RNA polymerase transcribes and replicates the negative sense vRNA. The positive RNA strand obtained is used as a template for the synthesis of new virion genome and for mRNA transcription and viral protein translation (Cros JF, 2003). All mRNA molecules are then transported back to the cytoplasm by the viral proteins NEP and M1 and once in the cytoplasm they are translated by the host cell machinery. The surface proteins HA, M2 and NA are synthesized in the endoplasmic reticulum (ER), glycosylated in the Golgi apparatus and finally transported to the cell membrane for virion assembly. The progeny virions assemble and bud at the plasma membrane (Figure 12).

The new progeny of virions remain initially bound to outside membrane sialic acid residues because of their interactions with HA spikes until NA sialidase activity remove them from cellular and viral glycoconjugates. For its peculiar activity, NA has also a role in preventing the aggregation of the new virions as well as in mediating their release. Once released from host cells the new virions can infect nearby cells and spread the infection.

2.3. Viral tropism and antigenic variation

Influenza A viruses circulate in a wide variety of animals, most of which are only transiently infected. The largest variety of influenza A viruses circulate in birds. Besides birds, additional animal reservoirs of influenza A viruses are found in mammalian species such as swine and horses.

The major determinants of the tropism of influenza viruses are the sialic acid molecoles because of their initial interaction with HA to start infection. Sialic acid residues are nine-carbon monosaccharides present in variable amounts on the surface of different cell types, usually bound to galactose through α2,3 or α2,6 linkages. HA from different viruses show a preferential binding avidity for the type of sialic acid linkage. Thus, viruses that infect humans bind preferentially to SA

with α2,6 linkages, whereas avian viruses bind mostly to SA in an α2,3 configuration (Ito T, 1998; Ito T, 2000; Ito T, 1997). The human tracheal epithelial tissue preferentially express SA with a2,6 linkages, whereas avian epithelial gastrointestinal tissue (where influenza viruses replicate in avian hosts) contain mainly SA in an a2,3 configuration. Of relevance, pig tracheal tissue has both kinds of SA linkages, and swine can thus be infected with viruses that recognize both types of receptors, hence, these animals have often been proposed as a mixing vessel for the generation of new strains from co-infections of avian and mammalian viruses.

It is noteworthy that Influenza A viruses evolve constantly using different mechanisms. Three are the best known mechanisms able to generate further variability in influenza A viruses. The most important is the lack of proofreading activity of the viral RNA polymerase during replication of the influenza genomic RNA segments, which results in a high level of point mutations, phenomenon that is also known as antigenic drift. The permanent antigenic drift in the principal targets of the immunological response, the proteins HA and NA, is the cause of the constant need to review the viruses that are included in the yearly prepared vaccines. The antigenic drift that has occurred in influenza A viruses for thousands of years has led to the current diversity of HA and NA subtypes. The second mechanism, known as antigenic shift, relies in the segmented nature of viral genome. This peculiar characteristic permits the formation of new progeny viruses with novel combination of segments when two or more different virus subtypes infect a single cell. This process is capable of introducing new proteins in circulating viral populations that can drastically change the biological properties of the virus. Antigenic shift is commonly associated with appearance of pandemic influenza viruses. A third mechanism associated with evolution of influenza A viruses is recombination by template switching. This type of recombination may involve genetic material either from more than one origin or two different

viralRNAsegments, and these nonhomologous recombination events could be associated with changes in viral pathogenicity.

3.1. Neisseria meningitidis

Neisseria meningitidis is a gram negative, encapsulated bacterium, which is generally a commensal that colonizes the mucosal epithelium of the nasopharynx of the human population. Colonizing strains can belong either to hypervirulent lineages which are generally associated with disease, or to carriage strains that provides a reservoir for meningococcal infection and can also contribute to establish host immunity (DS, 2009). For still unknown reasons, the carriage strains can invade the pharyngeal mucosal epithelium and, in the absence of bactericidal serum activity, disseminate into the bloodstream, causing septicaemia. In a subset of cases, bacteria can also cross the blood-brain barrier and infect the cerebrospinal fluid, causing meningitis.

With the exception of sporadic case reports, all known disease-causing meningococcal strains are surrounded by a capsule made up by complex polysaccharides, which confers resistance to phagocytosis and complement-mediated lysis. Even if the capsular polysaccharide (CPS) inhibits bacterial adhesion because it masks the action of meningococcal adhesins, it is known to be crucial for bacterial to survive in the blood.

Based on the immunogenicity and chemical structure of the CPS, *N. meningitidis* (*Nm*) can be classified into at least 13 serogroups A, B, C, E-29, H, I, K, L, W-135, X, Y, Z, and 29E (SE, 1953). Among them, only six serogroups (A, B, C, W-135, X, Y) have been associated with meninogococcal disease and are thus considered pathogenic. Further classification into serosubtype, serotype and immunotype is based on class 1 outer membrane proteins (PorA), class 2 or 3 (PorB) outer membrane proteins and lipopoly[oligo]saccharide structure, respectively (Rosenstein NE, 2001; Stephens DS, 2007)

3.2. Colonization and carriage

The first step known to establish carriage and invasive meningococcal disease is the colonization of the upper respiratory mucosal tract by *Nm*. The bacterium can be acquired through inhalation of respiratory droplets and secretions.

This acquisition can be either asymptomatic, or (infrequently) give rise to a local inflammation, invasion of mucosal surfaces, access to the bloodstream and fulminant sepsis, or focal infections such as meningitis (Stephens DS, 2007). Meningococcal disease usually occurs 1–14 days after acquisition of the pathogen.

Acquisition may also result in upper respiratory and pharyngeal meningococcal carriage. The duration of carriage can vary from days to months. The probability of meningococcal disease after the acquisition of *Nm* declines very sharply, such that invasive disease becomes unlikely 10–14 days after acquisition.

3.3. Meningococcal adhesion and cell invasion

The adhesion to the respiratory epithelium is essential for *Nm* survival, colonization and transmission, and is also a prerequisite for invasive meningococcal disease. Upon contact with human cells, the meningococci forms microcolonies and adheres using pili. *Nm* has evolved numerous surface-exposed adhesive structures that facilitate interactions with human cells. Bacterial host-specificity resides in the structural specificity of the meningococcal ligands for human molecules, which can range from nutrients, to serum/secreted proteins and surface-located adhesion receptors. Mechanisms of meningococcal adhesion are multifactorial, dynamic and display temporal changes during the course of infection. After the initial colonization, there is a loss or down-regulation of the capsule, which sterically masks the outer membrane proteins. This event is key to unmask adhesins that serve to mediate subsequent adhesion to the human epithelium. Antigenic and phase variation of meningococcal outer membrane proteins (OMPs) also play an

important role, and the presence of multiple adhesins compensates for phase variation and may lead to an altered tissue tropism. Close adherence of meningococci to the host epithelial cells results in the appearance of cortical plaques and the recruitment of factors leading to the formation and extension of epithelial cell pseudopodia that engulf the bacteria (DS, 2009). This intracellular lifestyle can give the bacteria the opportunity to evade host immune response, finding more available nutrients, and eventually, to further cross the epithelium entering the blood stream (DS, 2009). Intracellular meningococci reside inside membranous vacuoles and are capable of translocating through basolateral epithelial tissues by transcytosis within 18-40 hours. Within the cells, meningococcus has to express again the capsule, which can prevent antibody and complement deposition (M., 1995), is anti-opsonic and anti-phagocytic and therefore aids survival in blood (M., 2009). Once in the bloodstream, meningococci may multiply rapidly to high numbers and eventually translocate across the blood-brain barrier, proliferate in the central nervous system and cause meningitis. These later steps in invasion are still poorly understood. The ability to cause invasive disease is influenced by a multiplicity of environmental and microbial factors, as well as from the absence of host's protective antibodies.

3.4. Anti-meningococcal vaccines

Several meningococcal vaccines are available against the distinct serogroups. Vaccines against meningococcal serogroups A and C have been developed and tested in clinical trials (Costantino P, 1992) (Anderson EL, 1994); (Fairley CK, 1996). The first trials conducted in the United Kingdom with the meningococcus C conjugate showed a dramatic decline in the incidence of serogroup C disease in all age groups ((Borrow R, 2000) (Miller E, 2001) with an efficacy of 97 and 92 per cent for teenagers and toddlers, respectively. Conjugate vaccines against

meningococcus are now available as monovalent (A or C) or as different tetravalent formulations (A, C, W-135 and Y).

The most critical target for vaccination is meningococcus B (MenB), which is responsible for 32 percent of all cases of meningococcal disease in the United States and for 45–80 percent of the cases in Europe. Conventional biochemical and microbiological approaches have been of little help in the development of a vaccine able to induce broad protection against menB. A polysaccharide-based vaccine approach could not be used for group B meningococcus, since the principal component of its CPS that is a polymer of *Æ*(2-8)-linked N-acetylneuranimic acid., which is also abundantly expressed in human tissues. Alternative approaches to develop MenB vaccines have focused on the use of surface-exposed proteins contained in outer membrane preparations (outer membrane vesicles, OMVs). The first OMV vaccines were developed in Norway and Cuba and showed efficacy in humans ranging from 50 to 80 per cent (al, 1999). However, while each vaccine was shown to induce good protection against the homologous strain, both failed to induce protection against heterologous strains (Rosenstein NE, 2001). The major protective antigen in both these vaccines is PorA, the most abundant outer membrane protein, which is known to be highly variable across different isolates of serogroup B *N. meningitidis*.

To overcome these limitations, a novel multicomponent recombinant protein-based vaccine, named 4CMenB or Bexsero®, has been recently developed by Novartis Vaccines and Diagnostics against group B meningococcal strains. Bexsero® is now approved in Europe and Australia.

4CMenB is based on antigens identified through an innovative genetic approach known as ‘reverse vaccinology’ and combines OMVs from the New-Zealand epidemic strain (NZ98/254) with three major protein antigens: factor H-binding protein (fHbp), Neisserial Heparin-Binding Antigen (NHBA) and Neisserial adhesin A (NadA) (Giuliani MM, 2006) (Figure 13). Two of these main antigens,

fHpb (sub-variant 1.1) and NHBA (peptide 2), are present as fusion proteins to two minor antigens, GNA2091 and GNA1030, respectively. Another vaccine against serogroup B, developed by Pfizer, has been approved in America and contains two alleles of the recombinant fHbp.

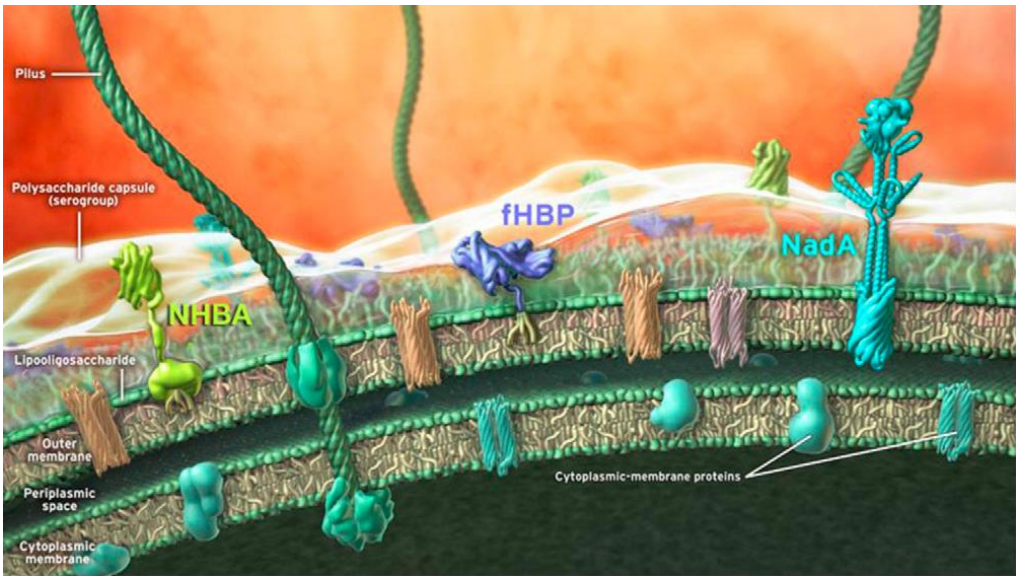

Figure 13_Schematic representation of the 4CMenB vaccine antigens on the surface of *N. meningitides*. The main antigens identified through reverse vaccinology approach (NHBA, fHbp and NadA) are depicted (from Vaccine, 2012).

3.5. Factor H binding protein (fHbp)

Factor H binding protein (fHbp or GNA1870) was the first discovered antigen effective in inducing bactericidal antibodies. It was identified by screening the genome of one of the most virulent strains: MC58. fHbp is known to bind specifically to human factor H (fH), an inhibitor of the alternative complement pathway. Since the evasion of the human complement system is key for *Nm* to cause the invasive disease, different studies have been addressed the role of fHbp

in host invasion and it has been shown that the its deletion results in increased susceptibility of most strains of *Nm* to killing in either serum or in whole blood.
The three-dimensional (3D) solution structure of fHbp has been resolved by nuclear magnetic resonance (NMR), by spectroscopy and by X-ray crystallography.

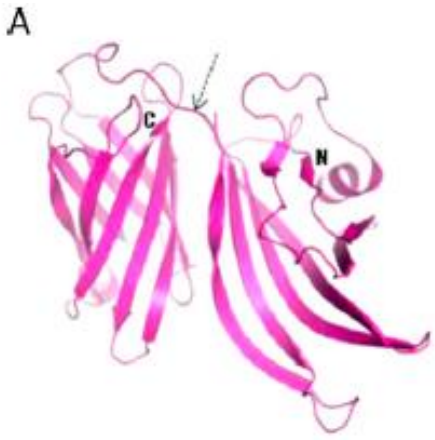

Figure 14_Structure of fHbp. The currently known structure of the fHbp formed by two beta-barrel domains (one domain N-terminal and the other C-terminal) connected by a short linker (from Vaccine, 2012)

These studies revealed that the protein is composed of two domains connected by a short linker: an N-terminal domain of 8 beta-strands, forming a highly curved anti-parallel beta-sheet, and a C-terminal domain that is a well-defined beta-barrel of 8 anti-parallel beta strands (Figure 14). Although fHbp is known to have ~300 sequence variants, multiple-sequence alignments show that the residues forming of the hydrophobic cores of both C- and N-terminal domain are well conserved predicting that the final 3D structure should be the same in all variants. The fHbp proteins can be classified into three genetic and immunogenic variants: fHbp-1, fHbp-2 and fHbp-3, which are not cross-protective, and can be further divided into subvariants. Among each variant, fHbp sequences are conserved across different strains (92 to 100%), while between the 1-3 variants sequence conservation is low (63%). This diversity has an important impact on the immunological features of fHbp, since members of each variant induce a strong protective immune response against meningococcal strains carrying homologous alleles but not against strains expressing distantly related variants (Masignani V, 2003).

References

1. A. Gottschalk Neuraminidase: the specific enzyme of influenza virus and Vibrio cholera. [Revue]. - 1957. - Vol. Biochemica et biophysica acta.
2. Agematsu K Nagumo H, Yang FC, et al. B cell subpopulations separated by CD27 and crucial collaboration of CD27+ B cells and helper T cells in immunoglobulin production. [Revue]. - 1997. - Vol. Eur J Immunol.
3. al Awdeh.Z.L. et Isoelectric focusing in polyacrilamide gel and its application to immunoglobulins [Revue]. - 1968. - Vol. Proc.Natl.Acad.Sci. U.S.A.
4. al Seidman J.G. et Multiple related Immunoglobulin Variable-region genes identified by cloning and sequence analysis [Revue]. - 1978. - Vol. Proc.Natl.Acad.Sci. U.S.A.
5. al Tappero JW et Immunogenicity of 2 serogroup B outer-membrane protein meningococcal vaccines: a randomized controlled trial in Chile [Revue]. - 1999. - Vol. JAMA.
6. Alt F.W. et al. Ordered rearrangement of immunoglobulin heavy chain variable region segments. [Revue]. - 1984. - Vol. EMBO.
7. Amanna IJ1 Slifka MK, Crotty S. Immunity and immunological memory following smallpox vaccination. [Revue] // Immunol Rev. - 2006 Jun. - pp. 211:320-37..
8. Anderson AS Jansen KU, Eiden J New frontiers in meningococcal vaccines [Revue]. - 2011. - Vol. Expert Rev Vaccines .

9. Anderson EL Bowers T, Mink CM, Kennedy DJ, Belshe RB, Harakeh H, Pais L, Holder P, Carlone GM. Safety and immunogenicity of meningococcal A and C polysaccharide conjugate vaccine in adults. [Revue]. - 1994. - Vol. Infect Immun..

10. Blink EJ1 Light A, Kallies A, Nutt SL, Hodgkin PD, Tarlinton DM. Early appearance of germinal center-derived memory B cells and plasma cells in blood after primary immunization. [Revue] // J Exp Med.. - 2005 Feb 21. - pp. 201(4):545-54..

11. Borrow R Fox AJ, Richmond PC, Clark S, Sadler F, Findlow J, Morris R, Begg NT, Cartwright KA. Induction of immunological memory in UK infants by a meningococcal A/C conjugate vaccine. [Revue]. - 2000. - Vol. Epidemiol Infect..

12. Cagigi A Du L, Dang LV, et al. CD27(-) B-cells produce class switched and somatically hyper- mutated antibodies during chronic HIV-1 infection. [Revue]. - 2009. - Vol. PLoS One..

13. Costantino P Viti S, Podda A, Velmonte MA, Nencioni L, Rappuoli R. Development and phase 1 clinical testing of a conjugate vaccine against meningococcus A and C. [Revue]. - 1992. - Vol. Vaccine.

14. Cros JF Palese P. Trafficking of viral genomic RNA into and out of the nucleus: influenza, thogot and Borna disease virus [Revue]. - 2003. - Vol. Virus Res.

15. David Tarlinton Kim Good-Jacobson Diversity Among Memory B Cells: Origin, Consequences, and Utility [Revue]. - 2013. - Vol. Science .

16. DC Stephens Biology and pathogenesis of the evolutionarily successful, obligate human bacterium Neisseria meningitidis [Revue]. - 2009. - Vol. Vaccine.

17. DS Stephens Biology and pathogenesis of the evolutionarily successful, obligate human bacterium Neisseria meningitidis. [Revue]. - 2009. - Vol. Vaccine .

18. Early P., Huang,H., Davis,M.,Calame,K., & Hood,L. An immunoglobulin heavy chain variable region gene is generated from three segments of DNA: VH, D and JH [Revue]. - 1980. - Vol. Cell.

19. Fairley CK Begg N, Borrow R, Fox AJ, Jones DM, Cartwright K. Conjugate meningococcal serogroup A and C vaccine: reactogenicity and immunogenicity in United Kingdom infants. [Revue]. - 1996. - Vol. J Infect Dis..

20. Fecteau JF Cote G, Neron S. A new memory CD27-IgG+ B cell population in peripheral blood expressing VH genes with low frequency of somatic mutation. [Revue]. - 2006. - Vol. J Immunol. .

21. Fletcher LD Bernfield L, Barniak V, Farley JE, Howell A, Knauf M, et al. Vaccine potential of the Neisseria meningitidis 2086 lipoprotein [Revue]. - 2004. - Vol. Infect Immun.

22. García-Sastre Rafael A. Medina & Adolfo Influenza A viruses: new research developments [Revue]. - 2011. - Vol. Nature.

23. Giuliani MM Adu-Bobie J, Comanducci M, Aricò B, Savino S, Santini L, Brunelli B, Bambini S, Biolchi A, Capecchi B, Cartocci E, Ciucchi L, Di

Marcello F, Ferlicca F, Galli B, Luzzi E, Masignani V, Serruto D, Veggi D, Contorni M, Morandi M, Bartalesi et al A universal vaccine for serogroup B meningococcus [Revue]. - 2006. - Vol. Proc Natl Acad Sci USA.

24. Good-Jacobson David Tarlinton and Kim Diversity Among Memory B Cells: Origin, Consequences, and Utility [Revue]. - 2013 . - Vol. Nature.

25. Hammarlund E1 Lewis MW, Hansen SG, Strelow LI, Nelson JA, Sexton GJ, Hanifin JM, Slifka MK. Duration of antiviral immunity after smallpox vaccination [Revue] // Nat Med.. - 2003 Sep. - pp. 9(9):1131-7..

26. Hua-Xin Liao Marc C. Levesque, Ashleigh Nagel, Ashlyn Dixon,Ruijun Zhang, Emmanuel Walter, Robert Parks, John Whitesides, Dawn J. Marshall,Kwan-Ki Hwang, Yi Yang, Xi Chen, Feng Gao, Supriya Munshaw, Thomas B. Kepler, Thomas Denny, M. Anthony Moody,Haynes High-throughput isolation of immunoglobulin genes from single human B cells and expression as monoclonal antibodies [Revue]. - 2009. - Vol. J Virol Methods..

27. Ian J. Amanna Nichole E.Carlson and Mark K. Slifka Duration of Humoral Immunity to Common Viral and Vaccine Antigens [Revue] // N Engl J Med. - November 8, 2007. - pp. 357:1903-1915.

28. Ian J. Amanna Nichole E.Carlson, and Mark Slifka Duration of Humoral Immunity to Common Viral and Vaccine Antigens [Revue]. - 2007. - Vol. The New England Journal of Medicine.

29. Ian J.Amanna Mark K. Slifka, shane Crotty Immunity and immunological memory following smallpox vaccination [Revue]. - 2006. - Vol. Immunological reviews.

30. IC. MacLennan Germinal centers [Revue]. - 1994. - Vol. Annu Rev Immunol.

31. IMGT. The International ImMunoGeneTics information system: [Revue]. - http://www.imgt.org.

32. Ito T Couceiro JN, Kelm S, Baum LG, Krauss S, Castrucci MR, Donatelli I, Kida H, Paulson JC, Webster RG, Kawaoka Y. Molecular basis for the generation in pigs of influenza A viruses with pandemic potential. [Revue]. - 1998. - Vol. Journal of Virology.

33. Ito T Suzuki Y, Sazuki T, Takada A, Horimoto T, Wells K, Kida H, Otsuki K, Kiso M, Ishida H, Kawaoka Y. 2000. Recognition of N- - glycolylneuraminic acid linked to galactose by the alpha2,3 linkage is associated with intestinal replication of influenza A virus in ducks [Revue]. - 2000. - Vol. Journalof Virology.

34. Ito T Suzuki Y, Takada A, Kawamoto A, Otsuki K, Masada H, Suzuki T, Kida H, Kawaoka Y. Differences in sialic acid-galactose linkages in the chicken egg amnion and allantois influence human influenza virus receptor specificity and variant selection. [Revue]. - 1997. - Vol. Journal of Virology.

35. Kracker S. & Radbruch,A. Immunoglobulin class switching: in vitro induction and analysis [Revue]. - 2004. - Vol. Methods Mol. Biol.

36. Lefranc M-P Lefranc G. The Immunoglobulin FactsBook [Revue]. - 2001. - Vol. Academic Press London.

37. M. Achtman Epidemic spread and antigenic variability of Neisseria meningitidis. [Revue]. - 1995. - Vol. Trends Microbio.

38. M. Virji Pathogenic neisseriae: surface modulation, pathogenesis and infection control. [Revue]. - 2009. - Vol. Nat Rev Microbiol..

39. Mark K. Slifka Rustom Antia, Jason K. Whitmire and Rafi Ahmed humoral immunity due to Long-Lived Plasma Cells [Revue]. - 1998. - Vol. Immunity.

40. Masignani V Comanducci M, Giuliani MM, Bambini S, Adu-Bobie J, Arico B, et al Vaccination against Neisseria meningitidis using three variants of the lipoprotein GNA1870 [Revue]. - 2003. - Vol. J Exp Med.

41. Matlin KS Reggio H, Helenius A, Simons K. Infectious entry pathway of influenza virus in a canine kidney cell line. [Revue]. - 1981. - Vol. Journal of Cell Biology.

42. Matsuda F Ishii K, Bourvagnet P, Kuma K, Hayashida H, Miyata T et al. The complete nucleotide sequence of the human immunoglobulin heavy chain variable region locus. [Revue]. - 1998. - Vol. J Exp Med.

43. Max E.E., Seidman,J.G., & Leder,P. Sequences of five potential recombination sites encoded close to an immunoglobulin kappa constant region gene. [Revue]. - 1979. - Vol. Proc. Natl. Acad. Sci. U. S. A.

44. Miller E Salisbury D, Ramsay M. Planning, registration, and implementation of an immunisation campaign against meningococcal serogroup C disease in the UK: a success story. [Revue]. - 2001. - Vol. Vaccine.

45. Min Zhang Gopesh Srivastava and Liwei Lu The Pre-B Cell Receptor and Its Function during B Cell [Revue]. - 2004. - Vol. Cellular & Molecular Immunology.

46. Muramatsu M Kinoshita K, Fagarasan S, Yamada S, Shinkai Y, Honjo T. Class switch recombination and hypermutation require activation-induced cytidine deaminase (AID), a potential RNA editing enzyme [Revue]. - 2000. - Vol. Cell.

47. Oettinger M.A., Schatz,D.G., Gorka,C.,& Baltimore,D. RAG-1 and RAG-2, adjacent genes that synergistically activate V(D)J recombination [Revue]. - 1990. - Vol. Science.

48. R.A. Lamb R.M. Krug Orthomyxoviridae: the viruses and their replication [Revue]. - 2001. - Vol. FEBS letters.

49. Ramsden D.A., Baetz,K., & Wu,G.E. Conservation of sequence in recombination signal sequence spacers [Revue]. - 1994. - Vol. Nucleic Acids Res..

50. Rosenstein NE Fischer M, Tappero JW. Meningococcal vaccines. [Revue]. - 2001. - Vol. Infect Dis Clin North Am.

51. Rosenstein NE PERKINS BA, Stephens DS, POPOVIC T, Hughes JM Meningococcal Disease [Revue]. - 2001. - Vol. N Engl J Med.

52. Rozanski CH Arens R, Carlson LM, et al. Sustained antibody responses depend on CD28 function in bone marrow-resident plasma cells. [Revue]. - 2011. - Vol. J Exp Med..

53. S. Tonegawa Somatic generation of antibody diversity [Revue] // Nature. - 1983. - pp. 575-581.

54. SE Branham Serological relationships among meningococci [Revue]. - 1953. - Vol. Bacteriol Rev.

55. Seifert M Kuppers R. Molecular footprints of a germinal center derivation of human IgM+(IgD+)CD27+ B cells and the dynamics of memory B cell generation [Revue]. - 2009. - Vol. J Exp Med..

56. Slifka MK1 Antia R, Whitmire JK, Ahmed R. Humoral immunity due to long-lived plasma cells. [Revue] // Immunity. . - 1998 . - pp. 8(3):363-72..

57. Stephens DS Greenwood B, Brandtzaeg P Epidemic meningitis, meningococcaemia, and Neisseria meningitidis. [Revue]. - 2007. - Vol. Lancet.

58. Storb U Stavnezer J. Immunoglobulin genes: generating diversity with AID and UNG [Revue]. - 2002. - Vol. Curr Biol..

59. Tarlinton Kim L.Good-Jacobson and David M. Moultiple routes to B-cell memory [Revue]. - 2012. - Vol. International Immunology.

60. Thomas Tiller Eric Meffre, Sergey Yurasov, Makoto Tsuiji, Michel C. Nussenzweig and Hedda Wardemann Efficient generation of monoclonal antibodies from single human B cells by single cell RT-PCR and expression vector cloning [Revue]. - 2008. - Vol. J Immunol Methods.

61. Traggiai E1 Puzone R, Lanzavecchia A. Antigen dependent and independent mechanisms that sustain serum antibody levels. [Revue] // Vaccine. . - 2003 Jun 1. - pp. Suppl 2:S35-7..

62. Traggiai Elisabetta Immortalization of Human B cells: analysis of B cell Rertoire and Production of Human Monoclonal Antibodies [Revue]. - Vol. Methods in Mol Biol .

63. U. Grawunder T.M. Leu, D.G. Schatz, A. Werner, A.G. Rolink, F. Melchers, et al. Down-regulation of RAG1 and RAG2 gene expression in preB cells after functional immunoglobulin heavy chain rearrangement [Revue]. - 1995. - Vol. Immunity, 3 (5) .

Outline of the thesis

B cells are crucial components of adaptive immune responses. The way by which B cells interface and sense the external 'danger' is through their BCR. The initial heterogeneity of B cells created by the random rearrangement of V(D)J gene segments enables recognizing a multitude of foreign antigens. In the course of human life this vast repertoire of antibody is continuously re-shaped in order to generate a pool of diversified MBCs and PBs with different antigen specificities.

Different studies are underlying the importance of dissecting the BCR repertoire of different B cell subsets following vaccination to gain insights on the dynamics of the vaccine response and to predict vaccine safety. This approach could help in understanding the specificity, the frequency and also the class of memory cells required to mediate protection, as well as the individual variability in the breadth of the response. Moreover, this analysis could allow discriminating useless versus harming responses. An increased knowledge on B cells, and in particular on MBCs and PBs responding to a given vaccine antigen, could be key for designing more effective vaccines able to stimulate and guide the 'right' immune memory responses.

Due to the relevance of these types of studies, the principal objective of my PhD thesis was to investigate and follow the response of both MBCs and PBs over time after vaccination by sequencing the variable part of the Ig genes of single cells (through single cell PCR. scPCR of paired VH and VL) and by profiling the antibody repertoire changes

However, when I started my PhD there were different challenges in introducing this approach, mainly represented by the lack of tools to identify and isolate antigen specific MBCs and by the low efficiency of amplification of Ig scPCR obtained in MBCs compared to the pool of PBs. This has led my project to be divided in two parts. In the first part of my dissertation I will present the results published in a

manuscript (Bardelli M, 2013) of an efficient approach developed to identify and sort HA specific MBCs as well as to amplify VH and VL genes by the use of scPCR. The robust technique developed in Novartis enabled to monitor quantitative and qualitative changes in the distribution of HA binding across different B cell subsets following vaccination, and to obtain enriched population of HA specific B cells for molecular cloning of paired VHVL Ig genes.

The overall PCR efficiency we obtained in this first study by amplifying VH-VL genes from single memory B cells isolated from frozen hPBMCs ranged between 17-35%, as described also in literature. To optimize the entire procedure of Ig-scPCR, before moving to clinical samples, a new set of primers was designed for both RT and PCR steps. The application of this strategy to different B cell subsets enables to rescue the 60-80% of PCR products with an efficiency comparable in all cell types and improved in respect with the one obtained before.

In the second part of my dissertation I will present the study that I have performed in the last year of my PhD aimed at broadly characterizing at phenotypic and molecular level the unexplored repertoire of circulating PBs and MBCs recruited in the interaction with Factor H Binding Protein (fHbp) antigen following Meningococcus B vaccination. PBs and fHbp-specific MBCs isolated *ex vivo* from human PBMC collected from two subjects before and at different time points after MenB vaccination have been characterized for their BCR repertoire. Moreover a comparison of the overall repertoire across the two individuals has been performed. The obtained results are described in a manuscript currently in preparation to be submitted and presented in this thesis.

Ex vivo analysis of human memory B lymphocytes specific for A and B influenza hemagglutinin by polychromatic flow-cytometry

Monia Bardelli[1], Liliana Alleri[1*], Francesca Angiolini[1*§], Francesca Buricchi[1], Simona Tavarini[1], Chiara Sammicheli[1], Sandra Nuti[1], Elena Degl'Innocenti[2], Isabelle Isnardi[2], Elena Fragapane[1], Giuseppe Del Giudice[1], Flora Castellino[1] and Grazia Galli[1#]

[1]Novartis Vaccines and Diagnostics srl, 53100 Siena, Italy, [2]Novartis Institutes for Biomedical Research, CH-4056 Basel, Switzerland

Published in PLoS One. 2013 Aug 15;8(8):e70620.

**these Authors gave equal contribution to this work*

§ Present address: European Institute of Oncology, 20141, Milan, Italy

 # Corresponding author: Grazia Galli Research Center, Novartis Vaccines and Diagnostics srl Siena, 53100, Italy. Email: graziagalli@gmail.com Phone: +39 055 331053 Fax: +39 055 331053

Abstract

Understanding the impact that human memory B-cells (MBC), primed by previous infections or vaccination, exert on neutralizing antibody responses against drifted influenza hemagglutinin (HA) is key to design best protective vaccines. A major obstacle to these studies is the lack of practical tools to analyze HA-specific MBCs in human PBMCs *ex vivo*. We report here an efficient method to identify MBCs carrying HA-specific BCR in frozen PBMC samples. By using fluorochrome-tagged recombinant HA baits, and vaccine antigens from mismatched influenza strains to block BCR-independent binding, we developed a protocol suitable for quantitative, functional and molecular analysis of single MBCs specific for HA from up to two different influenza strains in the same tube. This approach will permit to identify the naive and MBC precursors of plasmablasts and novel MBCs appearing in the blood following infection or vaccination, thus clarifying the actual contribution of pre-existing MBCs in antibody responses against novel influenza viruses. Finally, this protocol can allow applying high throughput deep sequencing to analyze changes in the repertoire of HA^+ B-cells in longitudinal samples from large cohorts of vaccinees and infected subjects with the ultimate goal of understanding the *in vivo* B-cell dynamics driving the evolution of broadly cross-protective antibody responses.

Introduction

The surface glycoprotein hemagglutinin (HA) plays a critical role in influenza virus infection, by anchoring viruses to surface sialic-acid residues on host cells and by mediating the subsequent fusion of viral and host cell membranes. Antibodies blocking these interactions are the only widely recognized correlate of protection from infection. Both influenza infection and vaccination prime durable immune memory in humans (1-3). Priming of immune memory by overt or subclinical influenza infection can occur early in life, thus most human immunizations occur in the context of pre-existing immunity. Influenza HA is highly susceptible to mutations and drifted variants capable to escape pre-existing neutralizing antibodies emerge continuously. For this reason influenza vaccines must be reformulated yearly. Whether, and to what extent, pre-existing memory B-cells (MBCs) play a role in preventing infection by new influenza variants is poorly understood (4-5).

Convincing evidence showing that MBCs are recruited in early plasmablast responses to infection or vaccination has been collected by several groups (6-10), also during the 2009 pandemic (10-12). Most of this information has been obtained by applying the best state-of-the-art technologies for molecular cloning and expression of paired heavy and light variable immunoglobulin (IgV_HV_L) genes to arrays of single plasmablasts from multiple subjects (6,8-11). This has been possible because plasmablasts are identifiable by flow-cytometry based on the expression of well-defined surface markers but mostly because they appear in large numbers in the blood one week following infection or vaccination and therefore don't need to be selected based on antigen specificity (6). Applying similar approaches to analyze the repertoire of pre-existing antigen specific-MBCs would be key to verify their actual contribution in plasmablast responses to drifted HA antigens, as well as in antigen-driven germinal center reactions that ultimately generate long-lived antibody secreting cells and memory B-cells expressing

antibodies of refined specificities. A major obstacle to move in this direction is the lack of practical markers to identify rare antigen-specific MBCs within the bulk of MBCs present in *ex vivo* human PBMCs. Successful attempts to analyze and sort by flow-cytometry mouse B-cells binding to fluorochrome-labeled soluble HA molecules have been reported several years ago (13). Unfortunately, applying similar approaches to the analysis of PBMC samples from human influenza patients or vaccinees has proved challenging so far (14-15), due to non-specific binding of HA to the surface of all human leukocytes.

We explored different approaches to sort HA-specific MBCs and found that an efficient method to prevent non specific binding of influenza HA is pre-saturation of PBMCs with influenza mono-bulk vaccine antigens (that is, monovalent bulk vaccine antigen before final formulation into multivalent mixtures, filling, and finishing) from a strain mismatched to the one used as fluorescent bait. By using influenza A and B mono-bulks as saturating reagents, we developed a staining protocol suitable for direct flow-cytometric analysis of B-cells specific for HA from up to two different mismatched influenza strains in the same human PBMCs sample. This technique can be applied to monitor quantitative and qualitative changes in the distribution of HA binding across different B-cell subsets following vaccination, and to obtain enriched population of HA-specific B-cells for molecular cloning of paired V_HV_L-Ig genes. This protocol provides a unique tool to compare HA-specific B-cell repertoires across cohorts of subjects with different histories of influenza exposure and to obtain information suitable for the development of novel influenza vaccines.

Results

Detection of BCR-dependent binding to soluble influenza recombinant HA baits

To identify B-cells engaged into BCR-specific interactions with influenza HA we first tried to stain PBMCs with monoclonal antibodies against the B-cell marker CD20 and the B-cell memory marker CD27 mixed with a recombinant H1 bait (rH1), or with human serum albumin (HSA), both conjugated with the Alexa-488 fluorochrome (A488). When stained with rHA, PBMCs gated on live singlets (Fig.1A) showed a high and diffuse fluorescent signal on both B and non B-cells, while staining with HSA-A488 only gave background signal (Fig.1B).

Human influenza HA is known to bind α2,6 sialic-acid residues (16), which are expressed on human leukocytes and are particularly abundant on B lymphocytes (17-18). We tried to block this interaction by adding a 100-fold molar excess of soluble sialopentasaccharides containing α2,6-linkage to the staining solution. While this prevented indiscriminate binding of rH1 to most leucocytes, it was not sufficient to block rH1 binding to all B lymphocytes (Fig.1B). Little, or no improvement was observed in experiments in which we pre-incubated PBMCs with compounds known to bind to α2,6-sialic-acid residues with high affinity, such as α-fetuin, or the *Sambucus nigra* lectin (19) (data not shown).

We then evaluated the possibility of removing sialic-acid residues from PBMC surfaces, or covering them with vaccine subunit mono-bulk antigens, purified from an influenza A subtype mismatched to that of the fluorescent HA bait. Equal numbers of PBMCs from the same donor were incubated for 30 minutes either at 37°C with *Clostridium perfringens* type VIII neuraminidase (NA), or on ice with a vaccine mono-bulk H3N2 antigens (from A/Panama/2007/1999). Both PBMCs samples were then stained with anti-CD20, anti-CD27 and an A488-tagged rH1 bait. Following either treatment the frequency of H1-binding B-cells was greatly reduced (2.2% of total B-cells in the NA-treated sample and 0.5% in the

H3N2-pre-saturated sample) and most of the $H1^+$ B-cells expressed the CD27 B-cell memory marker (Fig. 1C).

Because these staining patterns were consistent with that expected for MBCs binding to H1 through BCR-specific interactions, we sorted $H1^+$ B-cells from both samples to verify their specificity by ELISPOT. To induce resting B-cells to differentiate into antibody secreting cells (ASC), the two sorted $H1^+$ B-cell populations were cultured with CpG and IL-2, in the presence of autologous CD20-negative ($CD20^{neg}$) feeder cells, in a ratio of 1:200 to achieve a cell density of at least 10^6 cell/ml. To exclude interference from *ex vivo* activated H1-specific plasmablasts putatively included among $CD20^{neg}$ cells, an aliquot of $CD20^{neg}$ cells was also mixed with H1-negative ($H1^{neg}$) B cells sorted from the NA-treated sample and placed in culture with CpG and IL-2. Unsorted PBMCs were also activated in the same way to assess the starting frequency of $H1^+$ ASC precursors. The results from these experiments showed that the two $H1^+$ B-cell populations generated comparable numbers of ASC producing H1-specific IgG and at enriched frequencies as compared to unsorted PBMCs (Fig. 1D). The frequency of ASC producing H1-specific IgG detectable in cultures of $CD20^{neg}$ cells mixed with $H1^{neg}$ B cells was instead greatly reduced as compared to unsorted PBMC, showing that the contribution from H1-specific IgG ASC eventually generated from *ex vivo* activated $CD20^{neg}$ plasmablasts was negligible. However, 95% of total IgG producing ASC generated from $H1^+$ B-cells sorted from H3N2-pretreated PBMCs produced H1-specific antibodies; conversely, only 19% of IgG-ASC generated from $H1^+$B-cells sorted following neuraminidase treatment were H1-specific (Fig. 1D).

These results were confirmed in 2 other experiments in which the proportion of H1-specific IgG-ASC generated from $H1^+$ B-cells sorted from H3N2-, or NA-pretreated PBMCs accounted for 85-100% and 19-23% of total IgG-ASC, respectively.

Based on these results, we concluded that blocking BCR-independent binding sites with mismatched influenza subunit antigens increases the specificity of identifying $H1^+$ B-cells and decided to utilize this staining approach in the subsequent experiments.

Figure 1

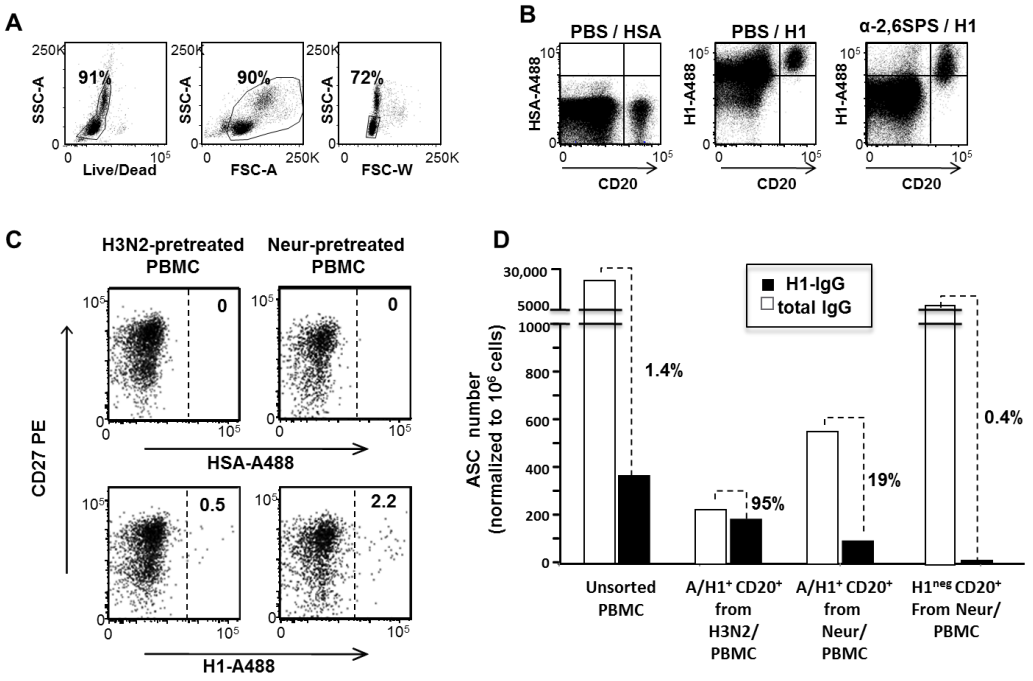

Figure 1. Blockade of sialic-acid binding sites reveals BcR-dependent binding to influenza HA. A-B. Diffuse binding of rH1 to untreated human PBMC. Thawed PBMCs from an anonymous blood donor were first stained with Live/Dead then with an anti-CD20 mAb mixed with Alexa488-conjugated human serum albumin (PBS/HSA), or Alexa488-conjugated rH1 from the A/California/07/2009 strain (PBS/rH1), or a solution of sialopentasaccarides containing the Alexa488-conjugated rH1 (α-2,6-SPS/H1Cal). The strategy for gating on single live lymphocytes is shown in A; rH1 binding to CD20 negative ($CD20^{neg}$) and $CD20^+$ cells is shown in B. **C.** Blockade of sialic-acid binding sites reveals putative BcR-specifc binding of rH1. PBMCs from a single donor were split in 8 tubes (10^7PBMC/each), 4 tubes were incubated with H3N2 mono-bulk subunit vaccine antigens from the A/Panama/2007/1999 strain (left dot plots), and 4 tubes with neuraminidase (right dot plots). Then the PBMCs were incubated with anti-CD20 and anti-CD27 mAbs and A488-HSA (upper plots), or A488-rH1 (lower plots). Shown is the distribution of rH1 binding on memory ($CD27^+$) and naïve ($CD27^-$) B cells identified in the $CD20^+$ gate. **D**. Specificity of rH1 binding. $H1^+$ B-cells sorted from H3N2- (n=1372) or neuraminidase- (Neur) (n=2233) treated PBMCs were mixed with sorted autologous $CD20^-$ cells in the ratio of 1:200 and activated in vitro with CpG and IL-2 for 5 days. As controls, cultures of unsorted PBMCs, as well as of autologous $CD20^{neg}$ cells mixed with H1-negative ($H1^{neg}$) B cells sorted from neuraminidase-treated

PBMCs (n=30,000) in the ratio of 1:10 were run for 5 days in the presence of CpG and IL-2. After 5 days, cells from each culture were harvested, washed, counted and assayed by ELISPOT to enumerate cells secreting IgG and H1N1-specific IgG. To facilitate comparisons between different cell cultures and across experiments depicted in different figures, the results are expressed as numbers of antibody secreting cells (ASC) normalized to 10^6 cultured cells assayed by ELISPOT.

Sensitivity and robustness of flow-cytometric analysis of HA-specific B-cell frequencies in *ex vivo* PBMCs

To obtain insights into the sensitivity and robustness of this approach, the frequencies of resting HA-specific IgG MBCs were measured both by flow-cytometry and by B-cell ELISPOT in PBMCs from 4 donors and in three different experimental sessions. For flow-cytometric analysis we used rH1 from the A/Solomon Island/03/2006 strain. The specificity of the $H1^+$ B-cell subset was verified by ELISPOT following activation of sorted $H1^+$ B-cells with CpG, IL-2 and autologous $CD20^{neg}$ B cells for 5 days (Fig. 2 A and B) using PBMC from a fifth donor. The capture antigen used in the ELISPOT assay was the H1N1 mono-bulk subunit from the same vaccine strain. To assess the frequency of $H1^+$ B cells expressing the IgG isotype among total $H1^+$ B cells detected in each of the four donors, an anti-IgG mAb was added to the staining protocol (figure 2 C).

The results of these comparisons showed that the frequencies of H1-specific IgG MBCs detected by flow-cytometry and by ELISPOT were linearly correlated and that the correlation was statistically significant (Fig. 2D; $R^2 = 0.73$; $p = 0.0005$). In addition, the variability of H1-specific IgG MBC frequencies measured by either method was comparable (Fig. 2E).

These results support the notion that our staining protocol can be applied for measuring HA^+ MBC frequencies in *ex vivo* PBMCs samples, with comparable sensitivity and robustness to conventional ELISPOT assays.

Figure 2

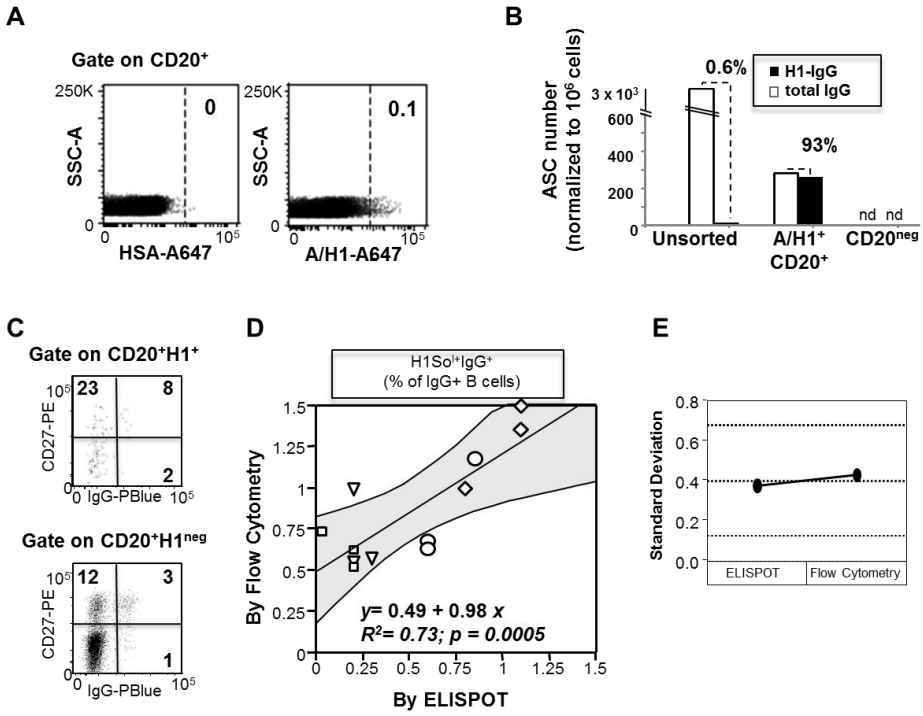

Figure 2. H1$^+$ IgG$^+$ MBCs frequencies measured by flow-cytometry and by ELISPOT correlated linearly

A-B. Specificity of the staining with the rH1 bait from A/Solomon Island/3/06. PBMCs ($1.6x10^8$) from anonymous blood donors were stained with Live/Dead, incubated with an H3N2 mono-bulk vaccine subunit (from A/Panama/2007/1999), and then stained with Alexa647-conjugated HSA ($6x10^7$), or Alexa647-conjugated rH1 ($1x10^8$), and with an antiCD20 mAb. **A.** Binding pattern of HSA (A647-HSA; left panel) and of rH1 (A647-rH1; right panel) in the CD20$^+$ B-cell gates. **B.** H1$^+$ B-cells identified in A were sorted (n=8215), mixed with autologous CD20^{neg} cells in the ratio of 1:50 and activated with CpG and IL-2 for 5 days *in vitro*. Unsorted PBMC and CD20^{neg} cells were also cultured in the same manner as controls. After 5 days, equal numbers of cultured cells were harvested and assayed by ELISPOT for numbers of cells secreting IgG and IgG specific for H1N1 (from A/Solomon Island/3/06). Results are expressed as number of antibody secreting cells (ASC) normalized to 10^6 cultured cells assayed by ELISPOT. Nd indicates undetectable ASC. **C.** Distribution of IgG$^+$ B-cells among H1^{neg} and H1$^+$ B cells expressing or not the CD27 B cell memory marker; shown is one representative subject. **D.** Replicates of frozen PBMCs from 4 anonymous blood donors were assayed by conventional ELISPOT, or incubated with an H3N2 mono-bulk vaccine subunit and stained with rH1, and anti-CD20 plus anti-human IgG antibodies. The scatter plot depicts paired values of H1$^+$ IgG$^+$ B-cell frequencies measured by flow-cytometry (y-axis) and by ELISPOT (x-axis) across three different experimental sessions. Shown are: the regression line with the related 95% confidence interval (gray areas), slope, intercepts, R^2 and p-value. **D.** Variability plot showing mean standard deviations of the measurements done by ELISPOT and flow-cytometry. The three dotted lines mark the grand mean and the upper and lower control limits.

Simultaneous identification of B-cells specific for HA from A and B influenza strains in *ex vivo* PBMCs

Next we assessed whether this approach was suitable to identify B-cells specific for HA from different influenza A subtypes, or from a type B influenza strain. PBMCs from two anonymous blood donors were pre-incubated with mono-bulk antigens from an influenza B vaccine strain and then stained with rHA from either A/H1N1 or A/H3N2 subtypes. Alternatively, PBMCs from a third donor were first pre-incubated with mono-bulk antigens from an influenza A/H3N2 subtype and then stained with B/rHA. B-cells putatively engaged in BCR-dependent binding to the rHA antigens were identified in each sample. Since applying a stringent gate only on bright H3+ or B/HA+ cells (rectangles in left panels of Fig. 3A) would have not permitted to obtain sufficient numbers of cells for ELISPOT tests, the sorting gates were set with lower stringency (dashed lines in left panels of Fig. 3A). In each sample HA^+ B-cells distributed across memory ($CD20^+CD27^+$) and putatively naïve ($CD20^+CD27^-$) B cells in comparable manner to HA^{neg} B cells (Fig. 3B). All the HA^+ B-cell populations were sorted and activated *in vitro* with CpG, IL-2 and autologous $CD20^{neg}$ B cells, to verify the specificity of the staining by ELISPOT. Unsorted PBMC, as well as autologous $CD20^{neg}$ B cells mixed with HA^{neg} B cells were also placed in culture as controls and activated in the same manner. After 5 days in culture, all the sorted HA^+ B-cell populations were enriched in B-cells expressing IgG specific for the HA baits. Fig. 3C depicts the results from a representative experiment where the fold enrichments in IgG-ASC specific for H3 (from A/Brisbane/10/07), H1 (from A/California/07/09) or B/HA (from B/Brisbane/60/08) were 210x, 29x, and 180x, respectively. No IgG-ASC specific for HA were detected in cultures of $CD20^{neg}$ B cells and HA^{neg} B cells (Fig. 3 C). In this experiment the highest frequency of ASC producing HA-specific IgG HA was observed in the cultures of $H1^+$ B-cells (68% of total IgG producing ASC), for which the most stringent sorting gate was applied (Fig. 3A and C, middle

panels). Comparable results were obtained with PBMCs from other two donors (not shown).

We then explored the possibility of combining two baits from different influenza strains to analyze B lymphocytes binding to either HA antigen in the same PBMC sample. Fig. 4 depicts the results obtained with PBMC from a single donor that were split into two tubes and either pre-incubated with a B/HA vaccine mono-bulk and stained with equal amounts of A647-rH3 and A488-rH1 (Fig. 4A), or pre-incubated with an A/H3N2 vaccine mono-bulk and stained with the A488-rH1 paired with an A647-B/rHA (Fig. 4B). $H1^+$ B-cells were detected at comparable frequencies, irrespective of the type of the mono-bulk used as blocking agent (0.4 and 0.3 % of total $CD20^+$ B-cells), and segregated apart from B/HA^+ or $A/H3^+$ B-cells. The results obtained from the analysis of PBMCs from 16 different donors stained with A647-rH3 and A488-rH1 confirmed that the $H1^+$ and $H3^+$ B-cell subsets were largely non-overlapping (Fig. 4C). B-cells putatively cross-reactive with H1 and H3 were detected in 13 out of 16 subjects at frequencies 10 to 100-fold lower than those of B lymphocytes binding only to the H1 or the H3 bait (Fig. 4C, insert).

Overall, these results show that, by designing appropriate staining protocols, flow-cytometry can offer the unique opportunity to identify and sort single B-cells with restricted or cross-reactive binding capacity against different antigens.

Figure 3

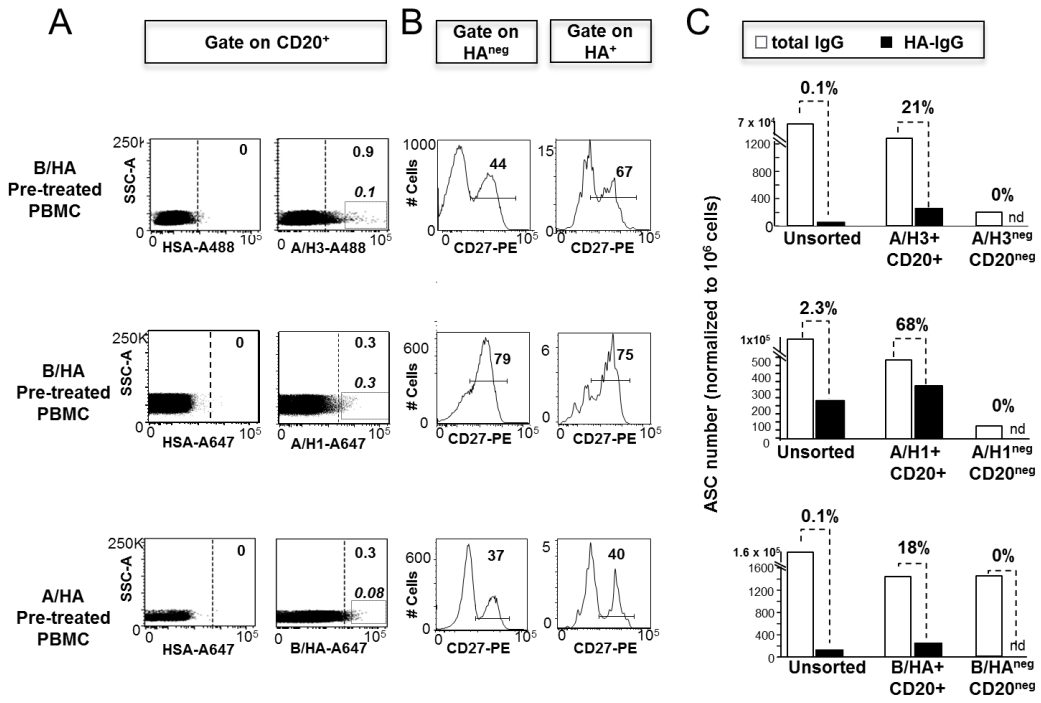

Fig 3. Identification of B lymphocytes specific for HA from A and B influenza strains in *ex vivo* PBMCs samples

PBMCs from different anonymous blood donors were pre-incubated with vaccine mono-bulk subunits from the B/Brisbane/60/2008 (B/HA pretreatment), or the H3N2 A/Panama/2007/1999 strain (A/HA pretreatment) and then stained HSA, rH3 (from A/Brisbane/10/2007), rH1 (from A/California/07/2009), or B/HA (from B/Brisbane/60/2008), as indicated. **A.** Staining pattern observed on $CD20^+$ cells in PBMC stained with the different rHA bait. The rectangular gates identify brilliant HA+ B-cells; the dotted vertical lines mark the gates used to sort HA^+ B-cells for the ELISPOT assays. **B**. Expression of the CD27 memory marker on HA^+ and HA^{neg} B cells identified based on the sorting gates. **C.** $H3^+$ (n=15,234), $H1^+$ (n=6482) and B/HA^+ (n=26,803) B-cells identified in A were sorted, mixed with autologous $CD20^{neg}$ cells (in the ratio of 1:20, 1:100 and 1:33) and activated with CpG and IL-2 for 5 days *in vitro*. Unsorted PBMC and $CD20^{neg}$ cells mixed with HA^{neg} B cells were also cultured in the same manner, as controls. After 5 days cultured cells were harvested and assayed by ELISPOT for the number of cells secreting IgG and IgG specific for mono-bulk subunits from the vaccine strain homologous to the sorting bait. Results are expressed as numbers of antibody secreting cells (ASC) normalized to 10^6 cultured cells assayed by ELISPOT. Nd indicates undetectable ASC.

Figure 4

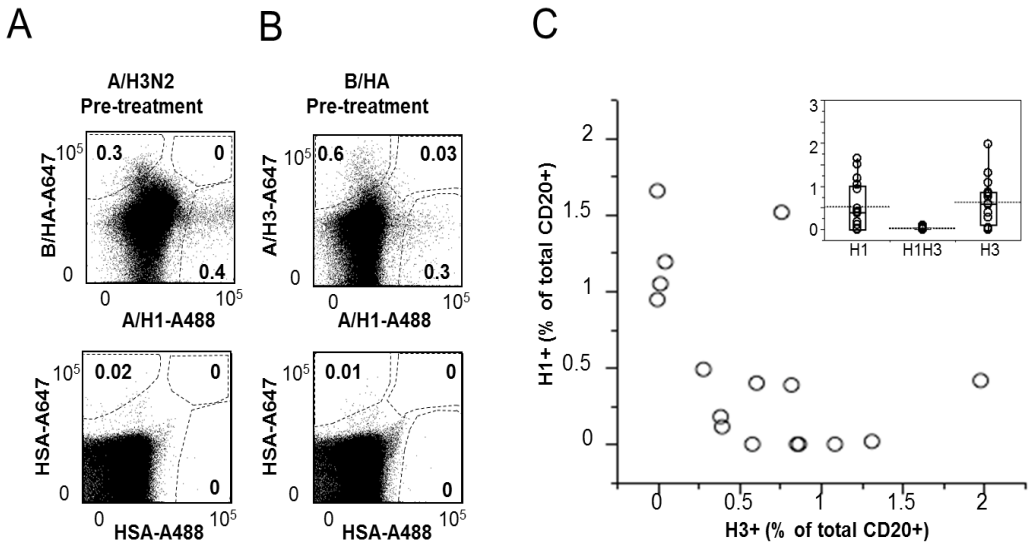

Figure 4. Simultaneous identification of B lymphocytes specific for HA from different influenza strains in *ex vivo* PBMCs samples

A. PBMCs from an anonymous blood donor were pre-incubated with subunits from either B/Brisbane/60/2008 or A/Panama/2007/1999 (H3N2), and then stained with anti-CD20 mAb, HSA conjugated with A488 and A647, with A647-rH3 (from A/Brisbane/10/2007) and A488-rH1 (from A/California/07/09), or with A647-rB/HA (from B/Brisbane/60/2008) and A488-rH1 (from A/California/07/09). The staining patterns observed in the CD20+ B-cell gate are shown. **B.** PBMCs from 16 anonymous blood donors were pre-saturated with B/Brisbane/60/2008 and then stained with anti-CD20 mAb, A647-rH3 (from A/Brisbane/10/2007) and A488-rH1 (from A/California/07/09). The scatter plot depicts paired values of $H1^+$ (y-axis) and $H3^+$ (x-axis) B-cells. The insert box plot depicts the distribution of $H1^+$, $H3^+$ and $H1^+H3^+$ B-cells in the same 16 donors. Mean values are indicated by dotted lines.

Molecular cloning of HA^+ B-lymphocytes

Next, we assessed whether B-cells sorted based on HA binding are suitable for molecular cloning of IgV_HV_L genes. To this aim, PBMCs from four blood donors were first incubated with B/HA vaccine antigens and then with an anti-CD20 mAb and the rH1-A647 and rH3-488 baits. B-cells that bound to H1 ($H1^+$ B-cells) and B-cells that did not bind to either H1 or H3 ($H1^{neg}H3^{neg}$ B-cells) were sorted from two donors; from the other two donors we sorted $H1^+$ B-cells and few cells binding to H3 ($H3^+$ B-cells).

To clone paired V_HV_L sequences we applied the single cell RT-PCR Ig-gene amplification protocol previously described (20-21). The efficiency of molecular cloning ranged between 17% and 38%. Since these cells were obtained from frozen PBMCs, we couldn't directly compare these values to the 40-60% cloning efficiency obtained using freshly isolated PBMCs by the authors of the RT-nested PCR protocol (21). Reassuringly, however, pairs of V_HV_L sequences were obtained with comparable efficiencies from HA^+ and HA^- B-cell subsets sorted from the same donor (38% for $H1^+$ and 22% for $H1^{neg}H3^{neg}$ B-cells from donor #3, 17% for both $H1^+$ and $H1^{neg}H3^{neg}$ B-cells from donor #4), suggesting that BCR-binding by rHA had no substantial impact on cell viability and mRNA degradation.

All arrays of sorted cells comprised single clones; only in one donor we found two $H1^+$ clones that expressed identical V_HV_L rearrangement with few different mutations (clones 53 and 87 from donor #2, Supplementary Table 1).

The distribution of V_H and V_L gene family use was similar across the different arrays of sorted B-cells, as well as across the four donors (Fig. 5). Use of V_H3 segments was dominant in HA^+ B-cells from three out of four donors; the second most represented family being V_H4 and the remaining V_H1 or V_H5 (Fig. 5A). The D_H3 family was most frequently used in HA^+ B-cells from 3 donors, followed by D_H2 and D_H6 and at lower frequency by D_H1, D_H4 and D_H5 (Fig. 5B). The most frequently expressed JH segments were from either the J_H4 or the J_H6 family,

followed by J_H5, J_H3, J_H2 and J_H1 families (Fig. 5C). Similarly, genes from the V_K1 and V_K3 families were most frequently expressed in all arrays of clones and most of them were rearranged with J_K1 or J_K4 genes, less frequently with J_K2, J_K3 and J_K5 genes (Fig. 5D and 5E).

Overall, no biases were found in the distribution of V_H and V_L gene families used by $H1^+$ or $H1^{neg}H3^{neg}$ clones from the two donors analyzed in this manner (Fig. 5). An in depth analysis of V_L regions from $H1^+$ and $H1^{neg}H3^{neg}$ B-cells showed that, in donor #4, these two B-cells subsets carried remarkable differences. As shown in Fig. 5F, V_L sequences cloned from $H1^+$ B-cells of subject #4 displayed significantly higher numbers of mutations leading to dissimilar amino acid substitutions than V_L sequences from $H1^-H3^-$ B-cells ($p<0.036$, one-tail Wilcoxon non-parametric test). Conversely, no differences were found when comparing mutations leading to similar amino acid substitutions in V_L regions (Fig. 5H), suggesting that the $H1^+$ and $H1^{neg}H3^{neg}$ B-cells could have evolved under different antigen-driven selection pressures. No differences were ever found between numbers of mutations leading to either dissimilar, or similar, amino acid substitutions in the V_H regions (Figs. 5 G and I).

In conclusion, these results show that the protocol developed to identify single HA-specific B-cells by flow-cytometry is applicable for molecular cloning and in-depth analysis of paired IgV_HV_L genes.

Figure 5

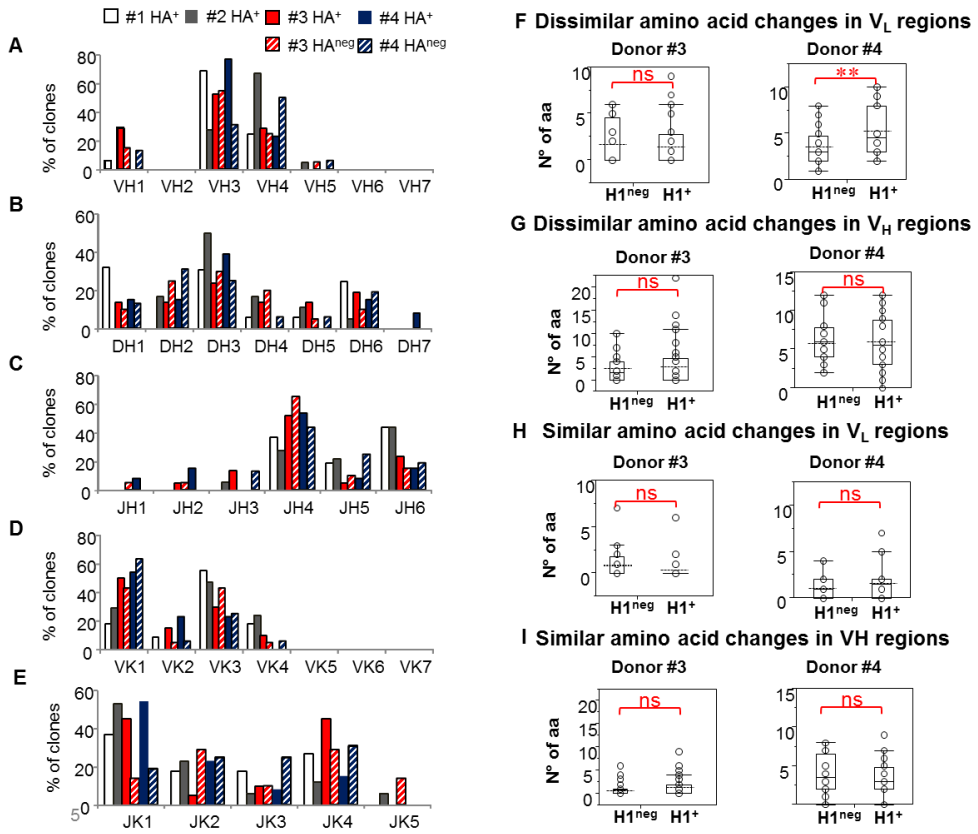

Figure 5. Molecular cloning of HA$^+$ B lymphocytes
PBMCs from 4 anonymous blood bank donors were stained as in Figure 4B. Single H1$^+$, H3$^+$, or H1^{neg}H3^{neg} CD20$^+$ B-cells were sorted to perform molecular cloning and analysis of their paired V_HV_L Ig regions as described in Material and Methods section. **A-E**. Distribution of V_H (A), D_H (B), J_H (C), V_k (D) and J_k (E) gene use across arrays of B-cells sorted from each donor (16 and 18 HA$^+$ clones from donors #1 and #2; 35 HA$^+$ and 20 HA^{neg} clones from donor 3; 16 HA$^+$ and 16 HA^{neg} clones from donor #4. **F-I.** Number of mutations in H1$^+$ and H1^{neg} CD20$^+$ B-cells from donors #3 and #4, which cause dissimilar (F, H) or similar (G, I) amino acid substitutions in V_H (G,I) and V_L (F,H). NS and ** indicate not significant, or significant ($p<0.036$) difference between mean numbers of mutations by one-way Wilcoxon non-parametric test.

Analysis of qualitative and quantitative changes in HA+ B-cells induced by vaccination

Finally we asked whether the method we developed could be applied to analyze quantitative and phenotypic changes in the pool of HA-binding B cells induced by influenza vaccination. For this analysis we took advantage of the availability of PBMCs samples collected at baseline and at days 21 and 43 after vaccination from four volunteers enrolled in a study performed during the 2007/2008 northern hemisphere influenza season (E.F. et al. manuscript in preparation). These samples were incubated first with H3N2 mono-bulk antigens and then with an A647-rH1^{+} (from the 2007/2008 H1N1 vaccine strain A/Solomon Island/03/2006) and monoclonal antibodies against the CD20 B-cell marker, the CD27 memory marker and IgG.

At baseline, all subjects had measurable numbers of H1^{+} B-cells (Figs. 6A and 6B). Following vaccination, the frequencies of circulating H1^{+} MBCs cells increased from 1.5 to 8 fold over baseline values (Figs. 6A and 6B). In three out of four subjects the expansion of H1^{+} B-cell paralleled the rise of circulating antibodies capable of blocking hemagglutination. A delayed expansion of H1^{+} B-cells, measurable at day 43 was observed in subject c, which was the only subject with high antibodies against the H1N1 strain at baseline (Fig. 6B).

It is important to note that vaccination also induced remarkable changes in the distribution of H1^{+} B-cells across different MBCs subsets. At baseline, the majority of H1^{+} B-cells distributed across mature memory (CD27^{+}) and immature IgG-switched memory cells (CD27^{neg}IgG^{+}) B-cells (Figs. 6A and 6C). By day 21, the proportion of H1^{+} B-cells expressing both the CD27 memory marker and an IgG-switched immunoglobulin receptor increased in all subjects to values that were 2 to 4-fold higher than those observed at baseline (Fig. 6C, upper right panel). The proportion of H1^{+} B-cells with naive (CD27^{neg}IgG^{neg}) or immature memory (CD27^{neg}IgG^{+}) phenotypes decreased in parallel (Fig. 6C, lower panels).

Comparable changes were never observed in the population of $H1^{neg}$ B-cells (Fig. 6A lower panels, and data not shown).

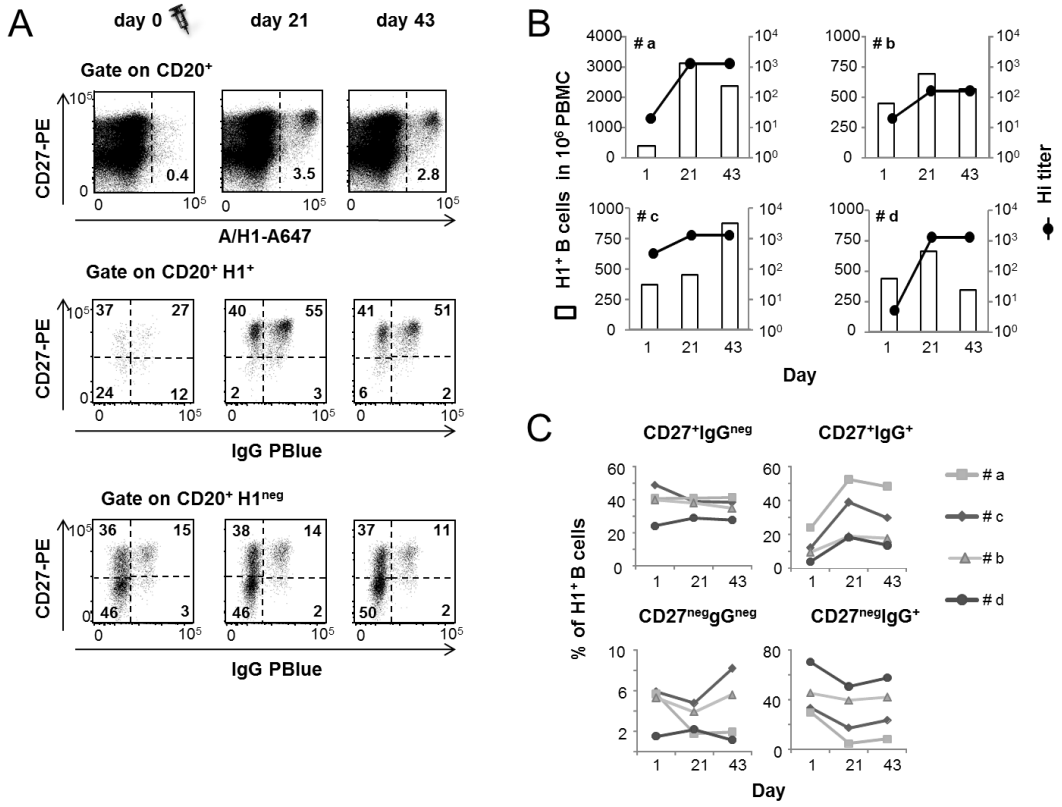

Figure 6. Vaccination induced changes in the pool of H1+ B-cells
PBMCs samples collected before (day 0) and at 3 and 6 weeks after vaccination from four seasonal influenza vaccinees, were pre-incubated with H3N2 subunit (from A/Panama/2007/1999) and then stained with rH1 A/Solomon Island/3/06) and mAbs anti-CD20, anti-CD27 and anti-human IgG. **A.** Dot plots gated on $CD20^+$ B-cells showing the distribution of $H1^+$ (middle panels) and $H1^{neg}$ (bottom panels) B-cells from donor #a across: the mature memory ($CD27^+$) and putatively naive ($CD27^{neg}$) CD20+ B-cell subsets (upper panels); un-switched mature memory ($CD27^+IgG^-$), IgG-switched mature ($CD27^+IgG^+$) and immature ($CD27^{neg}IgG^+$) memory B-cells. **B.** Numbers of circulating $H1^+$ $CD20^+$ B-cells in 4 vaccinees before and at 3 and 6 weeks after seasonal vaccination are overlaid with paired titers of antibodies inhibiting virus-induced hemmaglutination measured in their blood. The frequencies of $H1^+$ B-cells are normalized according to the frequencies of $CD20^+$ B-cells in 10^6 PBMCs. **C.** Distribution of circulating $H1^+$ and $H1^{neg}$ B-cells across same subsets identified in **B** in all vaccinees.

Discussion

Our findings demonstrate that B-cells carrying immunglobulin receptors specific for type A or B influenza HA can be identified in *ex vivo* PBMCs by using fluorochrome-tagged rHA as antigenic baits and unlabeled mismatched mono-bulk vaccine subunit antigens to block BCR-independent binding. Circulating HA^+ B cells identified in this manner in samples collected before and after vaccination can be further characterized for relative frequency and phenotype, as well as being sorted for further in depth analysis.

As antigenic bait, we used different recombinant full-length HA molecules, produced by Protein Sciences in the baculovirus-insect cell expression system. We opted for using rHA, instead of the influenza vaccine mono-bulk subunit preparations as bait for several reasons. First, the data available show that these soluble rHA preparations form trimers and higher order of structures, which retain hemagglutination activity and the expected antigenic properties of HAs (22). In addition, rHA preparations do not contain other influenza proteins, while mono-bulk vaccine subunits contain HA and some NA. Finally, these rHA are commercially available and can be used by most laboratories.

There were two main obstacles to identifying, with high specificity, HA^+ MBC circulating in human blood.

First, when added directly to untreated PBMCs, the rHA baits bind to all human blood leucocytes. This result is in apparent conflict with previous findings from the Baumgarth's lab supporting the use of flow-cytometry to analyze influenza HA specific B-cells (13). Using lymph node cells from mice immunized with the influenza PR8 virus and soluble PR8 HA as bait, they did not observe BCR-independent binding and succeeded in obtaining an enriched population of HA-specific B-cells (13). Such conflicting data can be reconciled by recent results showing that α2,6-N-acetyl sialic-acid residues, known to interact with high affinity with human influenza HA (16), are expressed at high levels on all human B

lymphocytes, independently of their activation status, either as intrinsic component surface-expressed glycoproteins, or bound to the lectin domain of B-cell-restricted CD22 inhibitory receptors (23). Conversely, most mouse B-cells express low levels of α2,6-N-acetyl sialic-acids on their surfaces, which transiently increase only in activated B-cells engaged in germinal center reactions (23). Intriguingly, Baumgarth's group reported that close to 90% of the HA^+ B-cells identified in PR8 immunized mice expressed surface markers characteristic of germinal center B-cells (13).

In line with the hypothesis that multimeric interactions between rHA and CD22-linked α2,6- N-acetyl sialic-acids could be responsible of the diffuse binding of HA to human B-cells, the addition of short α2,6-sialylated pentasaccharides to the staining solution displaced rH1 from most human leukocytes but not from B-cells. Conversely, rH1 binding to human B lymphocytes was blocked when PBMCs were stained following a pre-incubation step with either *C. perfringens* NA, which cleaves α-2,3- α-2,6- and α-2,8-linked sialic-acids, or with H3N2 human influenza mono-bulk antigens, which are known for preferential binding to α-2,6-sialic-acids. Of note, $H1^+$ B-cells isolated from NA-treated PBMCs still contained a large number of cells producing IgG of unknown specificity. Because NA is less than 50% active at the pH and temperature conditions that preserve cell viability, the inefficiency of preventing non-specific HA binding by NA treatment was anticipated. In contrast, up to 95% of $H1^+$ B-cells sorted from H3N2-preated PBMCs were confirmed as HA-specific by ELISPOT, supporting the use of this approach to prevent BCR-non-specific binding of fluorochrome-labeled rHA antigens.

The second obstacle to specific sorting of MBCs with HA baits was that the specificity of the HA^+ B-cell population was influenced by the stringency of the gates applied in the analysis. Because human beings are exposed to a multiplicity of different antigenic challenges, finding a true universal negative control appears

impossible. The use of autologous proteins, like HSA, is helpful to set the lowest gate for BCR-independent recognition. However, the use of such controls is clearly insufficient when dealing with pathogen receptor antigens, like HA, capable of multimeric interactions with their ligands. In our experience, the mean fluorescence intensity of HSA-stained B-cells is often substantially lower than that of *bona fide* HA^- B-cells stained with labeled rHA. Thus, to identify HA^+ B-cells with great specificity we set the gate on brilliant HA^+ B-cells. Repeated measurements of $H1^+IgG^+$ B-cell frequencies in replicates of PBMC samples by this staining approach provided a series of values linearly correlated with those obtained by ELISPOT assays, and with similar range of variability across different experimental sessions. Clearly, a robust standardization of the gating strategy would require parallel flow cytometric and ELISPOT analyses of large number of samples across different laboratories. It is encouraging, however, that the results obtained by analyzing PBMC samples from influenza vaccinees confirmed the adequacy of our gating approach to monitor quantitative and qualitative changes in HA-specific B-cell subsets induced by vaccination.

Quantitative analysis of MBCs before and after infection or vaccination has been so far performed by B-cell ELISPOT, or limiting dilution assays (24, 25). These assays proved useful at gaining knowledge of the kinetic and the magnitude of MBC responses to influenza strains that did or did not circulate in the human population (3, 12, 24, 25). The major limitation of these assays is that they are not suitable for functional and molecular analysis of the antigen-specific repertoire at the single cell level *ex vivo*.

We showed here that by combining rHA baits and monoclonal antibodies against surface B-cell markers our method is also suitable to analyze changes in the distribution of HA^+ B-cells across MBCs subsets at different maturation stages (26) including in subjects who eventually did not experience a substantial increase in total number of HA^+ MBCs. For our experiments we choose to restrict the analysis

to HA^+ B cells that expressed (or not) an IgG-switched BcR. A most in depth investigation of HA^+ B cells expressing IgM or IgA receptors is clearly feasible by adding appropriate mAbs in the staining, as shown in supplementary figure 1.

Overall, our observations provide strong support to the feasibility of standardizing flow-cytometry-based assays for monitoring directly in PBMC samples *ex vivo* quantitative and phenotypic changes induced in the repertoire of HA^+ B-cells by influenza infection or vaccination. Moreover, the staining approach presented here can be used to sort arrays of single B-cells with different HA-binding specificities and to perform molecular cloning and in depth analysis of the V_HV_LIg repertoires, as it is currently done with short-lived plasmablasts circulating early after antigenic challenge.

The possibility of combining two different HA baits in the same tube offers the opportunity of identifying rare circulating MBCs that cross-react between multiple influenza strains. Confirming the specificity of $H3^+H1^+$ B-cells identified in some of our samples was not feasible because the informed consents signed by the anonymous blood donors did not include producing monoclonal antibodies from their cells. In addition, the number of $H3^+H1^+$ B-cells in these samples was too low to apply an ELISPOT assay to verify their specificity. Nevertheless the results obtained by flow-cytometric analysis showed that the B-cells binding to A/H1 segregated completely from those binding the B/HA bait, consistent with the low amino acid sequence homology between these HA molecules and the absence of serological cross-reactivity between type A and B influenza strains (27-28). Conversely, and in line with recent findings reported by multiple groups who used most complex B-cell cloning procedures (15, 29), in several PBMC samples we identified extremely low frequencies of B-cells putatively cross-reactive to group 1 (H1) and 2 (H3) A influenza strains.

A major limitation of our approach is that MCBs that cross-react between the blocking HA and the bait HA will be missed. Thus, the rare MBCs cross-reactive

between type A H1 and H3 and B HA molecules as those recently discovered (14) would not be present in the sorted arrays of brightly stained MBCs unless they have extremely higher binding affinity to the fluorochrome-tagged HA baits as compared to the HA subunit used to block non specific binding.

Because human beings are exposed to annually changing antigenic variants of influenza HA, a deeper understanding of the protective potential of pre-existing MBCs repertoires is key to develop new and broadly protective vaccines. The approach reported here for direct analysis of HA-specific MBCs in *ex vivo* PBMC complements available methods to identify single plasmablasts, making possible to analyze all HA-specific B cell subsets circulating in the blood before and after vaccination. This will permit to verify the actual contribution of pre-existing MBCs in the generation of early plasmablasts and MBC expressing refined antibody specificities after infection or vaccination against novel (seasonal or pandemic) influenza viruses. With this complete set of tools longitudinal analyses of IgV_HV_LIg phenotypically characterized repertoires of plasmablasts and HA^+ MBCs from defined cohorts of subjects by deep sequencing will become possible, therefore allowing more rapid investigation of the *in vivo* B-cells dynamics driving the evolution of broadly cross-protective antibody responses against drifted influenza viruses. Greater understanding of these dynamics can aid the design of best vaccines for all ages and health conditions.

Materials and Methods

Human Blood samples and Ethics Statement

Leukopacs from anonymous healthy blood bank donors were collected during 2010-2011 season after written informed consent was provided and ethical approval granted by the Institutional Review Board of the Empoli City Hospital, the Comitato Etico Locale Azienda 11 Empoli. The history of influenza infection or vaccination of blood bank donors was unknown. Ethical approval for collecting blood and performing B-cell analyses from volunteers, enrolled across 2008 and 2009, in a Novartis' sponsored clinical study with trivalent seasonal influenza vaccine given with or without avian H5N1 vaccine formulated with MF59 adjuvant (ClinicalTrials.gov Identifier: NCT00620815), was granted by the Ethical Committee of the medical faculty of Ludwig-Maximilians-University Munich. All clinical investigations have been conducted according to the principles expressed in the Declaration of Helsinki. The results of this clinical study will be the subject of a forthcoming paper (Fragapane E. et al. unpublished data). PBMCs were isolated by conventional centrifugation over a Ficoll gradient, frozen and stored in liquid nitrogen as previously described (12). All subjects provided written informed consent. The informed consents did not include permission for producing monoclonal antibodies from donors' blood cells.

Conjugation of HA with fluorochromes

Recombinant HA (Protein Science) and HSA (Sigma-Aldrich) molecules were chemically labeled with Alexa Fluor 488 or Alexa Fluor 647 carboxylic acid succinimidyl ester (Molecular Probes, Invitrogen) following the manufacturer's instructions. Each protein antigen was incubated with the dye at a molar ratio of 1:10 for 1 hour at room temperature and then loaded into a Zeba desalting spin column (Thermo Scientific) to remove unbound dye. The degree of labeling was determined following the manufacturer's instructions, by measuring the absorbance of conjugated protein at the relevant wave length for each fluorochrome by

spectrophotometry. Protein concentrations were calculated by the BCA Protein Assay (Pierce, Thermo Scientific); the protein integrity was analyzed by SDS-PAGE.

Flow-cytometry

Frozen PBMCs were thawed at 37°C in PBS containing 2.5mM EDTA and 20 µg/mL DNAse (Sigma Aldrich). Samples were stained in tubes, each containing 10^7 PBMC, according to different protocols: i) For pre-saturation with mono-bulk vaccine antigens, PBMCs were first stained with Live/Dead Aqua (Invitrogen) diluted 1:500 in 100 µl, for 20 min in the dark. Then 50 µl of PBS containing 20% rabbit serum were added for further 20 min at 4°C to saturate Fc receptors. After two washes in 2 ml of PBS, PBMCs pellets were dissolved in 10 µl of PBS containing 30 µg/ml of vaccine subunit antigens (or 60 µg/ml in case of staining with 2 antigen baits) and incubated at 4°C in PBS. After 15 min, 10 µl of PBS containing 30 µg/ml (approximately 4 micromoles) of each fluorochrome-conjugated rHA bait were added, together with 50 µl of a cocktail of pre-titrated amounts of anti-CD20 PrCPCy5.5 (Becton Dickinson, clone L27), anti-CD27 PE (Becton Dickinson, clone L128) and anti-hIgG PacificBlue (Jackson ImmunoRes) monoclonal antibodies 1% FBS for 1 hour at 4°C. After two washes with 2 ml of 1% FBS/PBS cells were diluted in 1 ml of 5mM EDTA/PBS and acquired with the Canto II analyzer (Becton Dickinson, Pharmingen, San Diego, CA). ii) For neuraminidase pre-treatment, PBMCs pellets were diluted in 50 µl of PBS containing 0.1 to 5 M Type VIII neuraminidase from *Clostridium perfringens* (which cleaves α-2,3- α-2,6- and α-2,8-linked sialic-acid residues. # N5631 Sigma Aldrich), incubated for 30 min at 37°C and then washed 3 times with PBS. PBMCs were then stained as in i), but omitting the pre-incubation step with mono-bulk influenza antigens. iii) To saturate rHA binding sites for α2,6 linked sialic-acid residues, soluble sialopentasaccarides containing α2,6 linkage (provided by Dr. Paolo Costantino, Novartis VD) were incubated at 100-fold molar excess with

labeled-rHA for 15 min at 4° C. PBMCs were then stained as in i), but omitting the pre-incubation step with mono-bulk influenza antigens. iv) For pre-incubation with the Sambucus Nigra lectin (Vector Laboratories), PBMCs were stained as in i) adding as saturation agent 100 μl of a solution of PBS containing 10 to 100 μg/ml of the lectin for 15 min at 4°C, instead of mono-bulk influenza antigens. Flow-cytometric analysis was performed using the FlowJo software (Treestar Inc.). For antigen-specific B-cell sorting, PBMCs from the same donor stained at 10^7/tube were then pooled, diluted in 1 ml of 5mM EDTA/PBS and filtered through 30 μm cup filcon (Becton Dickinson). Samples were maintained on ice until sorting. Sorting was performed in high purity mode by a FACS Aria instrument (BD Biosciences, San Jose, CA) equipped with the BD FACSDiva v6.1.3 software using a 70 μm nozzle operating at 70 psi. Sorting gates were established in order to isolate brilliant HA^+ $CD20^+$ cells, unless differently specified. HA negative (HA^{neg}) B cells and CD20 negative ($CD20^{neg}$) cells were also sorted as negative controls or feeders for HA^+ and HA^{neg} B-cell cultures, respectively.

ELISPOT

In order to induce resting B-cells to differentiate into antibody secreting cells, unsorted PBMCs HA^+, or HA^{neg} B-cells were cultured *in vitro* in 0.2 ml of complete medium (RPMI with 100 units/mL penicillin, 100 μg/mL of streptomycin, 2 mM L-glutamine, 1 mM sodium pyruvate, and 0.1 mM not essential amino acids, 5%FBS; Invitrogen) containing 2.5 μg/ml of CpG (PRIMM, Milan, Italy) and 1000U/ml of IL-2 (Novartis). CD20- B-cells were added as feeders to HA^+ B-cell cultures in variable ratios (from 1:30 to 1:200) to achieve a cell density of at least 10^6/ml. After 5 days, cultured cells were washed 4 times in PBS, counted, diluted to equal concentrations in complete medium and plated in complete medium (200 μl/well) in serial 2-fold dilutions in duplicate-triplicate wells of ELISPOT plates pre-coated with HSA, influenza antigens or an

anti-human IgG antibody. ELISPOT plates (MultiScreen HTS^{TM} HA, Millipore) were coated over night at 4°C with 100 μg/ml of PBS containing 2.5 μg/ml of an anti-human IgG (BD Pharmingen), or 10 μg/ml of HSA (Sigma), H1N1 from A/California/07/2009 or A/Solomon Island/03/2006, or H3N2 from A/Brisbane/10/2007, or HA from B/Brisbane/60/2008. Following an overnight incubation at 37 °C and 5% CO_2, the ELISPOT plates were washed 4 times with PBS, then 4 times with 0.05% Tween20/PBS. Spots of antibody secreting cells were revealed with biotin-conjugated mouse anti human IgG (Southern Biotech) diluted in 4% BSA/PBS for 4 hours at 37 °C, followed by horse radish peroxidase-conjugated Streptavidin (ENDOGEN). The reaction was then developed with 3-amino-9-ethylcarbazole (AEC, Sigma). Automated spot counting was performed using the UV Spot ELISPOT plate Analyzer (CTL) and the Immunospot software v5.09 (CTL).

Single cell RT-PCR and sequence analysis of Ig variable regions

Single HA^+ and HA^- $CD20^+$ B-cells were sorted into ice-cold 96-well PCR plates pre-filled with 4 μl/well of 0.5X PBS containing 10 mM DTT (Invitrogen), 8 U RNasin (Promega), 0.4 U RNAse Inhibitor (QIAGEN). After sorting, plates were sealed, centrifuged and immediately transferred at −80 °C. cDNA synthesis was performed adding 10.5μl mix to the 96-well plate containing the sorted cells. The mix contains 150 ng of random hexamer primers (Roche), 0.5% v/v Igepal (SIGMA CA-630), 1U RNAse Inhibitor (QIAGEN), 4U RNAsin (Promega), 10mM DTT (Invitrogen), 0.5mM dNTP mix (Roche), 50U SuperScript III Reverse Transcriptase (Invitrogen), 5x Reverse Transcriptase Buffer (Invitrogen) diluted in nuclease free water (Invitrogen). The reaction was incubated at 25°C for 5', at 50°C for 60', and at 70°C for 15'. For the 1st PCR round 3.7 μl of cDNA template were mixed with forward primer mixes specific for the leader region and reverse primers specific for either IgH, IgK and Igλ constant regions (20-21) in 3 different plates. For the 2nd nested PCR round, 2.5 μl of the first round PCR product were

mixed with nested forward and reverse primers mixes (20-21). Both PCR reactions were performed in 96 well plates (Eppendorf) in a total volume of 25 µl/well of nuclease free water containing 1x GoTaq Hot Start Green Master Mix (Promega) and 0.2 µM of each primer or primer mix. Each round of PCR was performed for 50 cycles at 94°C for 30 seconds, 57°C (1^{st} PCR) or 59 °C (2^{nd} PCR) for 30 seconds and 72°C for 55 seconds (1^{st} PCR) or 45 seconds (2^{nd} PCR). PCR products were separated on 2% agarose gels and analyzed for the presence of 350-400 nucleotides products. Positive PCR products were purified from the wells of the plate using the QIAquick PCR Purification Kit (QIAGEN). PCR products were sequenced with the ABI 3730xl 96-capillary DNA analyzer (Applied Biosystems), using the second round PCR forward primer mix for the heavy chain products, the PanVK primer for the kappa light chain product, the second round reverse primer for the lambda light chain products. Sequences of the IgH/L V region were analyzed by IMGT/V-QUEST system.

Statistical analysis

A linear regression analysis was performed using the JMP 8.0.1 software to assess the presence of a linear correlation between frequency of $H1^+$ IgG memory B-cells measured by flow-cytometry, or by conventional B-cell ELISPOT. Variability analysis was performed to compare the repeatability of the two assays. To avoid assuming that frequencies of amino acid replacements had a normal distribution, the mean frequencies of amino acid replacements between arrays of $H1^+$ and $H1^{neg}$ B-cells were analyzed by one-way Wilcoxon non-parametric test as implemented in the stats package of R version 2.14 (http://www.r-project.org/).

Supplementary Figure 1

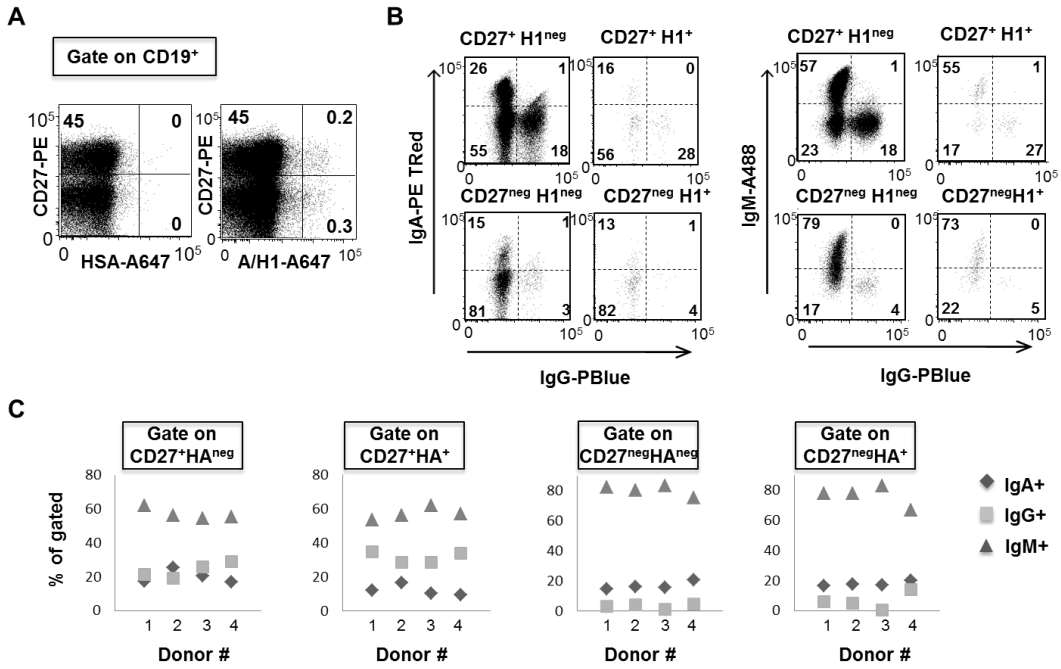

Supplementary Figure 1. Expression of IgM, IgA and IgG BcR among H1^{+} B-cells in steady state.

PBMCs from anonymous blood bank donors were pre-incubated with H3N2 subunit (from B/Brisbane/60/2008) and then stained with rH1 A/California/07/09 and mAbs anti-CD19, anti-CD27, anti-IgM and anti-IgG, or anti-IgA and anti-IgG. **A.** Dot plots gated on CD19^{+} B-cells showing the binding pattern of HSA or rH1 across mature memory (CD27^{+}) and putatively naive (CD27^{neg}) B-cells from donor #2. **B.** Dot plots showing the distribution of cells expressing IgA or IgG, or IgM BcR across CD27^{+} or CD27^{neg} H1^{+} and H1^{neg} B cells. **C**. Frequencies of IgA, IgM and IgG BcR across the same subsets identified in **B** in four different donors.

References

1. Yu X, Tsibane T, McGraw PA, House FS, Keefer CJ, et al. (2008) Neutralizing antibodies derived from the B-cells of 1918 influenza pandemic survivors. Nature 455(7212):532-6.
2. Amanna IJ, Carlson NE, Slifka MK. (2007) Duration of humoral immunity to common viral and vaccine antigens. N Engl J Med. 357(19):1903-15.
3. Sasaki S, Jaimes MC, Holmes TH, Dekker CL, Mahmood K, et al. (2007) Comparison of the influenza virus-specific effector and memory B-cell responses to immunization of children and adults with live attenuated or inactivated influenza virus vaccines. J Virol. 81(1):215-28.
4. Ellebedy AH, Ahmed R. (2012) Re-engaging cross-reactive memory B-cells: the influenza puzzle. Front Immunol. 3:53.
5. Dormitzer PR, Galli G, Castellino F, Golding H, Khurana S et al. (2011) Influenza vaccine immunology. Immunol Rev. 239(1):167-77.
6. Wrammert J, Smith K, Miller J, Langley WA, Kokko K, et al. (2008) Rapid cloning of high-affinity human monoclonal antibodies against influenza virus. Nature453(7195):667-71.
7. Pinna D, Corti D, Jarrossay D, Sallusto F, Lanzavecchia A. (2009) Clonal dissection of the human memory B-cell repertoire following infection and vaccination. Eur J Immunol. 39(5):1260-70.
8. Moody MA, Zhang R, Walter EB, Woods CW, Ginsburg GS et al. (2011) H3N2 influenza infection elicits more cross-reactive and less clonally expanded anti-hemagglutinin antibodies than influenza vaccination. PLoS One 6(10):e25797.
9. Wrammert J, Koutsonanos D, Li GM, Edupuganti S, Sui J et al. (2011) Broadly cross-reactive antibodies dominate the human B-cell response

against 2009 pandemic H1N1 influenza virus infection. J Exp Med. 208(1):181-93

10. Li GM, Chiu C, Wrammert J, McCausland M, Andrews SF et al. (2012). Pandemic H1N1 influenza vaccine induces a recall response in humans that favors broadly cross-reactive memory B-cells. Proc Natl Acad Sci U S A. 109(23):9047-52.
11. He XS, Sasaki S, Baer J, Khurana S, Golding H et al. (2012) Heterovariant Cross-Reactive B-Cell Responses Induced by the 2009 Pandemic Influenza Virus A Subtype H1N1 Vaccine. J Infect Dis. 207(2):288-96.
12. Faenzi E, Zedda L, Bardelli M, Spensieri F, Borgogni E et al. (2012) One dose of an MF59-adjuvanted pandemic A/H1N1 vaccine recruits pre-existing immune memory and induces the rapid rise of neutralizing antibodies. Vaccine. 30(27):4086-94.
13. Doucett VP, Gerhard W, Owler K, Curry D, Brown L, Baumgarth N. (2005) Enumeration and characterization of virus-specific B-cells by multicolor flow-cytometry. J Immunol Methods. 303(1-2):40-52.
14. Dreyfus C, Laursen NS, Kwaks T, Zuijdgeest D, Khayat R (2012). Highly conserved protective epitopes on influenza B viruses. Science. 337(6100):1343-8.
15. Hu W, Chen A, Miao Y, Xia S, Ling Z et al. (2012). Fully human broadly neutralizing monoclonal antibodies against influenza A viruses generated from the memory B-cells of a 2009 pandemic H1N1 influenza vaccine recipient. Virology 435(2):320-8.
16. Viswanathan K, Chandrasekaran A, Srinivasan A, Raman R, Sasisekharan V, et al. (2010). Glycans as receptors for influenza pathogenesis. Glycoconj J. 27:561–570.

17. Kamerling J P, Makovitzky J, Schauer R, Vliegenthart J F, Wember M. (1982).The nature of sialic-acids in human lymphocytes. Biochimica et Biophysica acta 714:351-355.

18. Zimmer,G, Suguri,T, Reuter,G, Yu,RK, Schauer, R. and Herrler, G. (1994) Modification of sialic-acids by 9-O-acetylation is detected in human leucocytes using the lectin property of influenza C virus. Glycobiology, 4, 343–349.

19. N Shibuya, I J Goldstein, W F Broekaert, M Nsimba-Lubaki, B Peeters and W J Peumans (1987) The elderberry (Sambucus nigra L.) bark lectin recognizes the Neu5Ac(alpha 2-6)Gal/GalNAc sequence. The Journal of Biological Chemistry 262(4):1596-601.

20. Wardemann H, Yurasov S, Schaefer A, Young JW, Meffre E, Nussenzweig MC.(2003) Predominant autoantibody production by early human B cell precursors. Science. 301(5638):1374-7.

21. Tiller T, Meffre E, Yurasov S, Tsuiji M, Nussenzweig MC, Wardemann H. (2008) Efficient generation of monoclonal antibodies from single human B cells by single cell RT-PCR and expression vector cloning. J Immunol Methods. 329(1-2):112-24.

22. Feshchenko E, Rhodes D, Felberbaum R, McPherson C, Rininger J, et al. (2012) Pandemic influenza vaccine: characterization of A/California/07/2009 (H1N1) recombinant hemagglutinin protein and insights into H1N1 antigen stability. BMC Biotechnol. 12(1):77.

23. Naito Y, Takematsu H, Koyama S, Miyake S, Yamamoto H et al. (2007) Germinal Center Marker GL7 Probes Activation-Dependent Repression of N-Glycolylneuraminic Acid, a Sialic-acid Species Involved in the Negative Modulation of B-Cell Activation. Mol. Cell. Biol. 27(8): 3008-3022.

24. Crotty S, Aubert RD, Glidewell J, Ahmed R. (2004) Tracking human antigen-specific memory B-cells: a sensitive and generalized ELISPOT system. J Immunol Methods. 286(1-2):111-22.
25. Galli G, Medini D, Borgogni E, Zedda L, Bardelli M, et al. (2009) Adjuvanted H5N1 vaccine induces early CD4+ T cell response that predicts long-term persistence of protective antibody levels. Proc Natl Acad Sci U S A. 106(10):3877-82.
26. Berkowska MA, Driessen GJ, Bikos V, Grosserichter-Wagener C, Stamatopoulos K, et al. (2011) Human memory B-cells originate from three distinct germinal center-dependent and -independent maturation pathways. Blood. 118(8):2150-8.
27. Krystal M, Elliott RM, Benz EW Jr, Young JF, Palese P. (1982) Evolution of influenza A and B viruses: conservation of structural features in the hemagglutinin genes. Proc Natl Acad Sci U S A. (15):4800-4
28. Schild GC & Dowdle WR (1975) in The Influenza viruses and Influenza. Ed Kilbourne ED (Academic New York).pp 315-372.
29. Corti D, Voss J, Gamblin SJ, Codoni G, Macagno A et al. (2011) A neutralizing antibody selected from plasma cells that binds to group 1 and group 2 influenza A hemagglutinins. Science. 333(6044):850-6.

Dissecting the Immunoglobulin repertoire of human fHbp-specific B cells and Plasmablasts in response to Meningococcus B vaccination

Liliana Alleri[1], Nicola Pacchiani[1], Giulia Torricelli[1], Silvia Guidotti[1], Stefano Censini[1], Maria Giuliani[1], Iwan Beuvink[2], Elisabetta Traggiai[2], Alessandra Mariani[1], Francesca Buricchi[1], Giuseppe Del Giudice[1], Grazia Galli[1] and Oretta Finco[1#]

[1]Novartis Vaccines and Diagnostics srl, 53100 Siena, Italy, [2]Novartis Institutes for Biomedical Research, CH 4056 Basel, Switzerland

Unpublished results

Abstract

Adaptive immune responses rely upon the establishment of a pool of antigen-specific B cells and Plasmablasts. Both cell types are the result of an affinity maturation process that re-shapes the repertoire of their immunoglobulins in the regions that directly interacts with the antigen (the variable region), or determining different effector functions (the constant region). This study summarizes the results obtained from the dissection of the un-explored repertoire of Plasmablasts and factor H binding protein (fHbp) specific memory B cells following Meningococcus B vaccination. The analysis of Variable (V), Diversity (D) and Joining (J) rearrangements of fHbp specific B cells isolated from two vaccinated subjects, before and at different time points after vaccination revealed the preferential usage of particular genes. An accurate bioinformatic analysis to reconstruct the affinity maturation process encompassed by fHbp-specific Ig sequences has brought to the selection of 6 sequences from the repertoire of the two individuals. The corresponding antibodies have been tested for antigen binding specificity and affinity. Interestingly we found that 4 antibodies were binding fHbp antigen with similar high affinity.

Introduction

Effective vaccines act stimulating the immune system to recognize and remember the pathogens that they target, through the generation and the maintenance of a serological memory. Successful immune response may last for a lifetime after vaccination or infections [1, 2, 3]. Different hypotheses have been proposed to explain such durable responses and it is noteworthy that all these hypotheses rely upon the establishment of a pool of long-lived Antigen (Ag)-specific Plasmacells and Memory B cells (MBCs) [4, 5].

Both cell types are the result of an affinity maturation process that re-shapes the repertoire of B cells responding to the eliciting antigen and generally occurs in specialized secondary lymphoid organs, also called germinal centers (GCs) [6]. Herein, activated B cells encompass somatic hypermutation (SHM), i.e. the introduction of point mutations, deletions and duplications in the germline sequence of V(D)J genes and class switch recombination (CSR) that initiates the gene-re-arrangements required to switch the immunoglobulin constant region from IgM to a different class (IgG, IgA or IgE) [7]. Following these events a multitude of clones, carrying modified immunoglobulin B cell receptors (BCRs) and thus differing in binding affinity to the antigen, are generated [8]. Finally, inside the GC, B cell clones that acquired improved affinity for the antigen achieve a proliferative advantage out-competing the others, which instead will die by neglect.

B cell differentiation in response to vaccine antigens is considered classically to develop along two pathways; one leads rapidly to the appearance of clusters of Plasmablasts (PBs) secreting antibodies, and the second leads to the appearance of GCs and generation of a pool of MBCs. Even if it is still controversial, there are several emerging evidences that Ag-specific PBs and MBCs undergo affinity maturation also without GC formation in extra-follicular pathways [9].

Either following GC reaction or not, two populations of B cells carrying hypermutated and class switched BCRs, Ag-specific PBs and MBCs, start to

populate the human blood after infection or vaccination in different timeslots and with different kinetics. PBs, representing the early component of host defense, peak in the blood around day 8 after vaccination and return quickly to undetectable levels thereafter. Otherwise, Ag-specific MBCs circulate at enriched frequency in the blood peaking at 1 month after vaccination, and contracting slightly above or equal to baseline at later time points. The fascinating and still mysterious nature of these B cell populations makes the dissection of their repertoire of particular interest, especially in the vaccination field where the comprehension of the mechanisms able to induce a more affine BCR against the eliciting antigen could help in designing *ad hoc* vaccines able to stimulate particular and dedicated arms of the immune responses.

Different are the studies that have been focused on the characterization of the repertoire of PBs isolated after vaccination [10, 11, 12] to measure effector recall memory responses, but really few studies have investigated the relationship between MBCs and PBs populations [13]. Due to the paucity of studies looking into this aspect of immune memory, it is still unclear whether PBs and MBCs originate from the same clones of B cells capable of binding to the antigens before vaccination, or instead the precursors of PBs and MBCs correspond to distinct group of clones. Also unclear is the clonal nature and relationship of MBCs recruited and circulating at different time points after vaccination. Two are the main works in literature that investigated changes at molecular level in Immunoglobulin (Ig) genes between PBs and MBCs isolated after vaccination [13, 14]; both the examples refer to tetanus toxoid vaccination and revealed that a clonal relationship between PBs and MBCs could exist, especially suggesting that Ag-experienced MBCs could be recruited in recall responses, becoming precursors of newly generated PBs and MBCs.

In line with these observations, this study was designed to characterize at phenotypic and molecular level the un-explored repertoire of circulating PBs and

MBCs recruited in the interaction with the factor H binding protein (fHbp) antigen following Meningococcus B vaccination. We describe here the results obtained dissecting the BCR repertoire of both PBs and fHbp-specific B cells isolated *ex vivo* from human PBMC collected from two subjects before and at different time points after MenB vaccination. We compare the IgH and IgL repertoire of MBCs and PBs and we also compare the fHbp-specific repertoire of the two individuals. Finally, informatic analysis of the antibody heavy chain sequences from the two individuals allowed us to determine the lineage structure of the repertoire and to analyze and reconstruct the affinity maturation process encompassed by some Ig sequences.

Results

Selection of two vaccinees based on their serological and cellular responses to the antigen

To get a comprehensive picture of the dynamic changes in the repertoire of B cells responding to a vaccine antigen following vaccination, we took advantage of PBMCs samples collected during a Meningococcus B vaccine clinical trial. Enrolled subjects were healthy adults who received 3 doses of vaccine at 1 month interval and blood samples were collected at different time points after vaccination: day 0 (pre-vaccination), day 30 post-1st dose, day 7, day 30 and day 202 post-3rd dose of vaccination. The PBs response was analyzed at day 7 post-3rd; Ag-specific MBCs were analyzed at all other time points.

The antibody response against fHbp in plasma samples and the frequency of antigen specific MBCs and PBs in peripheral blood were measured at different timepoints after vaccination in 6 subjects. Notably, following vaccination all subjects showed an increase in the antibody titers against fHbp as compared to baseline, as well as an increase in the frequency of fHbp-specific B cells. Comparable levels of antibodies were found in all subjects, with two of them (sbj #1 and #2) showing a slightly higher titer. Figure 1 shows that IgG-switched memory B cells (IgG MBC) specific for fHbp were detectable in all subjects at baseline (mean frequency ranging from 0.00% to 0.06% of total IgG MBC). By day 30 post 3rd dose of vaccination, the frequency of fHbp-IgG MBC increased in all subjects (ranging from 0.14% to 0.71%) and was maintained above pre-vaccination level (range: 0.15% to 0.25%) at least until day 202 after 3rd dose, in all but one subject. At day 7 post-3rd dose the frequency of fHbp-IgG- PBs ranged from 1.46% to 11.35. Interestingly, we observed the highest frequency of fHbp-IgG-switched PBs in subjects #1 and #2 (11.35% and 8.9% respectively), who also showed the highest anti-fHbp IgG-titers in plasma. These two subjects have been therefore

selected for further B cell repertoire analysis on the basis of their serological and cellular response at different time points after vaccination.

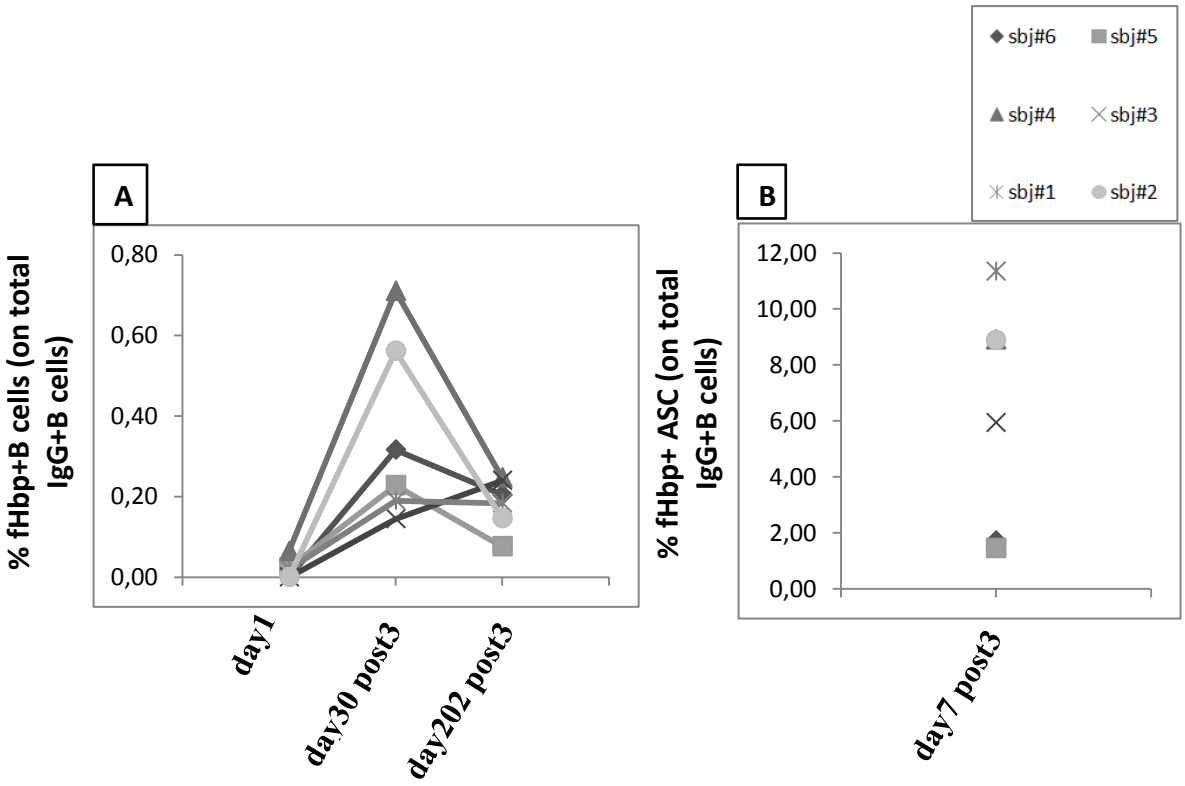

Figure 1_ Frequencies of IgG-switched memory B cells (IgG MBC) and PBs (IgG PBs) specific for fHbp detected in all subjects by Elispot. The frequency of fHbp-specific IgG MBC is expressed as percentage of total MBC producing antibodies in PBMC cultured with CpG and IL-2. Frequency of IgG PBs specific for fHbp is detected by ELISpot in resting PBMC collected at day 7 after 3rd dose of vaccination. Results are expressed as number of antigen specific antibody secreting cells (ASCs) in 10^6 PBMC. Each symbol represents an individual subject.

Ex vivo analysis of quantitative and phenotypic changes in the pool of fHBp binding B cells

Following this preliminary analysis, in order to get a comprehensive picture of the quantitative, phenotypic and molecular changes of the repertoire of fHbp specific B cells induced by vaccination we identified and isolated PBs at day 7 post-3rd dose of vaccination, as well as all B cells binding fHbp through their BCR directly from *ex vivo* PBMCs collected at day 0 (pre-vaccination), day 30 post-1st dose, day 30 and day 202 post-3rd dose of vaccination (Figure 2).

As shown in Fig.2A PBs were identified based on the differential expression of cluster differentiation marker, namely: CD3-, CD19+, CD20-, CD27++ and CD38++. To identify fHbp+ B cells we took advantage of the method previously developed by our group [15]. PBMCs samples were incubated with Alexa647 tagged-fHbp or Alexa647 tagged-Human Serum Albumin (HSA) as bait and monoclonal antibodies against CD19, CD27, anti- IgG, IgA and IgD. At baseline, both subjects had quite low numbers of CD19+ fHbp+ B cells with a frequency of 0,05 and of 0,03 for sbj #1 and #2 respectively, comparable to the negative control (HSA). Vaccination induced a slight and gradual increase of the frequencies of circulating fHbp+ B cells in the course of vaccination. At day30 post1st we observed a frequency of 0,09 and 0,05 for sbj #1 and #2 respectively. At day30 post 3rd we observed the higher frequencies of fHbp+ B cells with respect to other time points with frequencies of 0,15 and 0,1 for sbj #1 and #2 respectively. Interestingly, at day202 post3rd these frequencies were roughly maintained with a value of 0,16 and 0,08 for sbj #1 and #2. Despite this slight increase in frequencies, we observed substantial changes in the circulating pool of B cell subsets recruited in the interaction with fHbp, as shown in Figure 2B and 2C. At baseline, the rare fHbp+ B cells identified were mainly naive or natural effector (CD27+ or CD27- IgD+) B cells. Starting from day 30 post-1st dose to day 202 post-3rd dose of vaccination, the pool of circulating fHbp+ B cells expressing both the CD27 memory marker and an

IgG switched Ig BCR increased in both subjects, while the naive and natural effector B cells decreased.

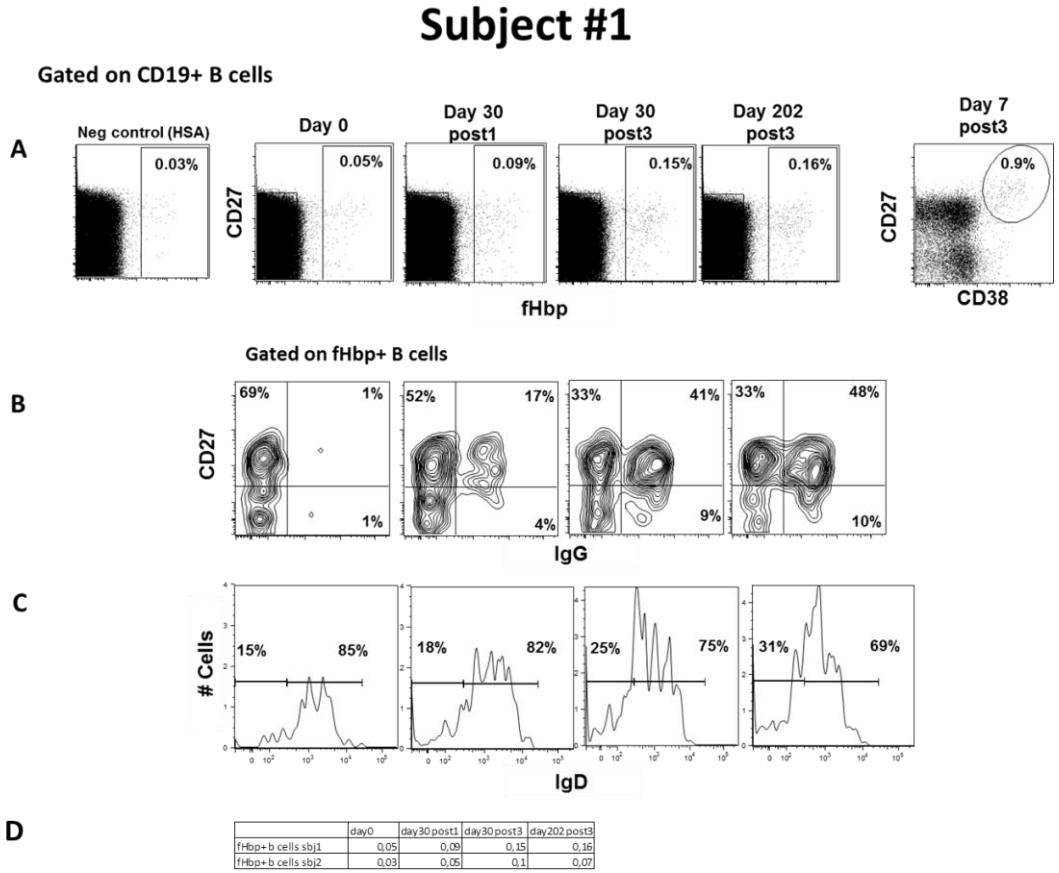

Figure 2_Identification of Plasmablasts and fHbp specific B cells in *ex vivo* PBMCs samples of vaccinees. PBMCs samples collected from sbj#1 and #2 at day 0 (pre-vaccination), day 30 post-1st dose, day 30 and day 202 post-3rd dose of MenB vaccination were incubated with fHbp Alexa647 and mAbs anti-CD19, anti-CD27 and anti-human IgG, IgA and IgD. PBMCs samples collected at day7 post-3rd dose were stained with mAbs anti-CD3, anti-CD19, anti-CD20, anti-CD27 and anti-CD38. **A)** Dot plots gated on $CD19^+$ B-cells showing the distribution of fHbp+ B-cells from sbj#1 across: the mature memory ($CD27^+$) and putatively naive ($CD27^-$) B-cell. **B)** and **C)** fHbp+ B-cells distribution across: naive or natural effector ($CD27^+$ or $CD27^-IgD^+$) B cell subsets, IgG-switched mature ($CD27^+IgG^+$) and immature ($CD27^-IgG^+$) memory B-cell subsets. **D)** Frequencies of fHbp+B cells in sbj#1 and #2 at the different timepoints after vaccination

Optimization of scPCR approach on memory B cells

Both plasmablasts and B cells binding fHbp were sorted as single cells in 96-well plates and analyzed for the rearranged V(DH)J genes of their BCR. Different were the protocols available in literature to amplify VH-VL genes from single cells but overall the efficiency on memory B cells isolated from frozen hPBMCs ranged between 17-35% [15, 13]. Thus, before moving to clinical samples, we optimized the entire procedure of Ig-scPCR by designing reverse primers specific for CH-CK-CL to be used in the retro-transcription reaction. We also designed new forward primers for Ig-nested PCR with a broader coverage of all VH and VL families' genes and reverse primers specific for the constant region of heavy and light chains (Table 1). By applying this strategy to both PBs and fHbp-specific B cell lysates we successfully rescued the 60-80% of PCR products. The PCR efficiency was comparable in both cell types and improved in respect with the one obtained before. Furthermore, the use of reverse primers specific for the constant region of heavy and light chains in PCR allowed determining the Ig class of the expressed Igs (figure 3).

GGAAGGTGTGCACGCCGCTGGTC	IgG CHrevRT	VHrev	RT GSP
CCTGGGGGAAGAAGCCCTGGACC	IgA CHrevRT		
GGGAATTCTCACAGGAGACGA	IgM CHrevRT		
CCTCTAACACTCTCCCCTGTTGAAG	CK revRT	VKrev	
CATTCTGYAGGGGCMACTGTCTTCTC	CL revRT	VLrev	
CACTCCCAGGTGCAGCTGGTGCAG	L-VH1_VH7 fw	FW	VH PCR1
TGGGTCTTRTCCCAGGTCACCTTG	L-VH2 fw		
AAGGTGTCCAGTGTSAGGTGCAG	L-VH 3fw		
GTCCTGTCCCAGGTGCAGCTGCAG	L-VH4_6 fw		
GAGTCTGTTCCGAGGTGCAGCTGG	L-VH5 fw		
GTGCCAGGGGGAAGACCGATG	IgG CH rev	Rev	
GCMGAGGCTCAGCGGGAAGAC	IgA CH rev		
GAGACGAGGGGGAAAAGGGTTG	IgM CH rev		
CAGGTGCCAGATGTGHCATCCAG	L-VK1 fw	FW	VK PCR1
CTGGATCCAGTGSGGATATTGTGATG	L-VK2 fw		
CCCAGATACCACCGGAGAAATTGTG	L-VK3 fw		
CTCTGGTGCCTACGGGGACATCGTG	L-VK4 fw		
CTGATACCAGGGCAGAAACGACAC	L-VK5 fw		
GAACACTCTCCCCTGTTGAAGCTCTTTG	CK rev 1st	Rev	
GGTCCTGGGCCCAGTCTGTGCTG	L-VL1 fw	FW	VL PCR1
GGTCCTGGGCCCAGTCTGCCCTG	L-VL2 fw		
TCTGTGRCCTCCTATGAGCTGAC	L-VL3 fw		
CTCTCGCAGCCTGTGCTGACTCA	L-VL4 VL5 VL9 fw		
GTTCTTGGGCCAATTTTATGCTG	L-VL6 fw		
GGTCCAATTCTCAGGCTGTGGTG	L-VL7 fw		
GAGTGGATTCTCAGACTGTGGTG	L-VL8 fw		
GTCAGTGGTCCAGGCAGGGCTGAC	L-VL10 fw		
GTGCTCCCTTCATGCGTGACC	CL rev 1st	Rev	
CCAGGTGCAGCTGGTGCAGTCTG	2ND_L-VH1_5_7 fw	FW	VH PCR2
CCAGGTCACCTTGAAGGAGTCTGGTC	2ND_L-VH2 fw		
TGAGGTGCAGCTGGTGGAGTCTGGGGGAG	2ND_L-VH3 fw		
CCAGGTGCAGCTGCAGGAGTCGGG	2ND_L-VH4_6_a fw		
CCAGGTGCAGCTGCAGCAGTGGGG	2ND_L-VH4_6_b fw		
CGATGGCCCCTTGGTGGARGCTG	IgG CH rev	Rev	
ACCTTGGGGCTGGTCGGGGATG	IgA CH rev		
GTTGGGGCGGATGCACTCCCTG	IgM CH rev		
GCCATCCAGATGACCCAGTCTCCATC	2ND_L-VK1 fw	FW	VK PCR2
GATATTGTGATGACCCAGACTCCACTCTC	2ND L-VK2 a fw		
GATATTGTGATGACTCAGTCTCCACTCTC	2ND_L-VK2_b fw		
GAAATTGTGTTGACACAGTCTCCAG	2ND_L-VK3_a fw		
GAAATTGTGATGACGCAGTCTCCAG	2ND_L-VK3_b fw		
GACATCGTGATGACCCAGTCTCCAG	2ND_L-VK4 fw		
GAAACGACACTCACGCAGTCTCCAG	2ND_L-VK5 fw		
GTTTCTCGTAGTCTGCTTTGCTCA	CK rev 2nd	Rev	
CAGTCTGTGCTGACTCAGCCGCCCTCAG	2ND_L-Vl1 fw	FW	VL PCR2
CAGTCTGCCCTGACTCAGCCTGCCTCCG	2ND_L-Vl2 fw		
TCCTATGAGCTGACACAGCCAC	2ND_L-Vl3_a fw		
TCCTATGAGCTGACTCAGGACC	2ND_L-Vl3_b fw		
CAGCCTGTGCTGACTCAATCGTCCTCTG	2ND_L-Vl4 fw		
TCAGCCTGTGCTGACTCAGCCRACTTC	2ND_L-Vl5 9fw		
TAATTTTATGCTGACTCAGCCCCACTC	2ND_L-Vl 6fw		
TCAGGCTGTGGTGACTCAGGAGCCCTC	2ND_L-Vl7 fw		
TCAGACTGTGGTGACCCAGGAGCCATC	2ND_L-Vl8 fw		
TCAGGCAGGGCTGACTCAGCCACCCTCGG	2ND_L-VL10 fw		
CACCAGTGTGGCCTTGTTGGCTTG	CL rev 2nd	Rev	

Table 1_ List of primers used to retro-transcribe and amplify VH and VL genes by scRT-PCR approach

MenB vaccination induces Ig class switch and a preferential VDJ usage in the pool of Fhbp-binding B cells.

We finally obtained 21 clones from day 0, 132 clones from day 30 post-1st, 105 clones from day 7 post-3rd, 95 clones from day 30 post-3rd and 94 clones from day 202 post-3rd from sbj#1. From sbj#2 we obtained 25 clones from day 0, 59 clones from day 30 post-1st, 185 clones from day 7 post-3rd, 46 clones from day 30 post-3rd, 205 clones from day 202 post-3rd. All sequences were analyzed with regard to their VH (DH) JH gene segment usage, CDR3 length and Ig class. For the majority of the sequences we were able to identify also the antibody class (figure 3). We found that at baseline both subjects had a pool of fHbp-specific B cells mainly composed by IgM natural effector B cells (88% and 80% of all the sequences in sbj #1 and #2 respectively) followed by IgA switched B cells (12 and16% of the sequences in sbj #1 and #2 respectively) and finally from IgG-switched B cells (0 and 4% in sbj #1 and #2 respectively) (Fig.3A and 3B). Starting from day 30 post-1st to day 202 post-3rd we observed substantial changes in the pool of fHbp-specific B cells. IgG-switched B cells begin to populate the antigen-specific B cell pool, increasing in sbj#1 from 12% at day 30 post-1st, to 47% and 51% at day 30 and at day 202 post-3rd, respectively, and in sbj#2 from 20% at day30 post 1st to 52% and 42% at day30 and day202 post 3rd. IgM natural effector, or IgM memory B cells decrease from approximately 80% at day 30 post-1st to 46% at both day 30 and day 202 post-3rd for sbj#1. This latter phenomenon was also observed for sbj #2 were IgM+ B cells decrease from 63% at day30 post 1st to 41% and 54% respectively at day30 and day202 post 3rd. A slight decrease was observed also for IgA-switched B cells in the course of vaccination (ranging from approximately 8% at day 30 post-1st to 7% and 3% respectively at day 30 and at day 202 post-3rd for subj #1 and from 18% at day30 post 1st to 7% and 4% respectively at day 30 and day202 post 3rd for sbj #2.

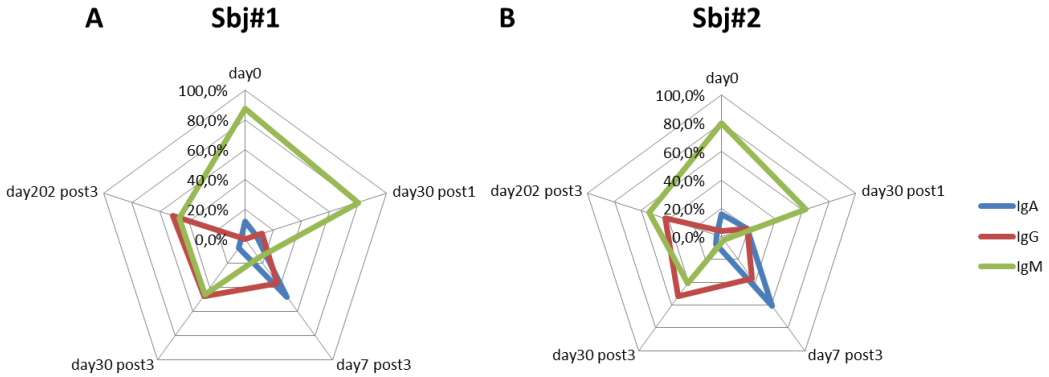

Figure 3_Ig class distribution of Plasmablasts and fHbp-specific B cells. The Ig class of all sequences obtained from sbj#1 and #2 (**A** and **B**) was determined after sequence analysis. The percentage of IgM, IgA and IgG of fHbp-specific B-cells isolated from day0, day30post1,day30 and day202 post3 and for PBs isolated at day7 post 3rd dose is reported is reported in this graph.

In parallel we looked also at the VH repertoire of fHbp-specific B cells. The bioinformatic tool used for this study analyzed the sequences into their likely germline gene segments and assigned sequences to inferred clonotypes. For both subjects we observed at all time points after vaccination a strong contribution of the VH3 gene family (figure 4), followed by the VH1. Looking at the individual gene segments, the most common VH gene at day 0 was VH3-74, followed by VH3-33 and VH3-15. At the following time points after vaccination there was a different pattern of VH genes expressed by the pool of fHbp-specific B cells. In particular, we observed the preferential expression of VH3-23 gene, followed by VH3-74, VH3-11, VH3-7 and VH1-18. Moreover, VH3-23 was most frequently rearranged with JH4, followed by JH6 (Figure 4). A total of 677 unique fHbp-specific sequences were isolated from both subject (342 and 335 sequences from sbj#1 and sbj#2 respectively) from all time points before and after vaccination except for day

7 post-3rd. The most common rearrangements VH3-23*04/JH6*02 and VH3-23*04/JH4*02 were present in samples from three and four time points, respectively. This could suggest that a large part of the fHbp-specific B cells repertoire in each subject is shifting over time after vaccination. On the other hand, there is also a small part of this repertoire that comprises clones that could derive from B cells expanded by the vaccination.

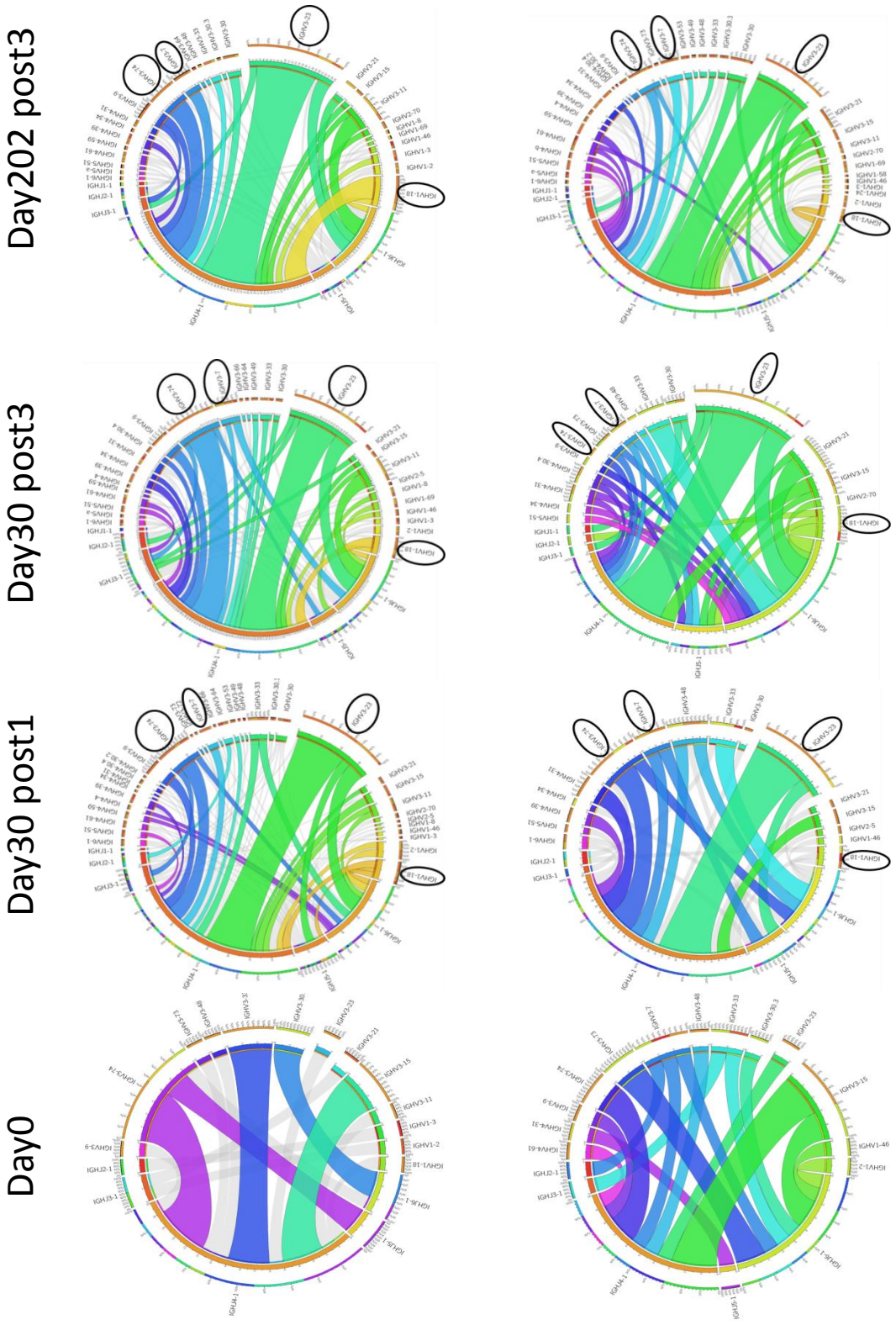
Day202 post3
Day30 post3
Day30 post1
Day0
Sbj #1
Sbj #2

Figure 4_ Circos plot showing the VHDJH gene usage in fHbp-specific B cells. Circos plots were generated for fHbp specific cells isolated from each timepoint. On the right half of each plot each VH gene segment is shown in a different color. The left half of each plot shows different JH gene segments. The colored ribbon corresponds to the frequency of a specific VH(D)JH gene segments combinations

Plasmablasts repertoire differs from fHbp-specific B cells repertoire.

Plasmablasts were identified and isolated based on the differential expression of CD surface markers (CD3-, CD19+, CD20-, CD27++ and CD38++). Compared to the memory B cells, the pool of plasmablasts was more heterogeneous both in terms of Ig-class switch and VH-VL repertoire. Indeed, the majority of plasmablasts were composed by IgA-switched B cell clones (48 and 60% of the sequences in sbj #1 and #2 respectively), followed by IgG (37% of the sequences in both subjects) and in a smaller part also from IgM (15% and 3% of the sequences in sbj#1 and #2 respectively) (Figure 3). Looking at the repertoire we observed the expression of a broader spectrum of VH genes. For both subjects we observed a strong contribution of VH3 gene family, followed by VH4 (Figure 5). Even if VH3-23 was the most expressed gene, V(DH)J rearrangements seems to derive from different clones in respect to the ones observed in the pool of fHbp-specific B cells. This finding could suggest that different precursor clones of B cells are recruited to populate the pool of Plasmablasts or Memory B cells after GC selection and affinity maturation. However we should not exclude that due to the nature of the MenB vaccine that is composed by three different recombinant antigens, Plasmablasts population is basically the result of different effective vaccine antigen components-specific B cells.

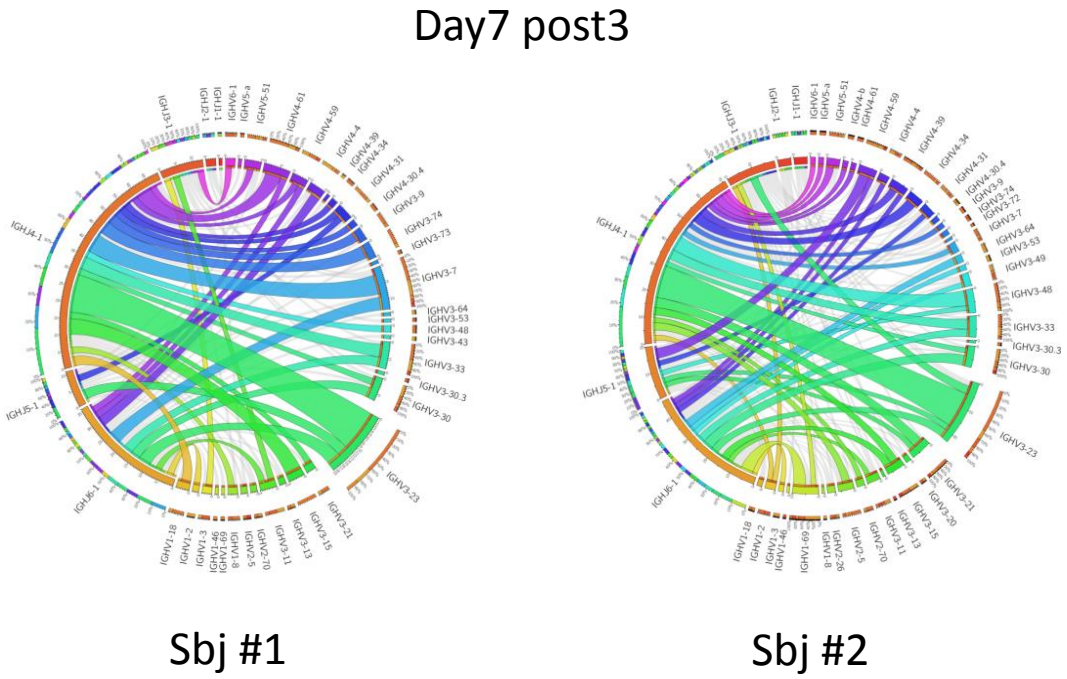

Figure 5_ Circos plot showing the VHDJH gene usage in PBs. Circos plot were generated for PBs isolated from day7 post 3rd dose of vaccination.

Generation of Fabs specific for fHbp.

One interesting question about the antibody repertoire in the compartment of antigen-specific BCR repertoire is if the most effective antibodies derive or not from positive selection in the GC reaction for higher affinity for the antigen, and possibly higher functionality. To answer this question we investigated the nature of the selection in this Ig sequences using dedicated software that relies on the assumption that affinity maturation strongly occurs along preferred paths in genotype space [16].

Following computational analysis of the repertoire we selected 6 Ig variable sequences identified in the two subjects at different time points after vaccination following preferential paths of mutations and possibly undergoing affinity maturation to be cloned and expressed as a fragment-antigen binding (Fab fragment). To generate the respective Fabs, VH and VL fragments were cloned into vectors and then expressed in Rosetta2(DE3) (Merk Millipore) strain. After purification, the binding specificity of the Fabs to fHbp was measured by Gyrolab immunoassay to determine both binding and affinity of the selected antibodies for fHbp. As shown in Figure 6, 4 of the selected antibodies generated from fHbp-specific B cells at different time points after vaccination were capable of binding the fHbp antigen, and all exhibited high binding affinities, with a W values ranging from 4,7 to 5,33 (Buricchi F. et al., manuscript in preparation).

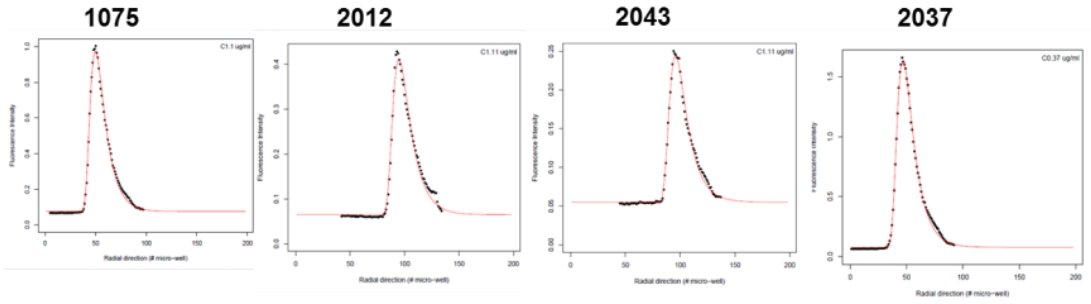

Fab name	Affinity vs fHbp (W)	St.dev
1075 (V3)	4,8	0,6
2012 (V8)	5,33	0,17
2043 (V7)	5,04	0,37
2037(V3)	4,7	0,26

Figure 6_ Characterization of anti-fHbp human Fabs. Gyrolab immunoassays were performed to determine the affinities of Fabs.

Discussion

The B cell repertoire is repeatedly shaped by the selection occurring in response to eliciting agents such as pathogens and vaccine antigens. The selection acts on the variable region, in the V(D)J gene segments, introducing sequential changes and redefining the specificity against the antigen domains [8]. Moreover also the constant region is modified switching from IgD+IgM+ BCR to different Ig classess, to mediate a more effective response recruiting the exact arm of effectors to clear the eliciting agents [7].

Different are the studies underlying the importance of dissecting the BCR repertoire of different B cell subsets following vaccination to get a comprehensive picture of the dynamics of the vaccine response. However, few studies looked at the repertoire of both PBs and antigen-specific MBCs. So far, the majority of the studies have focused only on the analysis of PBs [11, 12].

We dissected for the first time the variability among individuals in the breadth of the response to fHbp in terms of specificity, frequency and class of memory cells elicited by the multicomponent Meningococcus B vaccine. we also profiled the longitudinal changes of the repertoire at different time points after vaccination.

Two subjects were chosen among six vaccines, based on their serological and cellular responses to fHbp overtime after vaccination. By measuring both the antibody titers versus fHbp in plasma samples and the frequency of circulating fHbp-specific MBCs and PBs in peripheral blood we observed that there were overall no significant differences in the frequency of fHbp+ MBCs among the six subjects. Nevertheless two subjects showed higher serological and cellular responses to fHbp at day 7 post-3rd dose in respect to the other subjects. To dissect their VH and VL repertoire we isolated fHbp+ B cells by FACS at different time points before and after vaccination, and Plasmablasts at day7 post-3rd. Interestingly, we observed two main findings. Firstly, in the pool of fHbp+ B cells there are marked changes in the usage of the VDJ genes among cells isolated before and

after vaccination, underlined by the preferential expansion of some VH gene families induced by the vaccine, namely VH3-23 gene, followed by VH3-74, VH3-11, VH3-7 and VH1-18. Moreover we observed that starting from day30 post1st dose to day202 post 3rd dose, the VDJ usage across fHbp+ B cells isolated from each timepoint was comparable with the most common rearrangements VH3-23*04/JH6*02 and VH3-23*04/JH4*02 present in three and four time points, respectively. We did not observe the expansion of any particular clonal lineage but this could be due to the nature of the vaccine, being a multicomponent vaccine, or to the number of subjects and sequences analyzed. The approach used for the sequencing of the Ig genes has allowed also to gain the information on the Ig class of each single BCR expressed by the isolated fHbp+ B cells. By looking at the changes in frequencies of the different Ig classes identified longitudinally, it is clear that the antigen selects and models the specificity of the responding B cells also by inducing class switching from IgM, that represent at baseline on average the 85% of the repertoire reacting with fHbp to IgG at the peak of the response. In fact, unless carriage cases, vaccination should be likely the first encounter with these type B meningococcus antigens.

The second important finding is that MBCs and PBs elicited by MenB vaccination seems to derive from different clones. Previous studies demonstrated that a clonal relationship could exist between Ag-specific MBCs and PBs suggesting an involvement of Ag-experienced memory B cells in refilling newly generated PBs and MBCs at recall responses [13]. However, our finding could be explained by the intrinsic heterogeneity of PBs population generated by the encounter with different antigens present in the multicomponent MenB vaccine. Since our comparison between PBs and MBCs is done by looking at the heterogeneous pool of PBs and the restricted repertoire of fHbp+ MBC cells we do not exclude that this could limit our understanding on their possible relationship.

Finally it is noteworthy to underline that by performing a computational analysis of the fHbp specific repertoire of two individuals, and by looking at the changes of it at different time points after vaccination, it has been possible to identify six related VH sequences at different time points after vaccination, following a preferential paths of mutations. By expressing the corresponding antibodies we have formally demonstrated that four of them do actually bind fHbp, with a comparable high affinity. The similar sequence and affinity of the antibodies isolated by two different subjects might therefore by inferred to a maturation and affinity selection process preferentially induced by the vaccine antigen.

Overall this type of dissection represents the first longitudinal and in depth analysis of the evolution of Ig-BCR response of fHbp+ MBCs and Plasmblasts following vaccination. We strongly believe that extending this approach to a large number of vaccinated subjects and moreover to large cohorts of vaccinees of different ages receiving different vaccine formulations could be helpful in understanding the evolution of the adaptive immune response, as well as in discriminating useless versus harming responses. This approach could be key for designing more effective vaccines able to stimulate and guide the 'right' immune memory responses.

Materials and Methods

Vaccination protocol and blood sample collection

All subjects present in this study were enrolled in a study protocol and received three dose of the licensed vaccine against Meningococcus B strain. Blood and sera samples were collected at day0 (pre-vaccination), day 30 post-1st dose, day 7, day 30 and day 202 post-3rd dose of vaccination once the informed consent had been obtained from the individuals and after approval by the local ethical committee.

Gyrolab analysis to measure fHbp response in plasma samples and affinity of FAbs.

Both Plasma samples of six subjects and Fabs generated after cloning were tested for their specificity to fHbp by Gyrolab assay. All plasma samples were diluted 1:50 otherwise Fabs were tested at different concentration in order to calculate the affinity of each Fab. For both this assays, fHbp was biotinylated using use EZ-Link® sulfo-NHS-LC-Biotin (Thermo Scientific, cat # 21335) and used at a final concentration of 100 µg/ml. Sera or Fabs bound to fHbp were detected by using an anti-human alexa647-conjugated IgG at a concentration of 25 nM.

Analysis of fHbp-specific response of MBCs and PBs by ELISPOT assay

The frequencies of fHbp-specific IgG and IgM have been determined in PBs and MBCs of six subjects by Elispot assay. PBs collected at day 7 post 3rd dose of vaccination were thawed, counted and diluted to appropriate concentrations in complete medium (RPMI with 100 units/mL penicillin, 100 µg/mL of streptomycin, 2 mM L glutamine, 1 mM sodium pyruvate, and 0.1 mM not essential amino acids, 5%FBS; Invitrogen) and directly plated (200 µl/well) in serial 2 fold dilutions in duplicate wells of ELISPOT plates pre coated with HSA, fHbp or both anti- human IgG and IgM antibodies. Otherwise resting MBCs, once thawed and counted, were firstly cultured in vitro with complete medium containing polyclonal stimuli, 2.5 µg/ml of CpG (PRIMM, Milan, Italy) and

1000U/ml of IL 2 (Novartis), to induce the differentiation into antibody secreting cells. Following 5 days culture, cells were harvested and plated in ELISPOT plates as described with PBs. After incubation at 37°C and 5% CO2 for 2 hours, PBs or MBCs were removed and the plates were washed 6 times with 0.05% Tween20/PBS. Spots of antibody secreting cells were revealed with FITC-conjugated anti human IgG (Fc) diluted 1:8000 and biotin-conjugated anti human IgM (Fc) diluted 1:1000 in 4% BSA/PBS. After an overnight incubation at 37 °C, a step with horse radish peroxidase conjugated Streptavidin (ENDOGEN) followed. The reaction was finally developed with 3 amino 9 ethylcarbazole (AEC, Sigma). Spots were counted automatically using the UV Spot ELISPOT plate Analyzer (CTL) and the Immunospot software v5.09 (CTL).

Conjugation of fHbp with fluorochrome

fHbp (Novartis vaccine antigen) and HSA (Sigma Aldrich) molecules were chemically labeled with Alexa Fluor 647 carboxylic acid succinimidyl ester (Molecular Probes, Invitrogen) following the manufacturer's instructions. Briefly, each protein antigen was incubated with the dye at a molar ratio of 1:10 for 1 hour at room temperature and then loaded into a Zeba desalting spin column (Thermo Scientific) to remove unbound dye. The degree of labeling was determined following the manufacturer's instructions, by measuring the absorbance of conjugated protein at the relevant wave length for each fluorochrome by spectrophotometry. Protein concentrations were calculated by the Bradford Assay (da vedere catalogo); the protein integrity was analyzed by SDS PAGE.

Staining procedure for FACS analysis and sorting

Frozen PBMCs were thawed at 37°C in PBS containing 2.5mM EDTA and 20 µg/mL DNAse (Sigma Aldrich) and then divided into 2 ml Eppendorf tubes, each containing approximately 7x106 to 107 PBMC. Before incubating with the exact mix of Antibodies to differently identify Plasmablasts and fHbp-specific B cells, PBMC were first stained with Live/Dead Aqua (Invitrogen) diluted 1:500 in 100

µl, for 20 min in the dark. Then 50 µl of PBS containing 20% rabbit serum were added for further 20 min at 4°C to saturate Fc receptors. After washing with 1,5 ml of PBS, PBMCs were stained differently based on the B cell population to identify. To identify PBs, PMCS were finally incubated with 50 µl of mix containing the following pre-titrated monoclonal antibodies diluted in 1% FBS: anti-CD19 APC (Becton Dickinson), anti-CD20 PrCPCy5.5 (Becton Dickinson), anti-CD27 –PE (Becton Dickinson), anti CD3-PB (Becton Dickinson) and CD38 Alexa700 (ExBio). Otherwise, to identify fHbp specific B cells, PBMCs were firstly dissolved in 10 µl of PBS containing 10 µg/ml of Alexa 647-conjugated fHbp bait and then incubated with a mix of pre titrated amounts of monoclonal antibodies diluted in 1% FBS. The mix contained the following monoclonal antibodies: anti CD19 PrCPCy5.5 (Becton Dickinson), anti CD27-PE (Becton Dickinson), anti hIgG PacificBlue, anti IgA FITC and anti-IgD A700. The incubation was carried on for 1h at 4°C. After washing with 1,5 ml of 1% FBS/PBS cells were diluted in 1 ml of BSA (vedere prodotto a 4°C) and stored on ice before acquisition at FACS Aria. FACS data of each samples were analyze using FlowJo software.

Single PBs and fHbp-specific MBCs sorting and Ig RT-PCR

PBs and fHbp-specific B cells were isolated as single cells respectively from day 7 and from all others timepoints. The sorting was carried on in high purity mode by using a FACS Aria instrument (BD Biosciences, San Jose, CA) using a 70 µm nozzle operating at 70 psi. Two different sorting gates were established in order to isolate PBs and brilliant fHbp+ B cells. PBs were identified as CD3-CD19+CD20-CD27++CD38+ B cells, otherwise fHbp+ specific B cells were isolated as fHbp+ CD19+ cells. Cells were sorted as single cells in 96-well plates. The number of cells recovered from each timepoint was different based on the initial number of hPBMC after thawing and the frequency of Ag-specific B cells. Each well was previously pre-filled with 10 µl of a lysis buffer containing 1X RT-buffer, 0,7 µM of dNTPs, 10 mM DTT, 20U of RNase inhibitor, 0,5% of NP40. Plates were

prepared in a dedicated RNAse free area in order to avoid well to well contamination. After sorting, plates were sealed, centrifuged, labeled with subject code and vaccination time point and immediately transferred on dry ice and finally stored at -80°C. To generate the cDNA 5 µl of a mix containing Ig-gene specific primer (0,3 µM of each CH/CK/Cλ specific primer), 7,5 mM of MgCl2, 0,01 mM of DTT, 10 U of RNAse inhibitors and 50U of SSIII was added to each well. The RT-reaction was carried on at 50°C for 1h and at 85°C for last 5 minutes and cDNA was stored at -20°C if not used immediately after the RT reaction. Two rounds of Ig nested-PCR followed to amplify separately the heavy and the two light chains. To avoid well-to-well contamination all PCR mixes were prepared in an RNAse free area and the cDNA or PCR products were added in another laboratory. 3,5 µl of Ig cDNA template were used as template for the first round of PCR in a final volume of 25 µl of a mix containing 1X PCR buffer, 0,3 µM of a set of IgH, Igκ or Igλ variable region primers and 0,5 µM of either IgM, IgG and IgA or Igκ or Igλ constant region primers, 0,3 µM of dNTPs, 1X of Rediload, 1U of Pfx50 DNA polymerase and 5% of DMSO to enhance the performance of the PCR reaction. 1st round PCR was performed at 94°C for 2 min followed by 35 cycles of 94°C ×15s, 57°C ×60 s, 68°C x60 s, and one cycle at 68°C×7min. In the nested 2nd round nested PCR 3 µl of either IgVH or Igκ or Igλ PCR products were added to the 2nd round PCR mix composed by 1X PCR buffer, 0,3 µM of both IgH, Igκ or Igλ variable region primers and IgM, IgG and IgA or Igκ or Igλ constant region primers, 0,25 µM of dNTPs, 1X Rediload, 5% of DMSO, 1U of PfX50 Taq DNA polymerase. The latter PCR was performed at 94°C for 2 min followed by 10 cycles of 94°C ×15s, 57°C ×60s, 68°C x60s, 20 cycles at 94°C ×15s, 60°C ×60s, 68°C x60s and one cycle at 68°C×7min. The sequences of primers are shown in table 1.

Sequence analysis

2nd round PCR products were directly loaded to a 1,5% agarose gel electrophoresis, taking advantage of mixing the Rediload buffer in the PCR reaction mixture before cycling, and were visualized by exposure to UV light for the presence of 350-450 nucleotides products for IgH and Igλ and of 550-600 nucleotides products for Igκ. Positive PCR products were purified with Agencourt Ampure beads (Beckman Coulter) and finally sequenced with the ABI 3730xl 96 capillary DNA analyzer (Applied Biosystems). Two sequencing reactions were carried on for each PCR products by using 2nd round PCR forward primer mix in one reaction and 2nd round PCR reverse primer mix in the second reaction in order to have the entire IgH/κ/λ sequence. Sequences were analyzed by Sequencer software and the Ig-germline sequences were inferred by the dedicated Ig-bioinformatics software. Sequences containing a stop codon or an out-of-frame rearrangement were considered as nonproductive and excluded from the analysis. The Ig class of each Heavy chain was determined by looking at the complementarity of the nucleotide sequence to the CH primer.

Cloning of VH and VL and expression in ad hoc E.coli

6 sequences of paired IgH and IgL were selected for cloning and expression. IgL PCR products were cloned by Polymerase Incomplete Primer Extension method (PIPE) (ref) in pETOmpHF vector, a modified pET21 (Novagen) containing a 5' OmpA leader sequence. In parallel, also IgH PCR products were amplified and cloned in a modified version of pET22b (Novagen) containing the sequence encoding the CH1 region of human IgG. The resulting RBS-PelB-VH-CH1-6xHis cassette was amplified and sub-cloned by PIPE method in the corresponding light chain expression vector. All PCR reactions were performed with KAPAHiFi HotStart ReadyMix (Kapa Biosystems) at 95°C x5 min, 25 cycles at 98 °C x20 sec, 55°C 30 sec, 72°C 30 sec/kb. Fabs were expressed in Rosetta2 (DE3) (Merk Millipore) strain in 50mL EnPresso B medium (BioSilta) supplemented with 100mg/L ampicillin and 10mg/L chloramphenicol in shaking flask. After 16h of

growth at 30°C and 160rpm, antibody expression was induced by the addition of 1mM IPTG and incubation at 25°C at 160rpm for 24h. Bacteria were harvested by centrifugation (7650xg for 20 minutes) and protein extraction was performed by chemical lysis in CelLytic Express (Sigma-Aldrich). Pellets were re-suspended in 10mL/g wet cell weight and incubated 15' at room temperature. The suspension was then centrifuged at 10000xg for 20 min at 4°C and the clarified lysates were loaded on 0.5mL of manually packed Ni-NTA affinity resin (Qiagen) gravity columns equilibrated with 20 mM Tris-HCl, 300 mM NaCl, 10 mM imidazole, pH 8. Columns were washed with 20 column volumes (CV) of equilibration buffer and with additional 20 CVs of 20 mM Tris-HCl, 300 mM NaCl, 30 mM imidazole, pH 8. Bound protein was eluted in 3 CVs of 20 mM Tris, 300 mM NaCl, 200 mM imidazole, pH 8, concentrated and and subject to analysis by non-reducing SDS-PAGE. Antibody quantification was performed by Bradford assay (Sigma-Aldrich).

References

[1] N. E. a. M. K. S. Ian J. Amanna, "Duration of Humoral Immunity to Common Viral and Vaccine Antigens," *N Engl J Med,* pp. 357:1903-1915, November 8, 2007.

[2] S. M. C. S. Amanna IJ1, "Immunity and immunological memory following smallpox vaccination.," *Immunol Rev,* pp. 211:320-37., 2006 Jun.

[3] L. M. H. S. S. L. N. J. S. G. H. J. S. M. Hammarlund E1, "Duration of antiviral immunity after smallpox vaccination," *Nat Med.,* pp. 9(9):1131-7., 2003 Sep.

[4] A. R. W. J. A. R. Slifka MK1, "Humoral immunity due to long-lived plasma cells.," *Immunity.* , pp. 8(3):363-72., 1998 .

[5] P. R. L. A. Traggiai E1, "Antigen dependent and independent mechanisms that sustain serum antibody levels.," *Vaccine.* , pp. Suppl 2:S35-7., 2003 Jun 1.

[6] M. IC., "Germinal centers," vol. Annu Rev Immunol, 1994.

[7] S. &. R. Kracker, "Immunoglobulin class switching: in vitro induction and analysis," vol. Methods Mol. Biol, 2004.

[8] K. Rajewsky, "Clonal selection and learning in the antibody system," vol. Nature , 1996.

[9] D. T. a. K. Good-Jacobson., "Diversity among Memory B Cells: Origin, Consequences, and Utility," *Science,* pp. 1205-1211, 13 September 2013: 341 (6151).

[10] C. C. J. W. M. M. S. A. N.-Y. Z. J.-H. L. M. H. X. Q. S. E. e. a. G.-M. Li, "Pandemic H1N1 influenza vaccine induces a recall response in humans that favors broadly cross-reactive memory B cells," vol. Proc. Natl. Acad. Sci. USA, 2012.

[11] D. K. G.-M. L. S. E. J. S. M. M. M. M. I. S. M. H. W. L. e. a. J. Wrammert, "Broadly cross-reactive antibodies dominate the human B cell response against 2009 pandemic H1N1 influenza virus infection," vol. J. Exp. Med., 2011.

[12] K. S. J. M. W. L. K. K. C. L. N.-Y. Z. I. M. L. G. C. H. e. a. J. Wrammert, "Rapid cloning of high-affinity human monoclonal antibodies against influenza virus," vol. Nature , 2008.

[13] G. C. M. H. R. K. D. C. L. P. D. T. Frölich D, "Secondary immunization generates clonally related antigen-specific plasma cells and memory B cells.," vol. J Immunol, 2010.

[14] M. K. J. D. G. W. K. Franz B, "Ex vivo characterization and isolation of rare memory B cells with antigen tetramers.," vol. Blood., 2011.

[15] A. L. A. F. B. F. T. S. S. C. N. S. D. E. I. I. F. E. D. G. G. C. F. G. G. Bardelli M, "Ex vivo analysis of human memory B lymphocytes specific for A and B influenza hemagglutinin by polychromatic flow-cytometry.," *PLoS One,* 2013.

[16] M. S. W. K. Z. R. Y. J. W. C. D. T. T. G. A. S. M. M. K. G. L. H. H. B. Kepler TB, "Reconstructing a B-Cell Clonal Lineage. II. Mutation, Selection, and Affinity Maturation.," *Front Immunol.* , 2014.

[17] L. A. K. A. N. S. H. P. T. D. Blink EJ1, "Early appearance of germinal center-derived memory B cells and plasma cells in blood after primary immunization.," *J Exp Med.*, pp. 201(4):545-54., 2005 Feb 21.

Discussion

The B cell repertoire is repeatedly shaped by the selection occurring in response to eliciting agents such as pathogens and vaccine antigens. The selection acts both on the Variable region, in the V(D)J gene segments introducing sequential changes and redefining the specificity against the antigen domains, and in the Constant region determining the switch from IgD+IgM+ BCR to different Ig class to mediate a more effective response recruiting the exact arm of effectors to clear the eliciting agents.

Different are the studies underlying the importance of dissecting the BCR repertoire of B cell subsets following vaccination to get a comprehensive picture of the dynamics of the vaccine response but a restricted number of them is looking at the repertoire of both the crucial components of the adaptive immune response: PBs and antigen-specific MBCs. So far, the majority of the studies have been focused only on the analysis of PBs. This has been possible because plasmablasts peak 7-8 days post-vaccination in peripheral blood reaching relatively high frequencies, furthermore they are identifiable by flow-cytometry based on the expression of well-defined surface markers without the need of selection based on antigen specificity. Otherwise the major obstacle in gaining insights on the antigen-specific MBCs population has been so far the lack of practical markers to identify rare antigen-specific MBCs within the bulk of MBCs present in ex vivo human PBMCs.

In line with all the previous observations, my PhD research activity has been focused firstly on the isolation of rare circulating antigen-specific MBCs and amplification of their VH and VL genes. Finally this methodology has been used to draw a comprehensive picture of the evolution of the B cell repertoire in both MBCs and PBs at different time points after vaccination in subjects receiving different vaccines.

At the time my PhD started, in our laboratory a methodology to identify rare MBCs specific for HA antigen from influenza virus was almost set up but there were no protocols available to retrotranscribe and amplify by PCR the VH and VL genes.
To practice in the techniques required for amplification, sequencing, and cloning of paired VH/VL Ig genes from single cells by RT and Ig-nested PCR, I spent two weeks at the Novartis Institute for BioMedical Research in Basel. Thereafter I continued to dedicate my efforts in optimizing the strategy learned in Basel to amplify VH and VL genes as well as to exploit the tools developed at Novartis Vaccines to identify rare circulating B cells specific for both the influenza hemagglutinin antigen (HA) and other vaccine antigens such as MenB antigens.
We demonstrated that B-cells carrying immunglobulin receptors specific for type A or B influenza HA could be identified in *ex vivo* PBMCs by using fluorochrome-tagged rHA as antigenic baits and unlabeled mismatched mono-bulk vaccine subunit antigens to block BCR-independent binding because of HA stickiness. We also showed that by combining rHA baits and monoclonal antibodies against surface B cell markers the method was suitable to analyze changes in the distribution of HA+ B cells across MBCs subsets at different maturation stages, including in subjects who did not experience a substantial increase in total number of HA+ MBCs. This observation provided a strong support to the feasibility of standardizing flow cytometry based assays for monitoring directly in PBMC samples *ex vivo* quantitative and phenotypic changes induced in the repertoire of HA+ B cells by influenza infection or vaccination. Moreover, we were able to sort arrays of single B cells with different HA binding specificities and to perform molecular cloning and in depth analysis of the VHVL Ig repertoires, as it was done with short lived plasmablasts circulating early after antigenic challenge. Since the methology was well established, we followed the same approach to dissect for the first time the individual variability in the breadth of the B cell response to fHbp, an antigen of the multicomponent vaccine developed in Novartis

against Meningococcus B. Specificity, frequency and class of the BCR of memory B cells elicited in response to fHbp have been described at different time points after vaccination in two individuals receiving the same vaccine..

We observed marked changes in the pool of fHbp+ B cells both in the usage of the VDJ genes among cells isolated before and after vaccination and in the type of class of Ig expressed by each cell. The results observed are compatible with the changes prompt by the antigen that selects and shapes the specificity of the responding B cells. Moreover we observed that the VDJ gene usage across fHbp+ B cells isolated at different timepoints was comparable, indicating a preferential expansion of selected VH gene families induced by the vaccine antigen. We did not observe the expansion of particular clonal lineages but this could be due to the type of vaccination and to the type of cells investigate. In fact, unless carriage cases, the vaccination should be the first encounter with this type of antigen.

Moreover we found that there was not a relationship between the Ig repertoire identified in MBCs and PBs after MenB vaccination although previous studies demonstrated that a clonal relationship could exist between Ag-specific MBCs and PBs suggesting an involvement of ag-experienced memory B cells in refilling newly generated PBs and MBCs at recall responses. However, our finding could be explained by the intrinsic heterogeneity of PBs population generated by the encounter with different antigens present in the multicomponent MenB vaccine. Since our comparison between PBs and MBCs is done by looking at the heterogeneous pool of PBs and at the restricted repertoire of fHbp+ MBC cells we do not exclude that this could limit our understanding on their possible relationship.

List of publications

- **Ex vivo analysis of human memory B lymphocytes specific for A and B influenza hemagglutinin by polychromatic flow-cytometry.**
  Bardelli M, **Alleri L**, Angiolini F, Buricchi F, Tavarini S, Sammicheli C, Nuti S, Degl'Innocenti E, Isnardi I, Fragapane E, Del Giudice G, Castellino F, Galli G.
  PLoS One. 2013 Aug 15;8(8):e70620. doi: 10.1371/journal.pone.0070620. eCollection 2013.

Acknowledgements